

MUSCLE-DIRECTED GENE AND ENZYME REPLACEMENT THERAPIES FOR
GLYCOGEN STORAGE DISORDER TYPE II, POMPE DISEASE

By

THOMAS JOSEPH FRAITES, JR.

A DISSERTATION PRESENTED TO THE GRADUATE SCHOOL
OF THE UNIVERSITY OF FLORIDA IN PARTIAL FULFILLMENT
OF THE REQUIREMENTS FOR THE DEGREE OF
DOCTOR OF PHILOSOPHY

UNIVERSITY OF FLORIDA

2003

Copyright 2003

by

Thomas Joseph Fraites, Jr.

This work is dedicated to the current and future subjects of clinical trials for GSDII and their families. Their courage has inspired and sustained our efforts.

ACKNOWLEDGMENTS

I would like to express my gratitude to my mentor and friend, Barry J. Byrne, M.D., Ph.D., for his guidance, patience, and constant support throughout my career thus far. I also thank my committee members (Drs. Jörg Bungert, Philip Laipis, and Glenn Walter) for their excellent guidance, input, and patience. Dr. Cathryn Mah has been a close confidante and advisor for many of these years, and her counsel has been invaluable to me. Additionally, I owe a great debt of gratitude to the many fine professors and instructors who have taught the various courses that I have taken over the past 7 years, both in the College of Medicine and the Warrington College of Business.

Dr. Byrne undertook initial work in viral gene therapy for GSDII in collaboration with Drs. Paul Kessler and Daniel Pauly at the Johns Hopkins University. I followed where they began. Drs. Grant Zhang, Colette apRhys, and Catalin Toma also contributed at critical points during the infancy of this project, and I am indebted to them for teaching me the basics of molecular biology and GSDII. Drs. Rochelle Hirschhorn and Arnold Reuser, who remain active contributors to this field, laid the groundwork for our attempts at gene replacement through their isolation of the human gene and characterization of both human acid α -glucosidase and the progression of GSDII in patients.

Drs. Nina Raben and Paul Plotz of the National Institutes of Health developed and provided the animal model that was essential for this work. Characterization of that model could not have taken place without the critical assistance and guidance of Drs. R. Andrew Shanely and Scott Powers, both of whom were at the time in the College of

Health and Human Performance at the University of Florida. Their time and efforts are acknowledged and are greatly appreciated.

My colleagues in the Byrne Laboratory (particularly my co-workers in Pompe disease, Denise Cloutier, Dr. Mary Rucker, and especially Kerry Cresawn) have been remarkable in their commitment to this work and their assistance to me. Irene Zolotukhin, Larysa Sautina, and the Vector Core Laboratory of the Powell Gene Therapy Center were also instrumental in this work, as they collectively produced the rAAV vectors that were used. Special thanks are extended to Mark Potter and Dr. Sergei Zolotukhin, who have been collaborators and colleagues since my arrival in 1997. Others within the laboratory have been supportive and provided critical knowledge at points along the way, including Sean Germain, Kevin Cahill, Greg Simon, and Mandi Walters.

The work described here represents the best efforts of a group of people who have worked for the better part of 7 years to carry rAAV-mediated gene therapy forward, always with an eye to the critical goal of clinical application. This work is passed and entrusted now to promising young scientists (among them Christina Pacak, Robert Mango, Melissa Lewis, and Stacy Porvasnik).

Special thanks are reserved for those people who make graduate school not only bearable but a truly enjoyable experience. Joyce Connors and Laura Miriel have been staunch supporters and facilitators of my educational process, and their contributions to my progress and completion cannot be overstated.

Finally, I would like to express my deepest appreciation to my family. My parents are the mainstays of my life and remain my pillars of support. My siblings, as always, are my inspiration.

TABLE OF CONTENTS

	<u>Page</u>
ACKNOWLEDGMENTS.....	iv
LIST OF TABLES	x
LIST OF FIGURES.....	xi
ABSTRACT	xiii
1 INTRODUCTION	1
Glycogen Storage Disease Type II.....	2
Infantile-Onset GSDII, Pompe Disease	3
Later-Onset GSDII.....	4
Nonclassic infantile-onset GSDII	4
Childhood- and juvenile-onset GSDII.....	4
Adult-onset GSDII.....	5
Standard of Care for GSDII	6
Biochemistry of Glycogen and Acid α -Glucosidase	7
Glycogen.....	7
Lysosomal Enzyme Biogenesis and Trafficking	9
Acid α -Glucosidase Trafficking, Maturation, and Enzymatic Activity	10
Mutational Analysis and Genotype-Phenotype Correlations.....	11
Animal Models of GSDII	12
Two strains of knockout mice	13
Conditionally expressing transgenic mice on the <i>Gaa</i> ^{-/-} background.....	14
Proposed Therapeutic Strategies For GSDII	16
Enzyme Replacement Therapies For Lysosomal Storage Disorders.....	16
Lysosomal Storage Disorders	17
Glycogen Storage Disease Type II	17
Gene Therapy For GSDII.....	21
Initial Gene Therapy Studies For GSDII	21
Adeno-Associated Virus	22
AAV serotype 2 vectors	23
Other serotype vectors and differential tissue tropism	24
Skeletal Muscle-Directed Gene Therapy with Recombinant AAV	24
Muscular dystrophies and other muscle-based gene therapies	26
Molecular fate and persistence of rAAV2 genomes in muscle	27
Myocardium-Directed Gene Therapy with Recombinant AAV	27
rAAV-Mediated Gene Therapies for Lysosomal Storage Disorders.....	29
Phenotyping Murine Models of Skeletal and Cardiomyopathies	29

Skeletal Muscle Phenotyping.....	30
Isometric force mechanics	30
Histopathology.....	31
Cardiac Phenotyping.....	31
Electrophysiology (EP) and electrocardiogram (ECG).....	31
Echocardiography and magnetic resonance imaging (MRI)	32
Hemodynamics and contractility	33
Summary	35
2 PHENOTYPIC CHARACTERIZATION OF A MURINE MODEL OF GLYCOGEN STORAGE DISEASE TYPE II, POMPE DISEASE	36
Methods and Materials.....	38
Enzymatic Activity Assays for Acid α -Glucosidase.....	38
Histochemical Staining.....	41
<i>In Vitro</i> Force-Frequency Measurements	41
Data Analysis.....	43
Results.....	43
<i>Gaa</i> ^{-/-} mice lack GAA enzymatic activity, resulting in aberrant glycogen accumulation	43
<i>Gaa</i> ^{-/-} mice have diminished skeletal muscle contractile properties.....	44
Discussion	46
3 FUNCTIONAL CONSEQUENCES OF INTRAVENOUS RECOMBINANT ENZYME REPLACEMENT THERAPY	48
Experimental Design and Rationale.....	48
Methods and Materials.....	48
Animal Procedures and Intravenous Delivery	48
Assessment of Skeletal Muscle Function	50
Results.....	50
Expression and Enzymatic Activity in <i>Gaa</i> ^{-/-} Mice After Intravenous Delivery of rhGAA.....	50
Restoration of Skeletal Muscle Contractile Force in <i>Gaa</i> ^{-/-} Mice After Intravenous Delivery of rhGAA.....	51
Discussion	52
4 SKELETAL MUSCLE-DIRECTED RECOMBINANT ADENO-ASSOCIATED VIRUS MEDIATED GENE THERAPY FOR GSDII	54
Methods and Materials.....	55
Molecular Cloning of rAAV Vectors Carrying the Human and Murine GAA Genes	55
Cell Lines and <i>In Vitro</i> and <i>In Vivo</i> Viral Transduction.....	56
Assays of GAA Activity and Glycogen Content	57
Immunocytochemistry	57
Perchloric Acid Extraction and ¹ H-NMR Spectroscopy.....	58
Assessment of Skeletal Muscle Function	59
Results.....	60

Expression and Enzymatic Activity in GSDII cells After <i>In Vitro</i> Transduction With rAAV2- <i>hGAA</i>	60
Stable, Long-Term Expression of Human or Mouse GAA in Mouse Muscle After <i>In Vivo</i> Delivery of rAAV2 Vectors	61
Preservation of Skeletal Muscle Contractile Force in Knockout Mice After Direct Intramuscular Delivery of rAAV2- <i>mGaa</i>	63
Treatment of <i>Gaa</i> ^{-/-} Mice With rAAV1- <i>mGaa</i> Leading to Rapid Overexpression of GAA and Glycogen Clearance.....	64
Treatment of Various Skeletal Muscles with rAAV1- <i>mGaa</i> Leads to Overexpression of GAA in <i>Gaa</i> ^{-/-} Mice	65
Discussion	67
5 CROSS-CORRECTION AFTER RECOMBINANT ADENO-ASSOCIATED VIRUS DELIVERY TO SKELETAL MUSCLE.....	72
Methods and Materials.....	73
Molecular Cloning of rAAV Vectors Carrying the Human and Murine GAA Genes.....	73
<i>In Vivo</i> Viral Transduction	73
Assays of GAA Activity	73
Assessment of Skeletal Muscle Function	74
Assessment of Immune Response to hGAA.....	74
Histological Assessment of Glycogen Clearance	75
Results.....	75
Study 1: Evidence of Cross-Correction of Distal Tissues with rAAV1- <i>mGaa</i> Delivery to Quadriceps Femoris in <i>Gaa</i> ^{-/-} Mice.....	75
Varied Enzymatic Activities in Injected and Distal Muscles after High-Dose Delivery of rAAV1-hGAA to Quadriceps Femoris	76
Partial Preservation of Soleus Contractile Force in <i>Gaa</i> ^{-/-} Mice after High-Dose Delivery of rAAV1-hGAA to Quadriceps Femoris	78
High-Dose rAAV1- <i>hGAA</i> Treatment Leads to a Rapid Immune Response to the GAA Transgene.....	79
Discussion	81
6 RECOMBINANT ADENO-ASSOCIATED VIRUS-MEDIATED GENE THERAPY FOR MYOCARDIAL DISEASE IN GSDII.....	85
Experimental Design and Rationale.....	85
Methods and Materials.....	86
Intramyocardial Injections	86
<i>In Vitro</i> Cardiomyocyte Transduction with rAAV1	86
Media and plate preparation	86
Dissection, cell isolation, and plating	87
Fibroblast growth arrest.....	88
Senescent cell culture	89
Results.....	89
Intramyocardial Delivery of rAAV.....	89
<i>In Vitro</i> Transduction of Rat Cardiomyocytes with rAAV1, 2, and 5.....	90

	Intramuscular Delivery of rAAV1- <i>hGAA</i> and Cross-Correction of the Myocardium	90
	Discussion	90
7	RECOMBINANT ADENO-ASSOCIATED VIRUS DELIVERY TO THE MURINE DIAPHRAGM	92
	Methods and Materials.....	93
	Packaging and Purification of Recombinant AAV1, 2, and 5 vectors	93
	Vector-Vehicle Preparation	94
	<i>In Vivo</i> Delivery	94
	Assays of β -galactosidase and GAA Enzymatic Activity	95
	Histological Assessment of Glycogen Clearance	96
	Biodistribution of Vector Genomes.....	96
	Results.....	97
	Efficiency of Transduction Using Gel-Based Delivery of rAAV <i>In Vivo</i>	97
	Varying Tropisms of rAAV Serotypes 1, 2, and 5 for Diaphragm <i>In Vivo</i>	97
	Biochemical Correction of Diaphragms of <i>Gaa</i> ^{-/-} Mice with Gel-Based Delivery of rAAV1-GAA	98
	Biodistribution of rAAV Genomes After Gel-Based Delivery	100
	Discussion	101
8	CONCLUSIONS AND FUTURE DIRECTIONS.....	104
	REFERENCES.....	107
	BIOGRAPHICAL SKETCH	124

LIST OF TABLES

<u>Table</u>	<u>page</u>
2-1. Acid α -glucosidase activities in tissue samples from Gaa knockout ($Gaa^{-/-}$) and wild-type control mice.....	38
2-2. Acid α -glucosidase activities for specific wild-type and $Gaa^{-/-}$ hindlimb skeletal muscle tissues.	44
2-3. Acid α -glucosidase activities for wild-type and $Gaa^{-/-}$ various cardiac, smooth, and skeletal muscle tissues.	44
5-1. Percent of wild-type acid α -glucosidase activities in various $Gaa^{-/-}$ tissues after quadriceps femoris delivery of rAAV1- <i>mGaa</i>	76
5-2. Acid α -glucosidase activities in $Gaa^{-/-}$ hindlimb tissues after quadriceps femoris delivery of rAAV1- <i>hGAA</i>	77
5-3. Acid α -glucosidase activities in $Gaa^{-/-}$ various cardiac, smooth, and skeletal muscle tissues after quadriceps femoris delivery of rAAV1- <i>hGAA</i>	77

LIST OF FIGURES

<u>Figure</u>	<u>page</u>
1-1. β -galactosidase staining of mouse tibialis anterior (skeletal muscle) transduced by rAAV2-CMV- β gal.	25
1-2. Left-ventricular pressure-volume curve.	34
2-1. Contractile function measurement apparatus.	42
2-2. Qualitative functional phenotype of $Gaa^{-/-}$ mice.	43
2-3. Force-frequency assessment of soleus (postural skeletal muscles) from 129X1 x C57BL/6 (wild-type control) and $Gaa^{-/-}$ mice.	45
2-4. Force-frequency assessment of diaphragm muscle strips from 6-mo-old 129X1 x C57BL/6 (wild-type control) and $Gaa^{-/-}$ mice.	45
3-1. Enzymatic activities after intravenous delivery of rhGAA.	51
3-2. Isometric force-frequency relationships in soleus muscles of $Gaa^{-/-}$ mice after intravenous delivery of rhGAA.	52
4-1. <i>In vitro</i> expression and lysosomal targeting of GAA in cells from GSDII patients.	61
4-2. Expression of recombinant human GAA in Balb/c mice after transduction with rAAV2- <i>hGAA</i>	62
4-3. rAAV2- <i>mGaa</i> -mediated transduction of skeletal muscle in $Gaa^{-/-}$ mice.	63
4-4. Force-frequency relationships of intact soleus muscles after direct intramuscular delivery of rAAV2- <i>mGaa</i>	64
4-5. rAAV1- <i>mGaa</i> -mediated transduction of tibialis anterior in $Gaa^{-/-}$ mice.	65
4-6. rAAV1- <i>mGaa</i> -mediated transduction of various skeletal muscles in $Gaa^{-/-}$ mice.	66
5-1. Force-frequency relationships of intact soleus muscles after intramuscular delivery of rAAV1- <i>hGAA</i> to the quadriceps femoris.	78
5-2. Naïve anti- <i>hGAA</i> antibody titers.	79

5-3. Tolerized anti-hGAA antibody titers.	80
6-1. Restoration of GAA activity after intramyocardial injection of rAAV2 and rAAV1.	89
6-2. <i>In vitro</i> transduction of neonatal rat cardiomyocytes with three serotypes of rAAV- β gal.	90
6-3. Current status of rAAV-mediated gene therapy for myocardial disease in GSDII.	91
7-1. Gel-based delivery preparation.	95
7-2. Free virus and gel-based delivery of rAAV- β gal vectors based on AAV serotypes 1, 2, and 5.	98
7-3. rAAV1-hGAA-mediated transduction of diaphragms <i>Gaa</i> ^{-/-} mice.	99
7-4. Biodistribution of rAAV1 vector genomes after gel-based delivery.	100

Abstract of Dissertation Presented to the Graduate School
of the University of Florida in Partial Fulfillment of the
Requirements for the Degree of Doctor of Philosophy

MUSCLE-DIRECTED GENE AND ENZYME REPLACEMENT THERAPIES FOR
GLYCOGEN STORAGE DISORDER TYPE II, POMPE DISEASE

By

Thomas Joseph Fraites, Jr.

December 2003

Chair: Barry J. Byrne

Major Department: Molecular Genetics and Microbiology

Our earlier studies showed the potential utility of gene replacement therapies for glycogen storage disorder type II (GSDII), or Pompe disease, using recombinant vectors based on recombinant adeno-associated virus serotype 2 (AAV2). GSDII results from defects in the gene encoding acid α -glucosidase (GAA), a lysosomal enzyme responsible for glycogen turnover in that compartment. Acid α -glucosidase knockout mice (*Gaa*^{-/-}) accumulate massive quantities of glycogen over their life span, leading to muscle wasting and loss of contractile function. Therefore, in concert with previous gene transfer studies, experiments were also undertaken to establish the skeletal muscle phenotype of *Gaa*^{-/-} mice to determine whether they can serve as appropriate models of human Pompe disease.

Our objectives were 1) to further characterize the *Gaa*^{-/-} model of GSDII; 2) to assess the efficacy of recombinant enzyme replacement therapy, an alternative to gene transfer; and 3) to further develop recombinant adeno-associated virus-mediated gene

therapies for GSDII. In particular, much of our recent work has been focused on the potential for systemic delivery of recombinant human GAA, either through enzyme or gene replacement strategies, to correct affected muscles. The ultimate goal of these efforts is, as always, to correct the primary enzymatic defect in the murine model — enabling functional correction and providing critical data to inform the design and completion of clinical trials in human GSDII subjects.

CHAPTER 1 INTRODUCTION

Cardiovascular disease remains the leading cause of death in both the United States and the State of Florida [1,2]. Advances in pharmacological and surgical interventions have vastly improved quality of life and life expectancy after diagnosis for a host of cardiovascular conditions. Despite these advances, effective treatments remain elusive for a number of cardiovascular diseases, particularly conditions of genetic origin. With the completion of the Human Genome Project in April 2003, investigators and patients alike are hopeful that more effective and specific therapies will soon be available. The bridges between emerging genomic information and therapeutic products will in many cases be biotechnology and biopharmaceuticals.

Among biotechnology products, genetic therapies hold the promise of ameliorating the symptoms of genetic diseases and reversing the underlying molecular defects that give rise to them [3,4]. At present, however, clinical use of genetic therapies for cardiovascular and musculoskeletal conditions is limited by a variety of remaining challenges in vector development, gene delivery, and demonstrated safety and efficacy in animal models. For some clinical conditions, biopharmaceuticals (such as recombinant enzymes or antibodies) are also promising candidates, and in some cases biopharmaceuticals are already the standard of care. For example, Genzyme Corporation, in collaboration with the National Institutes of Health, has developed a recombinant enzyme replacement therapy for Type 1 Gaucher disease. ImClone Systems Incorporated has developed a number of chimeric monoclonal antibody products that target specific

growth factors in neoplastic conditions. Unlike genetic therapies, these products are designed for repeated administration, and as a result may face obstacles related to immunogenicity and bioavailability.

We chose to address the primary genetic and biochemical defects in glycogen storage disease type II (GSDII), an inherited cardiac and skeletal myopathy, using recombinant adeno-associated virus as a gene transfer vector. In parallel and in collaboration with an industrial partner, we also sought to characterize the potential efficacy of recombinant enzyme replacement therapy (ERT) for GSDII. Using a genetically engineered knockout mouse strain, we addressed some of the challenges facing gene and enzyme replacement therapies. Specifically, we evaluated the efficacy of various gene transfer methods and materials; and used physiologic measures of cardiac and skeletal muscle contractility to assess the functional efficacy of gene transfer and enzyme replacement therapy.

Glycogen Storage Disease Type II

Glycogen storage disease type II (GSDII; Pompe disease; MIM 232300) is an autosomal recessive disorder caused by a deficiency of the lysosomal enzyme, acid α -glucosidase (GAA; EC 3.2.1.20) [5]. GAA is responsible for the cleavage of α -1,4 and α -1,6 linkages in lysosomal glycogen and maltose, leading to the release of monosaccharides. A loss or absence of GAA activity leads to massive accumulation of lysosomal and cytoplasmic glycogen in all tissues with significant pathologies observed in striated muscle [6], where apparent disruption of the contractile apparatus leads to generalized myopathy. The incidence of GSDII is estimated at 1:40,000, although the true incidence may be underreported due to the broad spectrum of symptomology.

Although the severity of the disease is clearly related to the age of onset, glycogen burden, and residual enzyme activity [7], attempts to classify GSDII according to strict age or genotype-phenotype guidelines have been thwarted by the simple heterogeneity of clinical presentation from individual to individual. Rather than well-delineated ages of onset or clinical course, broad overlaps exist between the age at diagnosis and the involvement of cardiac or skeletal myopathies. However, severe cardiomyopathy is almost always associated with infantile-onset, Pompe disease, and a more diverse clinical spectrum can be classified as later-onset GSDII.

Infantile-Onset GSDII, Pompe Disease

The most severe, infantile form of GSDII is known as Pompe disease, and it is caused by complete or nearly complete absence of enzymatic activity. First described by Pompe in 1932 [7], it is characterized by a rapidly progressing cardioskeletal myopathy, with profound cardiomegaly and hypotonia, skeletal muscle weakness, macroglossia, and in some cases, hepatomegaly. Glycogen deposition is observed in cardiac, skeletal, smooth muscle and liver; and in the central nervous system. However, no mental retardation has been recorded in GSDII infants. Patients often initially present with respiratory illness followed by cardiorespiratory symptoms that escalate rapidly and culminate in cardiorespiratory failure and death within the first 2 years of life. Electrocardiogram reveals a shortened PR interval (which is pathognomonic for Pompe disease) and large QRS complexes [6]. X-ray and echocardiography upon initial presentation reveal a markedly enlarged heart. In some cases, increased wall thicknesses of both ventricles and the interventricular septum (with concomitant shrinking of the ventricular cavities) are observed, leading to left-ventricular outflow-tract obstruction; in others, left-ventricular chamber dilation has also been reported. End-stage heart failure

results in either case, with diminished cardiac output and eventually ischemic and arrhythmic cardiac events.

A recent report reviewed case histories from the literature and one center's experience in the Netherlands [8]. The authors' experiences with twenty patients and 133 case reports in the literature both indicate that the median age for onset of symptoms is 1.6 mo; and the median age at death is between 6 and 8 mo. Among the approximately 150 cases reported, 10 patients (approximately 7%) lived beyond 1 year (adjusted for gestational age at birth), with 2 patients surviving beyond 1.5 years.

Later-Onset GSDII

There is a continuum of later onset disease that is accompanied by generalized cardiac, skeletal, and smooth muscle myopathies (although cardiac involvement is usually secondary to other myopathies). In general, age and severity of onset correlate to residual enzyme activities, with initial symptoms manifested in postural and other skeletal muscles; and more-severe progression leading to respiratory muscle weakness. Morbidity and mortality often relate to respiratory pathology.

Nonclassic infantile-onset GSDII

Nonclassic infantile-onset GSDII is classified here as a later-onset condition, primarily because of the predominance of skeletal muscular symptoms without apparent (or at least severe) cardiac involvement [6]. The actual age of onset can vary (from as early as within the first 6 mo of life, to later in infancy) with some correlation between the age of onset and absence of cardiomegaly [6,9].

Childhood- and juvenile-onset GSDII

Many later-onset patients present during the first decade, and in some cases are hard to distinguish from the non-classic infantile-onset group; clinical presentation can

overlap with classic cardiac symptomatology and generalized muscular myopathy. Most childhood- and juvenile-onset patients present with proximal skeletal muscle myopathy. The progression of disease is generally slower than in infantile-onset GSDII, but the age of onset does not strictly correlate with the age of death. In toddlers and young children, delayed or halted progression of motor milestones can be observed. In adolescents, symptoms can begin either as proximal muscle weakness or respiratory insufficiency. Most children and adolescents are mechanically ventilated as their condition deteriorates, and eventual mortality results from respiratory insufficiency as a result of diaphragmatic weakness [10], usually before the end of the third decade [6]. In one interesting case of juvenile-onset disease, an adult patient with childhood-onset muscular weakness but no evidence of vacuolization at age 26 died at age 31 of respiratory insufficiency [11]. Just before death, histological analysis revealed massive vacuolization exclusively in type I fibers, a finding (not mentioned in later reports) that may provide insights into pathogenesis of respiratory insufficiency in GSDII.

Adult-onset GSDII

Adult-onset GSDII usually manifests during the third to sixth decades [12] (in some cases after years of robust athletic activity) indicating a lack of early symptomatology. As with juvenile GSDII, symptoms often resemble limb-girdle muscular dystrophy, with later involvement of the diaphragm and respiratory muscles. Unlike other forms of GSDII, few reports exist of cardiac involvement in any adult-onset patients. Adult-onset GSDII is characterized by higher residual acid α -glucosidase activities than seen in other forms of the disease. As with other forms of GSDII,

examination of tissues from adult-onset subjects reveals significant enlargement of lysosomes with substantial glycogen accumulation.

Clinical manifestations of late-onset GSDII, particularly among juveniles and adults, are reportedly caused primarily by increased muscle protein breakdown. Bodamer and colleagues reported that protein turnover in GSDII subjects was increased by 31% compared to control subjects, with a concomitant increase in mean resting energy expenditure [13]. Recent evidence indicates that in addition to generalized protein turnover, specific deficiencies and mistrafficking of the dystrophin-associated protein complex (DAP) may be secondary effects of adult-onset GSDII [14].

Standard of Care for GSDII

Early attempts to treat GSDII were unsuccessful, including a high-protein diet, β -adrenergic drugs, thyroid and steroid hormones, and bone marrow transplantation [15,16]. For instance, despite the finding that protein turnover is substantially increased in GSDII subjects, only 25% of all reported subjects show an improvement of muscle or respiratory function after a high-protein diet [13]. Recent evidence suggests that dietary supplementation with L-alanine may have some beneficial effect in later-onset patients [17]. One case was also reported in which a patient with late infantile presentation (12 mo old at diagnosis) was treated with L-alanine supplementation for over 3 years, with some resolution of cardiac hypertrophy but progressive skeletal muscle myopathy nonetheless [18]. Because of the age at diagnosis and the heterogeneity of clinical course among late-infantile patients, there is some question as to whether the supplementation therapy had any effect at all. In any event, currently only palliative care is widely available, including nasogastric feeding and ventilatory support.

Biochemistry of Glycogen and Acid α -Glucosidase

Acid α -glucosidase is one of a family of lysosomal hydrolases that are responsible for processing of glycogen and recycling of monosaccharides. Glycogen enters the lysosome by a variety of autophagic mechanisms and is then available for complete digestion by GAA, which cleaves α -1,4 and α -1,6 glycosidic linkages to produce single glucose residues. Significant pathologies arise in GSDII patients despite normal levels and activity of cytoplasmic glycogen synthetic and hydrolytic enzymes.

Glycogen

Glycogen is a highly branched glucose polymer; and is the major storage form of carbohydrates in animals. While glycogen is synthesized and broken down in most human tissues, it is most abundant in liver (up to 6%) and muscle (1%). Considerable data have been accumulated regarding the differential metabolism of glycogen in these two tissues, particularly regarding its mobilization by means of hydrolysis.

The glycogenesis pathway is almost the same in liver and muscle [19]. The first step (phosphorylation of glucose to glucose-6-phosphate) is shared with the first step in glycolysis of glucose, and is catalyzed by hexokinase and glucokinase in the muscle and liver, respectively. The conversion of glucose-6-phosphate to glucose-1-phosphate through a glucose-1,6-bisphosphate intermediate is followed by the synthesis of UDP-glucose from glucose-1-phosphate and UTP, a reaction that is catalyzed by UDPGlc-pyrophosphorylase. These steps are shared with several other pathways. The next three events are unique to glycogen synthesis. First, glycogenin, a 37-kDa protein, is glucosylated on a specific tyrosine residue by UDP-glucose in an autocatalytic manner. The linear extension of this glucose oligomer is then catalyzed by glycogen synthase,

which attaches further glucose molecules by means of the 1→4 position. When the length of these branches reaches a minimum of eleven residues, glycogen branching enzyme (amylo[1→4] → [1→6]- transglucosidase) transfers a portion of the nascent chain to a separate chain, forming branch points in the molecule. Repeated catalysis of the last two events causes the generation of large, extensively branched glycogen polymers.

The roles of glycogen in liver and muscle are distinct, and for this reason, two separate catabolic pathways exist for glycogenolysis [19]. Muscle glycogen is responsible for providing hexose units for glycolysis within the myofiber. Hepatic glycogen, on the other hand, is available as a means of maintaining blood glucose – these hexose units are for export to the bloodstream. In the cytoplasm, the two pathways are controlled by a distinct (muscle or hepatic) glycogen phosphorylase, which is responsible for hydrolysis of 1→4 linkages to yield glucose-1-phosphate, the rate-limiting step in both organs. After a specific transfer reaction, 1→6 branch points can be exposed, allowing the activity of debranching enzyme (amylo[1→6]glucosidase) to act on the molecule. In concert, these reactions free glucose-1-phosphate, which is convertible to glucose-6-phosphate by a phosphoglucomutase, and glucose-6-phosphate is then available for further glycolysis. In the liver and kidneys, a further, alternative step enables removal of the phosphate from glucose-6-phosphate to allow free glucose to diffuse into the blood rather than enter the glycolytic cycle. It should be noted that all of these reactions occur in the cytoplasm or microsomes at neutral pH, an environment much different than the lysosomal compartment where glycogenolysis is catalyzed by acid α -glucosidase.

The exact mechanisms for glycogen entry and storage in the lysosome are uncertain [20]. Current opinion in the literature attributes this process to either glycogen incorporation in autophagic vacuoles (which then fuse to lysosomes) or by microautophagy (in which glycogen directly invaginates the lysosomal membrane). In neither case are the signals that initiate the process known; nor are the specific transport mechanisms known, if any exist.

Lysosomal Enzyme Biogenesis and Trafficking

Lysosomal enzymes share a number of important features. They have an amino-terminal signal peptide that mediates co-translational transport into the lumen of the endoplasmic reticulum (ER) where they are glycosylated. Subsequent carbohydrate modification begins in the ER and continues in the Golgi compartment. In the *cis*-Golgi, two enzymes, GlcNAc phosphotransferase and phosphodiester acyl-glucosaminidase (uncovering enzyme), are responsible for addition of mannose 6-phosphate (M6P) residues to nascent lysosomal proteins. The primary transport pathway leads directly from the *trans*-Golgi network to the late endosomes and lysosomes [21]. However, some lysosomal proteins can be alternatively routed to the plasma membrane and enter the lysosomes *via* the endocytic pathway.

Three mechanisms of lysosomal targeting have been described. Most soluble lysosomal proteins acquire the mannose 6-phosphate recognition marker and depend on the phosphomannosyl receptor for their transport [21,22]. Some proteins, including acid phosphatase (which lacks the M6P recognition marker), are synthesized as transmembrane proteins and reach the lysosome *via* the plasma membrane. The third mechanism, which is poorly understood, also seems to involve some form of membrane association.

Both during transport and upon reaching the endo-lysosomal compartment, lysosomal enzymes undergo limited proteolysis. Often this process is limited to cleavage of the signal peptide in the ER, but it can involve more extensive cleavage at internal sites or the loss of amino- and carboxyl-terminal propeptides.

Acid α -Glucosidase Trafficking, Maturation, and Enzymatic Activity

This maturation process is part of the trafficking and biogenesis of acid α -glucosidase (GAA). A 110-kDa precursor form of acid α -glucosidase is core-glycosylated in the ER and acquires M6P residues in the *cis*-Golgi. Most of this inactive precursor is sorted from non-lysosomal enzymes and transported to the lysosomal compartment by the mannose 6-phosphate receptor (M6PR). Successive cleavage of the enzyme in late endosomes and lysosomes yields 95-, 76-, and 70-kDa forms of GAA, all of which are catalytically active [23].

Despite the specificity of intracellular lysosomal enzyme trafficking, about 10% of a glycosylated 105-kDa precursor is not sorted to the lysosomes and instead enters the secretory pathway [24,25]. As with other circulating lysosomal enzymes, this secreted GAA fraction can be recaptured by M6P receptors on the surface of cell membranes, internalized, and directed to the lysosome [26]; evidence suggests that GAA can be captured by both the cation-dependent and -independent forms of the M6P receptor. Therefore, GAA can reach the lysosome *in cis*, by means of *de novo* enzyme synthesis, or *in trans*, through an M6P receptor-mediated secretion-recapture pathway [27]. This understanding of the intra- and intercellular trafficking of lysosomal enzymes (and GAA in particular) has been critical to the development of both genetic and protein replacement therapies for GSDII.

At acidic, lysosomal pH (pH 4.0-5.0) GAA cleaves both α -1,4 and α -1,6 linkages of both high- and low-molecular-weight α -glucans, including glycogen, soluble starches, and maltose, as well as a number of artificial substrates. The most significant artificial substrate for our work is 4-methylumbelliferyl α -D-glucopyranoside (4-MUG). There are relatively few inhibitors or activators of GAA, and virtually none that are GAA-specific. Alkaline pH inactivates the enzymatic activity. Teleologically, GAA enzymatic activity is believed to be important for mobilization of neonatal hepatic glycogen stores, but (as evidenced by the steady accumulation of glycogen in the lysosomal compartments of GSDII patient tissues) this activity remains important throughout life.

Mutational Analysis and Genotype-Phenotype Correlations

Genotype-phenotype correlations have been difficult to establish for GSDII because of relatively small kindreds and the existence of several examples of family members with identical mutations but widely varying clinical course. However, in some cases the genotype leads to a predictably deleterious phenotype based on the extent of the mutation and the particular domain of the GAA enzyme in which it falls. To date, over 70 different mutations (along the entire length of the gene) have been identified and characterized in the human population, and some are known to have consistent, significant, deleterious effects.

Among mutations in Caucasian populations, the most common is an intronic mutation in intron 1 of the human *GAA* gene [20]. The mutation gives rise to splice variants in which exon 2 is either partially or completely deleted. The resulting mutant proteins, particularly those lacking exon 2, are completely null for GAA activity, since the translation initiation codon, signal peptide, and amino-terminal proteolytic processing

site are all located in exon 2. However, low levels of correctly spliced GAA mRNA can also be transcribed in these cells, leading to low levels of normal, functional enzyme. These low levels are able to perform the catalytic functions of GAA in the lysosomal compartment. As a result, the most common Caucasian mutation (in intron 1) gives rise to a milder phenotype, late-onset variant of GSDII. On the other hand, Δ exon 18 or Δ T525 mutations in exon 2 (or compound heterozygosity for the two) have been shown to result in a severe infantile-onset phenotype. These mutations are common among Dutch GSDII patients. The Δ exon 18 mutation leads to an in-frame removal of 55 amino acids, some of which are essential for enzyme maturation.

Despite seeming concordance between apparently obvious deleterious mutations and phenotype, several examples exist of patients carrying severely deleterious genotypes but presenting with mild to moderate phenotypes [20]. In particular, reports of homozygous Δ exon 18 mutations in adult patients have confounded geneticists and clinical investigators. Likewise, several examples of compound heterozygotes carrying two mutations that are deleterious when found in the homozygous state also provide reasons to question the strictness of genotype-phenotype prediction and correlation. These examples and others provide the first bases for hypotheses about modifier genes and other potential mechanisms of disease modulation in GSDII.

Animal Models of GSDII

Several naturally occurring and genetically engineered animal models of GSDII are currently available and were reviewed by Hirschhorn and Reuser [6]. Some strains of cattle are known to carry GAA mutations and exhibit various skeletal muscle phenotypes. Japanese quail also suffer from a disease that mirrors the juvenile form of GSDII. The Lapland dog in some ways mirrors the infantile form of GSDII because of its cardiac

presentation, but the disorder is not as uniformly or prematurely fatal in these animals. While differential GAA synthesis and/or activity exists in these animals (as well as a full spectrum of cardiac involvement) none of these naturally occurring examples of GSDII mimic human infantile Pompe disease, particularly when age of onset and death (relative to the life span of the species) is used as a measure of disease progression or severity.

Two strains of knockout mice

Two independent research teams engineered murine knockout models of GSDII [28,29]. While the strategies for creating these models were similar, the actual phenotypes of the two resulting strains of animals are markedly different [30]. For instance, Raben *et al.* [30] noted that knockouts on a 129SvJ x C57BL/6 background — backcrossed to the C57BL/6 strain — developed a more profound cardiomyopathy with earlier onset than knockouts of the same background backcrossed to FVB. Unfortunately, the targeted exons in these respective knockouts were different, leading to the possibility that the targeted allele may be differentially inactivated rather than affected by strain background. Still more confounding is a report from Kamphoven *et al.* [31] indicating that the knockouts on the FVB and C57BL/6 backgrounds are cardiomyopathic, but their data are unclear because of problems with anesthesia (and therefore heart rate and cardiac function) and a poor delineation of which of their reported data apply to each of the respective strain backgrounds.

In any event, variations in phenotype among the different knockout strains are reminiscent of the variegated phenotypes among the patient population; and suggest that despite seemingly similar genetic disruptions, other modulating factors play a role in the clinical presentation of this disorder. In addition, new models are continually being developed, including a number of transgenic strains on the knockout background with the

GAA cDNA under the control of a regulatable promoter (tetracycline response element) [32]. These models may provide a clearer understanding of the pathogenesis of Pompe disease.

Raben and colleagues developed the knockout strain that is currently in use at a number of institutions in the United States [28]. This strain was produced *via* targeted disruption of exon 6 of the murine *Gaa* locus. Homozygous knockouts (hereafter *Gaa*^{-/-}) have markedly reduced mobility and strength within 3.5 wk of age. The GAA activities in these mice are negligible and represent less than 1% of the wild-type activity. Observations in our laboratory showed that these activities are reduced throughout embryonic development and remain depressed throughout the lifespan of the animal. Decreased motor activities and grip strength were reported as indices of depressed muscle function, as well as hepatomegaly and cardiomegaly. These mice have emerged as the model of choice for pharmacologic and genetic therapies for GSDII in the United States.

Conditionally expressing transgenic mice on the *Gaa*^{-/-} background

Genetic engineering also facilitated the production of two unique lines of transgenic mice that serve as experimental models of GSDII treatment modalities. Using the tetracycline-regulatable (tet) promoter system developed by Bujard and colleagues [33], two transgenic mouse lines were created on the *Gaa*^{-/-} background in which the human GAA gene is transcriptionally regulated by a tet-transactivator. Transcription of the transactivator is (in turn) regulated by either the muscle-specific creatine-kinase promoter or liver-specific albumin promoter, respectively. The end results are two transgenic mouse lines that produce no murine *Gaa* enzyme and synthesize human GAA exclusively in muscle or liver, respectively [32]. Furthermore, GAA expression in these two tissues can be repressed by the presence of tetracycline or its doxycycline derivative

(tet-off); in animals, ingestion of doxycycline chow is commonly used to deliver the drug to target tissues.

These two strains of conditionally expressing animals provide some unique and interesting insights into the efficacy of various potential treatment modalities. Since GAA can reach the lysosome *in trans* by means of an M6P receptor-mediated secretion-recapture pathway, therapies for GSDII have been designed to provide high levels of circulating enzyme. Perhaps the most interesting finding from the conditionally expressing transgenics is that human GAA, when produced in high quantities in liver, can be both secreted from the liver and endocytosed by muscle and other tissues. Restoration of enzymatic activity and clearance of glycogen were also reported, confirming the long-held belief that circulating enzyme could be correctly trafficked and proteolytically processed in deficient tissues and, in turn, lead to correction of the primary biochemical defect.

Another potentially significant finding from these mice was that high levels of hGAA expression in skeletal muscle did not lead to the same extent of secretion or subsequent re-uptake in distal tissues as liver-derived expression. These results have great significance for gene transfer strategies, in which an appropriate organ must be selected for gene transfer and subsequent cross-correction. Raben *et al.* [32] observed that high levels of expression in skeletal muscle were unable to cause transfer of enzyme activity to the liver and other tissues; and that still-higher levels of expression were cytotoxic in muscle cells. One critical problem with these conclusions, however, is that they are not based on a direct comparison of transcription in muscle versus liver tissues in these respective strains. It is unclear, in other words, whether these results are applicable

on a transcript-to-transcript basis; or if they are unique to the particular levels of transcription in the strains of mice reported in this work. Perhaps the most important question that could not be addressed in these mice is whether therapeutic levels of enzyme activity could be transferred from one muscle to another, irrespective of the levels of activity restored to non-muscle tissues (i.e., tissues that are not directly involved in the pathogenesis of GSDII). Nonetheless, findings reported by Raben and colleagues suggest important issues to consider in designing preclinical or clinical treatment strategies.

Proposed Therapeutic Strategies for GSDII

Because of the unique potential for circulating bioavailability of GAA, both genetic and protein replacement therapies for GSDII are currently under investigation. Both of these strategies rely on the specificity of M6P receptor-mediated import of GAA. Gene therapy is particularly attractive under these circumstances because there is a theoretical possibility of continuous delivery of circulating, recombinant GAA *in trans* after transduction of a repository of producer cells.

Enzyme Replacement Therapies for Lysosomal Storage Disorders

Enzyme replacement therapies (ERTs) for lysosomal storage disorders (LSDs) have been under development since the discovery of their underlying enzymatic defects – in most cases a span of 30 to 40 years [34]. Despite the seeming uniformity of lysosomal enzyme trafficking, the heterogeneity of disease progression and primary organ pathogenesis among these diseases have led to unique challenges and approaches to enzyme replacement strategies.

Lysosomal Storage Disorders

Of the 40 known lysosomal storage diseases, Type 1 Gaucher disease, the nonneuronopathic variant, has been the most successful target for enzyme replacement therapy. Type 1 Gaucher disease is caused by the unchecked accumulation of a lipid called glucocerebroside due to a deficiency of β -glucocerebrosidase. To date, over 3000 subjects have been treated with imiglucerase (either purified from placenta or a more recent modified recombinant form). Since disease progression manifests in the nervous system, modifications must be made to the enzyme to facilitate its entry into macrophages, which then carry the enzyme to target tissues. Type 2 and Type 3 Gaucher disease present more difficult problems because pathogenesis and disease progression occur in the central nervous system, necessitating transit across the blood-brain barrier. Human trials of ERT for Fabry disease (deficiency of α -galactosidase A) and mucopolysaccharidosis type I (MPS I; deficiency of α -L-iduronidase) are also underway [34].

Glycogen Storage Disease Type II

Synthetic and processing pathways for acid α -glucosidase provide a rationale for intravenous delivery of recombinant GAA as a therapeutic modality. Enzyme replacement therapy has been attempted by a number of groups, beginning in the early 1970s [35,36]. Early attempts used protein purified from human placenta or urine, or bovine GAA. While those studies did not lead to long-term strategies for production of enzyme for widespread use, they did lead to two important findings. First, exogenously derived, intravenously delivered GAA could be taken up, *in vitro*, by cultured fibroblasts and skeletal muscle cells from GAA deficient patients. Second, the delivered enzyme

could mediate glycogen breakdown in those cells [27,37]. Reuser *et al.* [36] correctly surmised that differential uptake of these variously purified GAA proteins was directly related to the extent of phosphorylation on mannose residues. Further investigation by the same group confirmed that there are seven glycosylation sites on the native 110kDa protein; that proteolytic processing removes at least two of these sites; and, most importantly, that mutation or deletion of the second glycosylation site at Asn-233 prevents proper trafficking of GAA [38].

Since the cloning of human acid α -glucosidase [39,40], efforts in protein replacement therapy have focused on recombinant protein production and delivery. Recombinant human GAA (rhGAA) has been produced in Chinese hamster ovary (CHO) cell lines [41,42]; and in the milk of transgenic mice [43] and transgenic rabbits [44]. In the latter two cases, transgenic animals were engineered to secrete rhGAA from their mammary glands. After collecting milk from these animals, the protein was separated and purified. Kikuchi *et al.* reported transfer of enzyme activity and clearance of glycogen in Japanese quail after intravenous administration of CHO-derived material [42]. Similar results were observed in knockout mice using rhGAA derived from transgenic mice [45] and rabbits [44]. Promising results from these initial studies are the bases for ongoing, early-stage clinical trials [46]. Recent reports from human trials using recombinant protein replacement therapy show some promise [47-50].

The first trial, conducted at Sophia Children's Hospital in Rotterdam, Netherlands, included 4 infantile-onset subjects, all of whom demonstrated significant cardiac hypertrophy before 6 mo of age [47-49]. Three reports regarding these subjects have emerged — two from the 36-wk timepoint and one from the 72-wk timepoint. Two

subjects were enrolled very early after birth (2.5 and 3 mo, respectively) and 2 subjects were initiated at 7 to 8 mo of age. Twelve weekly intravenous doses of either 15 or 20 mg/kg rhGAA (depending on weight criteria) were administered; muscle biopsies were performed to assess the extent of glycogen clearance and transfer of enzymatic activity. After determining that all 4 subjects' enzymatic activities had increased substantially but not to normal levels, all subjects were increased to 40 mg/kg rhGAA per wk. In summary, all 4 subjects had significant decreases of left-ventricular mass indices at 36 wk [47,48]. After 72 wk, 1 patient had nearly complete reversal of all skeletal muscle symptoms and reached significant developmental milestones; while the other 3 subjects had significant clearance of glycogen (as assessed by periodic acid-Schiff base (PAS) staining) but persistent severe vacuolization and myofibrillar destruction [49].

The second trial was designed to test CHO-derived rhGAA, and was a Phase I/II, open-label, single-dose (5 mg/kg) study with 3 infantile-onset subjects [50]. All 3 subjects were less than 5 mo old at the initiation of twice-weekly intravenous administrations, and the primary endpoint was established as 1-yr survival with absence of cardiomyopathy. In that study, presence of neutralizing antibodies was also assessed, in addition to measures of left-ventricular mass and motor development. After approximately 60 wk of therapy, left-ventricular masses for all 3 subjects were reportedly decreased, with the most significant decrease observed in the subject who had the most pronounced hypertrophy at study initiation. None of the 3 subjects had restoration of enzymatic activity to normal levels, although 1 infant had activities roughly 8% of normal. Interestingly, this subject also had glycogen clearance from skeletal muscle as well as normal AIMS scores for motor development. Further investigation revealed that

this infant was also the only CRIM-positive subject and the only one not to develop neutralizing antibodies to rhGAA.

Genzyme Corporation initiated two more clinical trials in the United States [51]: one for subjects less than 6 mo of age (Phase II) and another for subjects between 6 and 36 mo old (Phase I/II). Both of these trials use rhGAA produced from a new CHO cell line using new purification methods, and both are either underway or currently enrolling patients. While no data are available from this trial yet, the material used in these patients has been tested in 2 strains of mice — *Gaa*^{-/-} and the liver-targeted transgenic described above. Not surprisingly, immunocompetent, hGAA-naïve *Gaa*^{-/-} mice developed a fulminant immune response to intravenously delivered rhGAA [52]; none of these mice survived beyond the seventh weekly dosing. The remaining studies were performed in liver-specific transgenic mice that express hGAA at low levels. Mice were treated weekly with either 20 or 100 mg/kg. The age at initiation varied from 1.5 mo to 6 mo; and the duration of treatment varied from 1 mo to 5 mo. The summary findings of the study are as follows: 1) differential uptake of rhGAA was observed in various muscle tissues in the following order: heart > diaphragm > other skeletal muscles; 2) higher doses of rhGAA led to more thorough clearance of glycogen and restoration of enzymatic activity; and 3) some relationship may exist between muscle fiber type and mannose 6-phosphate receptor density as assessed by histological methods. Paradoxically, Raben *et al.* observed that mice treated at 3.5 mo of age responded better than 1.5-mo-old treated mice, as assessed by enzyme activity, glycogen content, and locomotor activity.

As might be expected in tolerant mice, the highest dose of rhGAA had the most significant effect on restoration of enzymatic activity and glycogen clearance.

Interestingly, delivery of rhGAA to these mice was initiated at 6 mo, the oldest cohort in these studies. Despite efficacious transfer of enzymatic activity and clearance of glycogen, Raben *et al.* observed persistence of autophagosomes in skeletal muscle. These results are remarkably similar to the findings from the Dutch infantile enzyme replacement trial [49] (in which initiation of treatment in older patients led to less significant correction) and warrant further investigation.

Gene Therapy for GSDII

Initial Gene Therapy Studies for GSDII

The pursuit of viral and non-viral gene therapies for GSDII began in earnest after the cloning and characterization of the human *GAA* gene [39,40,53]. Gene replacement strategies offer the potential for long-term expression of a therapeutic protein after a single administration of vector, and early studies using viral vectors as a delivery system for *GAA* yielded promising results. Zaretsky *et al.* [54] showed effective transduction of *GAA*-deficient myoblasts with a recombinant retrovirus vector. Our group and others [55-57] constructed recombinant E1-deleted adenoviral vectors carrying the human *GAA* cDNA (rAd-*hGAA*) [58] and demonstrated their ability to direct expression of *GAA* both *in vitro* (in deficient fibroblasts); and *in vivo* after a single intramuscular or intramyocardial injection. Further studies showed that deficient fibroblasts (after transduction with rAd-*hGAA in vitro*) could serve as producer cells of recombinant *GAA*; that the recombinant protein could be secreted and recaptured by untransduced acceptor cells; and that the M6P receptor mediated the recapture process [58]. When a similar virus carrying the mouse *Gaa* cDNA (rAd-*mGaa*) was administered intravenously to *Gaa*^{-/-} mice [28], secretion of the enzyme was demonstrated *in vivo*, (with increased enzyme activity in both cardiac and skeletal muscle) [58]. These results showed that

viral vectors can direct the synthesis of recombinant GAA in deficient cells. The early onset and robust expression from recombinant adenovirus vectors established important proof of concept; however, adenovirus-mediated gene delivery elicited host immune responses in immunocompetent subjects (leading to transient expression of the transgene *in vivo*) [59].

Non-viral gene delivery systems have been used to deliver a host of genes *in vitro* and *in vivo*, including human GAA. Martinuik and colleagues are the primary proponents of this strategy, and reported the successful use of a “gene gun” approach to deliver plasmid DNA carrying the human GAA cDNA [60]. The results from that study were somewhat promising; however, repeated dosing was required in *Gaa*^{-/-} mice. The need for repeated dosing is indicative of transient expression of the transgene, a common problem among non-viral gene delivery methods and strategies.

Concerns about recombinant adenovirus safety and persistence and the transient nature of non-viral gene therapies have accelerated the search for alternative viral vectors. Adeno-associated virus (AAV) has emerged as an attractive alternative to adenovirus as a potential gene therapy vector, mainly because of its unique ability to integrate in a site-specific manner [61,62] and to persist long term in infected cells [63-66]. However, it has been suggested that recombinant AAV, unlike wild-type AAV, does not target integration to a specific location [67-69].

Adeno-Associated Virus

Early studies regarding the life cycle of adeno-associated virus (AAV) and its potential as a gene therapy vector were conducted by Berns and Muzyczka, and were reviewed by Muzyczka [70]). AAV is a member of the *Dependovirus* family and therefore requires the presence of a helper virus in order to initiate a productive viral

infection. In the absence of helper virus, wild-type AAV is characterized by its ability to stably integrate into terminally differentiated host cells. Kotin *et al.* [71] demonstrated that the integration of the wild-type virus occurs in a site-specific manner into human chromosome 19 q13.3-qter; the human target sequence for AAV integration (AAVSI) was later cloned and sequenced. The virus has a broad tropism for mammalian tissues. The most carefully described serotype (AAV2) uses the heparan sulfate proteoglycan and human fibroblast growth factor receptor 1 as its primary co-receptors for attachment and entry into host cells [72,73]. AAV has not been associated with any known human disease and does not elicit a fulminant immune response.

The AAV2 genome at once suggests its potential as a gene transfer vector. The two, 145-nucleotide inverted terminal repeats (ITRs), located at the viral termini, are the only *cis*-acting elements necessary for viral replication and latent integration. The wild-type virus carries the genes for 3 structural proteins (VP-1, -2, and -3) that comprise the viral capsid as well as for 4 nonstructural Rep proteins that are involved in viral replication, transcription, and integration. These genes may be deleted from the viral genome and replaced with therapeutic genes in order to produce recombinant virus. Production of recombinant virus requires delivery of the wild-type AAV and helper virus genes *in trans* [74].

AAV serotype 2 vectors

Recombinant AAV serotype 2 vectors have been under investigation for a number of years [70]) and as a group constitute the most characterized parvovirus-based vector system. Neither recombinant nor wild-type AAV2 cause any apparent pathologic effect on their hosts, and they do not seem to elicit a strong host immune response. Long-term expression *in vivo* has been reported in a variety of organs and tissues including the brain

and spinal cord [75-77], airway epithelium and lungs [78-80], kidneys [81,82], liver [83-85], intestines [86], and a host of muscle tissues (described in detail below). Recent advances in our laboratory and others at the University of Florida Powell Gene Therapy Center have made scalable production of rAAV2 vectors feasible [87-89].

Other serotype vectors and differential tissue tropism

Six serotypes of adeno-associated virus were originally identified (designated AAV1-6) [90-94], and two more were recently described [95]. Additionally, a report from Gao *et al.* [96] indicates the potential for extensive variation and mutation of the capsid region of the AAV genome within primate tissues. Of the original 6 serotypes, AAV6 closely resembles AAV1 in genotype and structure, and may not be functionally distinct. While most data with rAAV as a gene transfer vector has been gathered using AAV2-based vectors, recent studies showed increased transduction, particularly of skeletal muscle, using serotypes 1 [97,98] and 5 [99]. As preferential tropism of these varying serotypes becomes more finely characterized, advances in production of recombinant vectors will become increasingly critical. Efforts are underway at the University of Florida Powell Gene Therapy Center and other institutions to achieve scalable production of various serotypes of rAAV [100-103].

Skeletal Muscle-Directed Gene Therapy with Recombinant AAV

Early demonstrations of the successful use of rAAV2 as a gene therapy vector in muscle tissue were performed in our laboratory [64] and are the basis for a U.S. patent (U.S. Patent Number 5,858,351). Figure 1-1 is an example of rAAV2-mediated transduction of skeletal muscle; in this case the vector carried the gene for β -galactosidase (β gal). Xiao *et al.* [65] also demonstrated long-term transgene expression

in muscle from rAAV2 vectors, perhaps mediated by integration of the recombinant proviral genome into host cell chromosomes, although episomal persistence of rAAV2 vectors has been demonstrated in animals that do not have sequences similar to the human integration site [99]. Efficient transduction of skeletal muscle with rAAV2 vectors has been demonstrated previously with reporter [104] and secretable therapeutic genes, including erythropoietin [105]; VEGF [106]; factor IX [107]; and alpha-1-antitrypsin [108]. Pruchnic *et al.* showed preferential rAAV2 transduction of slow twitch skeletal muscle fibers [109], presumably due to a higher concentration on the surface of those fibers of the heparin sulfate proteoglycan (the primary receptor for AAV2) [110].

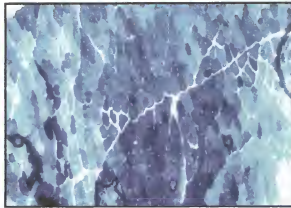


Figure 1-1. β -galactosidase staining of mouse tibialis anterior (skeletal muscle) transduced by rAAV2-CMV- β gal.

More recently, recombinant AAV vectors based on other serotypes have demonstrated greater transduction efficiencies in skeletal muscle [97,98,111]. In particular, nearly one log greater expression of a variety of transgenes has been shown when they are packaged in rAAV1 capsids compared to rAAV2. Similar findings were reported with rAAV6, although this serotype has not been as widely used. Evidence from the literature suggests that rAAV5 vectors may also lead to higher expression levels in skeletal muscle [112], though not to the levels achievable with rAAV1. Finally, a recent

report describing serotypes 7 and 8, isolated from non-human primates, provided data suggesting these two serotypes may be able to mediate transduction of skeletal muscle at levels between rAAV5 and rAAV1 [95].

These newer, alternative serotype vectors are far less characterized than rAAV2. For instance, among the 4 newer rAAV serotypes with skeletal muscle tropism (rAAV1, 5, 7, and 8, respectively), AAV5 is the only one for which the cellular receptors are known. Hauck and Xiao recently characterized the muscle-tropic elements of the AAV1 capsid using a domain-swapping scheme [113]. Despite this, the specific receptor or receptors that recognize or bind these muscle-tropic domains remain unknown.

Muscular dystrophies and other muscle-based gene therapies

While structural proteins are significantly more difficult to replace than soluble proteins, the efficiency of skeletal muscle transduction with rAAV vectors has made the treatment of a host of previously inaccessible musculoskeletal disorders feasible. Soon after rAAV2 vectors were demonstrated to be potent in skeletal muscle tissues, several groups began applying this vector system to a variety of different muscular dystrophies. Becker and Duchenne muscular dystrophies are caused by mutations in the dystrophin gene – the largest gene in the human genome. Because of its large size, the full-length cDNA cannot be packaged into rAAV, but mini- and micro-dystrophin constructs are under development and are being tested in the *mdx* mouse, a model of dystrophin-deficient X-linked muscular dystrophy [114-117]. Successful gene transfer using rAAV vectors for limb-girdle muscular dystrophy (LGMD) has also been reported for α -, β -, γ -, and δ -sarcoglycan genes in animal models. Two reports indicate the successful use of rAAV encoding the human δ -sarcoglycan gene in the BIO14.6 hamster [118,119], and two more indicate similar success in the TO-2 hamster, another genetic model of

cardiomyopathy with δ -sarcoglycan deficiency [120,121]. Significant improvement was also observed in a mouse model of δ -sarcoglycan deficiency [122]. Cordier *et al.* reported rescue of a γ -sarcoglycan-deficient mouse, again using the human cDNA [123]. More recently, Dressman *et al.* described the use of rAAV to deliver the human α - and β -sarcoglycan genes in knockout mice deficient in those two genes, respectively [124]. In some of these cases, robust over-expression was associated with a strong immune response and short-term transgene expression, but the mechanism by which the immune response was elicited is not known. Possible explanations for the immune response and/or cytotoxicity include the accumulation of immunoreactive protein aggregates or abnormal signaling resulting from inappropriate binding to cellular factors or cytoskeletal elements.

Molecular fate and persistence of rAAV2 genomes in muscle

Rep-deleted viral vector genomes have not been shown to integrate site-specifically, in contrast to their wild-type counterparts. Instead, persistence is often mediated by the formation of episomal forms, or in some cases, random-site integrants [125,126]. Persistence in muscle in particular is accomplished by formation of circular, concatemeric intermediates [99], the majority of which are found to be in a head-to-tail orientation. These episomal genome forms are fully functional templates for active transcription and mediate long-term gene expression. Song *et al.* [127] later established a role for DNA-dependent protein kinase (DNA-PK) in the conversion from linear genome concatemers to circular episomes.

Myocardium-Directed Gene Therapy with Recombinant AAV

While a number of reports describe the use of rAAV vectors in skeletal muscle to address clinically relevant problems, few studies have been published with regards to the

use of these vectors in the heart. Kaplitt *et al.* [128] were among the first to report transduction of the porcine heart with rAAV vectors, but the efficiency of the infection was quite low. Maeda *et al.* [129,130] were more successful *in vitro* in cultured cardiomyocytes. Svensson *et al.* [131], in a proof of principle study, demonstrated successful expression of a reporter gene after cardiac delivery, using both direct injection into the myocardium and intracoronary perfusion. Recently, direct delivery of rAAV encoding recombinant vascular endothelial growth factor (rVEGF) has been used to induce neovascularization in an ischemic mouse model [106]. Likewise, Kawada *et al.* have demonstrated restoration of cardiac function in dystrophic TO-2 hamsters [120] after direct intramural delivery of rAAV expressing δ -sarcoglycan.

Gene transfer to the myocardium has historically been challenging for a variety of reasons, including a lack of effective gene delivery methods. These difficulties have arisen in part because of the size of the rodent models typically used in proof-of-principle or genetic model studies. Mice in particular present unique challenges caused by their extremely rapid heart rates as well as the small cannulae and injectate volumes that are necessary for intravascular delivery. Since the efficiency of viral vector delivery is directly related to capsid binding to host cell receptors, dwell time in a particular capillary bed greatly affects transduction efficiency. In the case of mice, coronary flow may be too rapid for viral vectors to efficiently transverse the capillary endothelium into myocardial tissue. Direct injection of myocardial tissue may ameliorate some of these problems, but may present new limitations, particularly with regards to the distribution of vector within the heart wall.

Recent reports indicate that some of these obstacles may be overcome using mechanical, physiologic, and/or pharmacologic interventions. Logeart and colleagues [132] recently reviewed the relevant literature with regards to gene delivery in rodents and tested several permutations of mechanical and pharmacological enhancements. Likewise, the number of improvements in delivery and efficacy has dramatically increased in the past three years [120,121,133-139]. Several groups have employed methods that involve clamping the aortic root; others have cooled the subject to roughly 20°C; and still others have employed a combination of the two, with pharmacologic agents added to the mix. All of the reports cite higher levels and longer duration of transduction with recombinant adeno-associated virus vectors over adenovirus, and almost all have used some combination of hemodynamic and pharmacologic intervention.

rAAV-Mediated Gene Therapies for Lysosomal Storage Disorders

Recombinant AAV vectors have been used to address a variety of lysosomal storage diseases [140-146] including MPSI, MPSVII, and Fabry disease. The routes of administration and doses of these studies have varied greatly (particularly as production of vectors has improved) but promising results have been reported, particularly after intrahepatic or intramuscular delivery for Fabry disease [144,146].

Phenotyping Murine Models of Skeletal and Cardiomyopathies

The advent of murine knockout and transgenic techniques has given rise to a proliferation of mouse models of abnormal cardiovascular and musculoskeletal physiology. Many of these engineered mice are designed to mimic human genetic diseases. In those cases, useful mouse models of human disease are characterized by a measurable, distinct phenotype and their similarity to human pathophysiology. As a result, much emphasis has been placed in recent years on phenotypic analysis of various

mouse muscle groups. The goals of many of these techniques are to 1) accurately describe of the actual physiologic state of the animal in question and 2) to provide a rationale for comparison to human subjects. Desirable methods of phenotypic analysis should provide sensitivity, to detect small changes or differences in function, and scalability, in order to correlate measured function from the mouse to known human parameters.

Skeletal Muscle Phenotyping

Isometric force mechanics

Physiologists observed as early as the 17th century that muscles contract in response to stimulus from a nerve. As technology, instrumentation, and data recording methods became more sophisticated, it has become possible to attempt more precise studies of muscle physiology. One early observation was the relationship between force generation in muscle tissues in response to electrical stimulus. The concept of muscle fiber recruitment was introduced, which states that the number of active muscle fibers increases in response to the frequency of the external stimulus. In the case of isometric muscle contraction, this relationship is known as the force-frequency relationship, or FFR. Increases in stimulation frequency lead to concomitant increases in force up to a critical frequency, called the tetanic frequency, after which no further increases in force can occur [147]. The intrinsic tetanic contractile force of the muscle is determined by the contraction speed of the muscle. Using various *in vitro* systems, it is possible to determine the intrinsic contractile characteristics of a muscle by measuring its FFR. If collected properly, these data can also provide information with regards to the contractile speed of a muscle, also known as time to peak tetanus (TPT). Likewise, the rate of relaxation of the muscle can also be measured ($\frac{1}{2}$ RT) [148]. These indices give an

indication of the calcium-handling capacity of the muscle, another physiologic index of muscle function.

Histopathology

Other useful methods for phenotyping murine skeletal muscle include a variety of histopathological techniques. Cryostat sections of frozen tissues are the most commonly stained specimens, and an array of stains and methods can be employed to detect specific elements of skeletal muscle structure or physiological status. Tissue morphology can be assessed using toluidine blue, hematoxylin and eosin, Masson's trichrome, or immunostaining with specific antibodies against any number of subcellular organelles. Fiber typing can be performed using either a pH-based staining method or a specific set of antibodies developed by Schiaffino [149] and others, and distributed by several suppliers. Storage diseases, such as GSDII, are detected with periodic acid/Schiff base (PAS; stains carbohydrates), Alcian blue (mucopolysaccharides), and Sudan black B and Oil red O (lipids). A number of enzymatic assays can also be performed, indicating the subcellular localization and biochemical status of the mitochondria, lysosomes, and endoplasmic reticulum.

Cardiac Phenotyping

Electrophysiology (EP) and electrocardiogram (ECG)

Clinical electrocardiography has been used to diagnose and describe myocardial disease since the early 20th century. The use of bioelectrical signals in mice has been used more frequently in the context of the central nervous system (electroencephalography), however, early studies using electrocardiograms (ECG) from mice were performed as early as 1968 [150]. With the development of faster microprocessors and digital data collection, sampling rates are now available in a

frequency range that exceeds the normal heart rate of the mouse. Likewise, more careful investigations of appropriate anesthetic cocktails and regimes now enable the preservation of contractility and heart rate in anesthetized mice [151,152].

Perhaps the most important advances in recent years have been the development of more sensitive data acquisition methods and more effective software tools for analyzing data. Chu *et al.*[153] have developed a system for measurement of ECG in conscious mice and have coupled this system with software that can detect small changes in intervals and heart rate variability. Berul *et al.* [154,155] have made significant contributions to instrumentation with the development of an octopolar, intracardiac ECG recording catheter. They have also developed a sophisticated electrophysiologic (EP) protocol for mice that enables very sensitive localization and analysis of conductance phenotypes within the intact, *in situ* mouse heart.

Echocardiography and magnetic resonance imaging (MRI)

As with electrocardiography, the use of echocardiography has expanded with improvements in technology and data acquisition. The first description of its use with mice was reported as recently as 1993; however, in the intervening years improvements in equipment, particular smaller and higher frequency probes, have led to a large number of manuscripts describing the use of echocardiograms (hereafter “echos”) to assess a variety of murine cardiac parameters, including fractional shortening, ventricular septal thickness, left-ventricular (LV) internal dimension, LV posterior wall thickness, and derived LV mass [156]. As in humans, the same instrumentation has also been expanded to study rodent vascular function (i.e., flow), although this application has not been the focus of our interest.

Hemodynamics and contractility

Kiichi Sagawa and colleagues first used ventricular pressure-volume relationships as a window into myocardial function in the late 1960s and early 1970s [157]. The definitive text in this area of research was published in 1988 [158]. Ventricular volumes and pressures are recorded simultaneously using a catheter that contains a set of conductance electrodes and a wheatstone bridge-based micromanometer. With this data in hand, one can plot the left-ventricular (LV) pressure (ordinate) against volume (abscissa), as seen in Figure 1-2, which is taken from an isolated canine heart preparation. The curve has 4 distinct phases, which correspond to the phases of the cardiac cycle. Phase 1 is called isovolumic contraction, during which the LV generates substantial increases in pressure. At the end of Phase 1, the ventricular pressure (LVP) finally exceeds the aortic pressure (AoP), leading to the opening of the aortic valve and ejection from the ventricle. Phase 2 corresponds to LV ejection, which is commonly called systole. When the LV has ejected most of its volume, the pressure in the ventricle begins to fall, and the aortic valve closes. In order to fill again, the heart must relax and return to its resting state; Phase 3 corresponds to isovolumic relaxation. When the heart has completely relaxed, the pressure in the ventricle drops below the pressure in the left atrium (LAP), and the mitral valve opens, filling the ventricle with blood. Filling is referred to as diastole, and is represented by Phase 4 in the figure above. Thus, by traversing the pressure-volume curve counterclockwise, the heart completes a single cardiac cycle. Stroke volume (SV) is the ejected volume during a single cardiac cycle; in Figure 1-2 $SV \approx 12$ units ($40 - 28$), and stroke work (SW) is the area bounded by the pressure-volume curve. SW represents the total energy transferred to the blood during contraction of the ventricle.

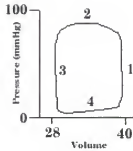


Figure 1-2. Left-ventricular pressure-volume curve

Manipulations of the load experienced by the ventricle lead to changes in the pressure-volume curve and provide insights into the inotropic (contractile) state of the heart. Changes in loading conditions (preload and afterload) will very clearly change the position of the end-systolic pressure-volume points; however, the locations of these points are constrained under constant contractile states. In other words, varying the return of blood to the heart, for example, will change the end-systolic pressure and volume, but for a given heart in a constant contractile state, the pressures and volumes are predetermined. The relationship between end-systolic pressures and volumes in a single heart under varying load conditions can be plotted as a single line, called the end-systolic pressure-volume relationship (ESPVR). The slope of this line varies with changes in the contractility of the heart, and is therefore referred to as the end-systolic elastance (E_{es}).

Until recently, the techniques and many of the principles outlined above were unavailable and infeasible in small rodents. In 1998, Georgakopoulos *et al.* [151] published the first report using a pressure-conductance catheter in mice and demonstrated striking fidelity in cardiac mechanics between mice and various other species, including humans. Since 1998, several advances have been made in catheter design and data analysis techniques [159-161], and an acceleration of publications using pressure-volume

relationships in mice has been observed. Of particular interest have been a few papers describing the contractile dysfunction of popular knockout mouse models of familial hypertrophic cardiomyopathy [162-164]. These reports have provided insight into which indices may provide some discernable phenotype in myopathic mouse hearts. In particular, Georgakopoulos *et al.* [165] have shown profound differences in the end-systolic pressure-volume relationship (ESPVR) in a mouse model of familial hypertrophic cardiomyopathy.

Summary

Glycogen storage disease type II (GSDII) is a cardioskeletal myopathy for which a genetic model has been created; recombinant enzyme replacement therapy has been developed; and gene therapy vectors are being tested. Recombinant viral vectors are promising tools to address this problem, and adeno-associated virus vectors have emerged as real candidates for GSDII and a host of other muscle disorders.

The application of gene therapeutics to genetic diseases will require extensive testing in animal models. While larger animal models can determine the toxicity of therapeutic modalities, genetically engineered mice are currently the gold standard for assessing phenotypic correction. Development of phenotypic methods has been rapid and dramatic, and assays for cardiac and skeletal muscles will continue to become more and more sensitive and specific.

CHAPTER 2

PHENOTYPIC CHARACTERIZATION OF A MURINE MODEL OF GLYCOGEN STORAGE DISEASE TYPE II, POMPE DISEASE

With the advent of transgenic technology, genetically engineered mice have become the system of choice for modeling the phenotypic progression of human diseases. Since the primary genetic defect in glycogen storage disorder type II (GSDII) results in absent or diminished biochemical activity of GAA, it is important to first demonstrate that the enzyme activity is indeed lacking in the knockout mouse strain, *Gaa*^{-/-}. A survey of GAA activities in various tissue beds was performed as part of the initial characterization of the mouse model. Aberrant accumulation of glycogen is another important facet of the disease. Histological staining for glycogen reveals dramatic increases of glycogen content in histological sections from knockout mice. Likewise, immunohistochemistry provides another method for detection of GAA in normal controls or successfully treated knockouts. Thus, biochemical activity and histological staining provide two methods of assessment for disease severity and progression in the knockout strain.

Measurement of skeletal muscle contractility in *Gaa*^{-/-} mice provides a third and more quantitative understanding of the phenotype of this knockout strain, as well as an index for functional improvement following a biochemical, pharmacological, or genetic intervention. The physiologic studies that we have undertaken offer precise quantitative assessment of mechanical force related to stimulation frequency in the skeletal muscles. In concert with biochemical and histological assessments of knockout and treated mice,

these measures provide an insight into the true functional, clinical effect of proposed therapies and treatment modalities.

Finally, hemodynamic assessment of *Gaa*^{-/-} mice provides yet another critical method with which one can assess the utility of these animals as models of Pompe disease as opposed to other forms of GSDII without cardiac involvement. The presence or absence of certain phenotypic traits, in concert with complete absence of enzymatic activity, may provide insights into either critical differences between human and mouse physiology or point to genetic and physiologic modifiers that may affect the course and progression of both human and murine GSDII.

In order to assess the efficacy of any therapeutic strategy in our knockout mouse model, it was first essential to establish the characteristic phenotype of our strain. All animal procedures described in this study were performed under the guidelines and oversight of the University of Florida Institutional Animal Care and Use Committee (IACUC). Likewise, it should be noted that all recombinant viral and other genetic materials were registered and used in accordance with regulations of the Biosafety Division of the University of Florida Environmental Health and Safety Office.

As was mentioned in Chapter 1, *Gaa*^{-/-} mice were originally developed and characterized by Raben and colleagues at the National Institutes of Health. Some of our characterization work recapitulated their efforts, particularly with regards to the enzyme activity measures. However, it was essential for our laboratory to duplicate their efforts in order to ensure that we would be able to perform these experiments in subsequent treated cohorts. Table 2-1 provides a summary of our combined findings with regards to enzyme activities in various tissues. For most of our studies, the tissues for investigation

included samples from heart, liver, and skeletal muscle from positive control (129X1 x C57BL/6 hybrid) and *Gaa*^{-/-} mice. Enzymatic assays were performed on tissue homogenates to determine the aggregate GAA activities of mice from these strains. Histochemical staining was also performed in order to provide a measure of glycogen content in respective tissues.

Table 2-1. Acid α -glucosidase activities in tissue samples from Gaa knockout (*Gaa*^{-/-}) and wild-type control mice.

	<i>Gaa</i> ^{-/-}	Wild-type
Heart	2.55 \pm 0.30	33.91 \pm 1.06
Liver	17.7 \pm 1.52	187.14 \pm 24.82
Skeletal muscle	3.27 \pm 0.15	39.74 \pm 0.58
Brain	0.62 \pm 0.04	57.0 \pm 4.5

Our data did not always exactly recapitulate the findings of Raben *et al.* (1998), in terms of raw numbers. In those cases, our results are listed in Table 2-1. Despite slight differences in raw numbers, however, we found the same dramatic differences in enzyme activity levels between wild-type and controls as reported in their work.

Methods and Materials

Enzymatic Activity Assays for Acid α -Glucosidase

Active GAA cleaves α -1,4 and α -1,6 linkages of carbohydrate chains. 4-methylumbelliferyl α -D-glucoside (4-MUG) is a chemical substrate for GAA cleavage that, when cleaved, yields a fluorescent product, 4-methylumbelliferone (4-MU). Cultured cells and excised tissues are can both be assayed for GAA activity using this substrate and reporter system. Cell lysates or excised tissues are thoroughly homogenized in 100 μ L sterile water, then centrifuged for 2 min at 5000 rpm, in order to separate crude cell debris. The supernatant is then assayed for GAA activity. Twenty μ L of each sample lysate is added to one well of a 96-well plate suitable for fluorescent light detection.

The substrate for the reaction is 2.2 mM 4-MUG. A stock solution of 75 mM 4-MUG is prepared by adding 988 μ L dimethyl sulfoxide (DMSO) to a bulk container of 25 mg 4-MUG (Sigma-Aldrich, St. Louis, MO). For a single well, 1.6 μ L 75 mM 4-MUG is diluted in 38.4 μ L 200 mM sodium acetate (pH 3.6), yielding a total substrate mix of 40 μ L per well. Sodium acetate is necessary not only to dilute the 4-MUG but more importantly to provide the acidic environment necessary for GAA activity. After mixing the diluted sample and substrate, the 96-well plate is wrapped in Parafilm and incubated at 37°C for 1 h. Standards of 4-MU (Sigma-Aldrich, St. Louis, MO) are also prepared. A stock of 1 mM 4-MU is prepared by adding 9.9 mg 4-MU to 50 mL sterile water. Subsequent standards are made from dilutions of this stock 4-MU. A typical dilution series yields standards that are 6.25, 12.5, 25, 50, and 100 μ M 4-MU, respectively. The GAA reaction is stopped after one hour of incubation with 200 μ L 0.5 M sodium carbonate (pH 10.7), which not only abolishes the acidic environment necessary for GAA activity, but also provides the alkaline environment required for 4-MU to fluoresce. Twenty μ L of each of the dilution series of 4-MU standards are then added to individual wells of the dish, along with 40 μ L sodium acetate and 200 μ L sodium carbonate. The plate is then read in a fluorimeter with a filter set that generates 360 nm excitation and 460 nm emission detection wavelengths. During the course of this study, two different fluorimeters have been used, the latter of which is a FLx800 microplate fluorescence reader (Bio-Tek Instruments, Winooski, VT). Using the standards included in this protocol, it is possible to calculate a standard curve (linear regression line) with 4-MU as the abscissa and relative fluorescence units (RFU) as the ordinate. All linear regressions for this study were generated using Microsoft Excel

(Microsoft, Redmond, WA). The data collected are then reported as nmol 4-MU/h, since the experimental protocol is designed to measure the amount of 4-MU that is liberated after one hour of incubation. However, this assay as described does not account for variations in the homogenization process and therefore protein content of the assay samples. Therefore, a protein assay must also be performed in order to normalize the reported activities to the amount of input total protein.

Two different protein assays have been used during the course of this study. Both have been based on Bio-Rad protein assay kits (Bio-Rad, Hercules, CA), and both assays are based on the Bradford dye-binding procedure. The assays use the binding properties of Coomassie Brilliant Blue G-250 dye and the assays result in increasingly intense blue coloration of solutions with increasing amounts of total protein. The latter kit (which produces much more consistent and linear results) is the Bio-Rad *DC* Protein Assay Kit. Microtiter plates are prepared with duplicates of diluted samples from homogenized tissues or cells. Standards are also prepared from a stock of bovine serum albumin (BSA) of known concentration. Originally, samples were prepared in 50 μ L total volume per well; with the *DC* Protein Assay Kit only 5 μ L were required. Standards are prepared at concentrations ranging from 0 to 5 μ g of BSA, also in 50 μ L. To each sample or standard well, 150 μ L of Bio-Rad reagent are added, for a total volume of 200 μ L. The reaction proceeds for 5 min, after which the entire microtiter plate is read at either 620 nm wavelength (previously) or 750 nm (*DC* Protein Assay Kit). Using the results from the two assays, one can then express the GAA activities of samples as nmol 4-MU released/h/mg total protein; for the purposes of these studies, this will be abbreviated as nmol/h/mg.

Histochemical Staining

Periodic acid-Schiff base (PAS) staining of tissue sections selectively stains glycogen with a pinkish tone. More intense staining is indicative of higher glycogen content; tissues in which glycogen is absent do not stain at all. Tissues for PAS staining were stored in 10% formalin and delivered to the Diagnostic Referral Laboratory (DRL) of the University of Florida for paraffin embedding, sectioning, and staining.

In Vitro Force-Frequency Measurements

A picture of the *in vitro* contractile assessment system is shown in Figure 2-1. *In vitro* contractile measurements were performed in collaboration with R. Andrew Shanely, Ph.D., and Scott K. Powers, Ed.D., Ph.D. as described previously [148,166]. Briefly, the mouse is anesthetized with a sub-lethal dose of sodium pentobarbital. After reaching a surgical plane of anesthesia, the diaphragm and/or soleus muscles are surgically excised and placed in a dissecting chamber containing Krebs-Henseleit solution equilibrated with a 95% O₂/ 5% CO₂ gas mixture. For contractile measurements, a diaphragm muscle strip, including the tendinous attachments at the central tendon and rib cage are dissected from the right ventral costal region. This diaphragm strip and the left (or right) soleus muscle are then independently suspended vertically between two lightweight plexiglass clamps connected to force transducers (Grass Instruments, Model FT03) in two separate jacketed tissue baths. Transducer output is amplified and differentiated by operational amplifiers and undergoes A/D conversion for analysis using a computer-based data acquisition system (Polyview, Grass Instruments). Each of the dual-jacketed tissue baths contain Krebs-Henseleit solution equilibrated with a 95% O₂/ 5% CO₂ gas (bath ~37 ± 0.5°C, pH ~ 7.4 ± 0.05, osmolality ~ 290 mOsm).

In vitro contractile measurements begin with determination of the muscle's optimal length (L_0) for isometric tetanic tension development. The muscle field is stimulated (modified Grass Instruments S48) along the entire length of the muscle strip with platinum electrodes (120 V). Muscle length is progressively increased until maximal isometric twitch tension is obtained. Once the highest twitch force is achieved, all contractile properties are measured isometrically at L_0 . Maximal twitch tension is determined from a series of single twitches and the following isometric characteristics can be determined: time to peak tension (TPT), half-relaxation time ($\frac{1}{2}RT$), and maximum rate of tension development ($+dP/dt$). The force-frequency relationship is examined using previously described methods. At the end of each study, the muscle strip length is measured, and the tissue is carefully dissected, blotted dry, and weighed. The muscle cross-sectional area (CSA) is estimated using the equation $CSA \text{ (cm}^2\text{)} = [\text{muscle strip mass (g)} / \text{fiber length } L_0 \text{ (cm)} \times 1.056 \text{ (g/cm}^3\text{)}]$, where 1.056 g/cm^3 is the assumed density of muscle. The calculated CSA is used to normalize tension, expressed as N/cm^2 .

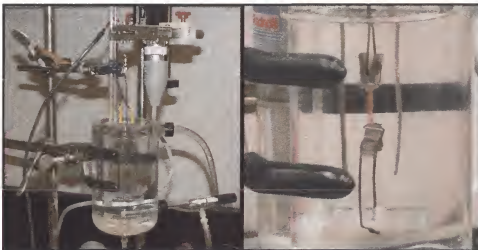


Figure 2-1. Contractile function measurement apparatus. A. Wide view of the bath, in which the entire water-jacketed bath, gas source, force transducer, and stimulating electrodes can be seen. B. Close-up view of the muscle tissue suspended between the Plexiglas clamps and the platinum electrodes.

Data Analysis

Data were collected using analog-to-digital conversion and stored directly as digital information. All data are expressed as means \pm standard error. Significance was ascertained for certain indices using student's t-test.

Results

***Gaa*^{-/-} mice lack GAA enzymatic activity, resulting in aberrant glycogen accumulation**

As demonstrated by Raben *et al.* [28] and Table 2-1 above, *Gaa*^{-/-} mice lack enzymatic activity. Glycogen accumulation begins prenatally in tissues of deficient mice, and increases with time. Positive PAS staining is observed in a variety of tissues, leading to a variety of pathologies. Qualitatively, *Gaa*^{-/-} develop severe skeletal muscle deficiencies, leading to curvature of the spine (kyphosis) and splayed hindlimbs (Figure 2-2). These findings led to the adoption of this mouse strain as a possible model of the human disorder.

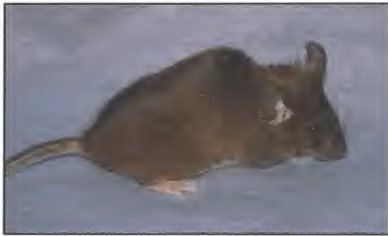


Figure 2-2. Qualitative functional phenotype of *Gaa*^{-/-} mice. Severe skeletal muscle weakness leads to an inability to support the animal's weight on the hindlimbs.

More recent characterizations in our laboratory have been marked by lower overall values for enzymatic activities but the same general relationship (Table 2-2). The reasons

for these lower values are not known, but could be explained by lot-to-lot variability in the substrate or product and the use of a new fluorometric instrument.

Table 2-2. Acid α -glucosidase activities for specific wild-type and *Gaa*^{-/-} hindlimb skeletal muscle tissues. SOL = soleus, GAST = gastrocnemius, TA = tibialis anterior, EDL = extensor digitorum longus, and QUAD = quadriceps femoris.

	SOL	GAST	TA	EDL	QUAD
Wild-type	5.23 \pm 0.45	5.91 \pm 0.73	12.21 \pm 0.72	31.06 \pm 3.66	5.53 \pm 0.21
(range)	4.69 – 6.47	5.16 – 7.58	10.5 – 14.01	22.6 – 37.35	5.04 – 6.05
<i>Gaa</i> ^{-/-}	0.39 \pm 0.07	0.43 \pm 0.19	0.26 \pm 0.06	0.64 \pm 0.11	0.06 \pm 0.03
(range)	0.16 – 0.62	0.08 – 1.17	0.24 – 0.42	0.42 – 0.94	0.03 – 0.08

We have also characterized the enzymatic activities in the heart, forelimb, and other muscles of interest (Table 2-3). These tissues also yielded lower values than we had initially observed, but were comparable to findings in later publications by Raben and her group at the National Institutes of Health.

Table 2-3. Acid α -glucosidase activities for wild-type and *Gaa*^{-/-} various cardiac, smooth, and skeletal muscle tissues. HRT = heart, DIA = diaphragm, TRI = triceps, TNG = tongue, and BLD = bladder.

	HRT	DIA	TRI	TNG	BLD
Wild-type	9.30 \pm 1.20	4.95 \pm 0.56	6.59 \pm 0.30	8.47 \pm 0.70	20.46 \pm 3.15
(range)	7.51 – 12.83	3.29 – 5.83	5.89 – 7.24	7.01 – 10.37	12.2 – 26.57
<i>Gaa</i> ^{-/-}	0.42 \pm 0.24	0.17 \pm 0.02	0.18 \pm 0.02	0.37 \pm 0.05	0.64 \pm 0.06
(range)	0.03 – 1.10	0.11 – 0.23	0.11 – 0.22	0.20 – 0.49	0.48 – 0.86

Gaa^{-/-} mice have diminished skeletal muscle contractile properties

In addition to general lethargy and wasting over time, we tested for specific decrements in skeletal muscle contractile properties. Force-frequency analysis was performed for *Gaa*^{-/-} mice over a range of ages, for both the soleus, a slow-twitch postural muscle, and the diaphragm, a mixed population of slow- and fast-twitch muscle fibers. Isometric force-frequency relationships in response to increasing stimulation frequencies are shown in Figure 2-3 for the soleus and in Figure 2-4 for diaphragm muscle strips. We observed an age-dependent decrease in force generation, a result that was expected.

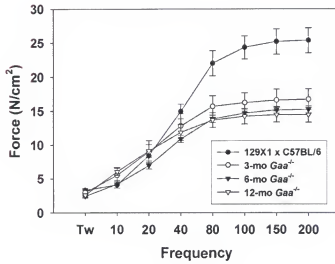


Figure 2-3. Force-frequency assessment of soleus (postural skeletal muscles) from 129X1 x C57BL/6 (wild-type control) and *Gaa*^{-/-} mice. Force measurements were recorded at each stimulation frequency and then averaged for each group. Each data point represents at least 6 soleus muscles.

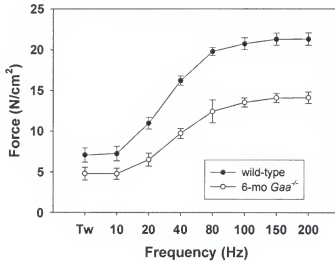


Figure 2-4. Force-frequency assessment of diaphragm muscle strips from 6-mo-old 129X1 x C57BL/6 (wild-type control) and *Gaa*^{-/-} mice. Force measurements were recorded at each stimulation frequency and then averaged for each group. Each data point represents at least 4 diaphragm strips.

Discussion

Characterization of animal models is a common requirement for genetic intervention studies. While the enzymatic defects of GSDII models are similar to their human counterparts, functional characterizations have yielded some interesting variations. The results reported here indicate that *Gaa*^{-/-} mice have some important functional deficiencies. Intracellular glycogen accumulation is a critical pathology that has been duplicated in this model. Likewise, destruction of myofibrillar networks was also observed. The precise causal pathway of myofibrillar degradation was not elucidated, but this process is not well understood in the patient population either. As a model of human disease, however, this pathology is relevant and similar to the clinical condition.

Impaired muscle function has important quality of life ramifications among juvenile and adult Pompe patients. *Gaa*^{-/-} mice have similar deficiencies in their ability to carry out normal murine activities. In particular, their mobility diminishes over time, and their postural muscle network fails to support their spinal column. Our studies also indicate that *Gaa*^{-/-} mice have difficulties standing on their hindlimbs, an important trait with regards to their ability to feed and drink in standard rodent housing. These qualitative measures indicate that *Gaa*^{-/-} mice experience similar general malaise and decreasing quality of life as the patient population.

Force assessments of isolated muscle samples confirm the observations of whole animal behavior. Our force-frequency assessments indicate that *Gaa*^{-/-} have an age-dependent decrement in their ability to contract. The specific causal pathway is unknown for these decreased measures; however, it is clear that the animal model experiences

similar decreases in muscle function to affected humans. These deficiencies may be directly caused by enlargement of the lysosomal compartment; lysosomal rupture and release of degradative enzymes; disruption of cellular metabolic pathways; programmed cell death (apoptosis) in response to altered cellular conditions; or an interplay between these and other factors and agents. Despite the multitude of candidate effectors, however, the functional ramifications are clear and quantifiable. These qualitative and quantitative findings of a real pathology in *Gaa*^{-/-} mice provide a basis for their use as a system in which to evaluate the feasibility of genetic interventions for GSDII, including genetic therapy using recombinant viral vectors.

CHAPTER 3

FUNCTIONAL CONSEQUENCES OF INTRAVENOUS RECOMBINANT ENZYME REPLACEMENT THERAPY

Intravenous delivery of recombinant enzymes has been pursued for a number of lysosomal storage diseases in order to address the primary enzymatic deficiencies that cause these diseases. As mentioned in Chapter 1, the unique biosynthetic and trafficking pathways for lysosomal enzymes provide a rationale for recombinant enzyme replacement therapy (ERT). In collaboration first with Novazyme Pharmaceuticals and later with Genzyme Corporation, we have sought to characterize the efficacy of ERT in *Gaa*^{-/-} mice. Our primary outcome measures were enzymatic activity and soleus contractile function.

Experimental Design and Rationale

To assess the bioavailability and uptake of GAA activity, we dosed *Gaa*^{-/-} mice with 60 mg/kg of recombinant human acid α -glucosidase (rhGAA) from three different preparation methods. Doses were delivered intravenously in order to mimic the delivery route for patients. Data were collected for 5-7 animals per group, with placebo-treated *Gaa*^{-/-} and wild-type control groups. This study was conducted in a blinded fashion until the collation of data at the end of all experimental procedures.

Methods and Materials

Animal Procedures and Intravenous Delivery

Preparations of recombinant human acid α -glucosidase (rhGAA) were provided by Novazyme Pharmaceuticals or Genzyme Corporation. Several different preparations

were provided over the course of two years; only one study is reported here. CHO-derived material which had a 45% binding capacity to the M6P receptor was labeled “BI”. A similar CHO-derived batch that was processed by Novazyme Pharmaceuticals was labeled “HP” and had 100% binding efficiency to the M6P receptor. A third preparation of material, labeled “GZ”, was prepared by Genzyme Corporation and had 20% binding capacity to the M6P receptor. The vehicle used for these preparations was comprised of mannitol, polysorbate 80, sodium phosphate dibasic heptahydrate, and sodium phosphate monobasic monohydrate. The protein and/or vehicle were supplied frozen in glass vials, which removed from the freezer and placed in an ice bath until thawed. The protein was administered within 2 h of thawing.

All animal procedures were performed in accordance with the guidelines of the University of Florida Institutional Animal Care and Use Committee. Mice were anesthetized *via* intraperitoneal (IP) delivery of avertin (2,2,2-tribromoethanol). Avertin is prepared as a 1.2% solution and used at a dose of 0.2 mL/10 g bodyweight. Avertin stock solution consists of 25 g 2,2,2-tribromoethanol (Sigma-Aldrich, St. Louis, MO) in 15.5 mL *tert*-amyl alcohol (2-methyl-2-butanol). The solution is mixed greater than 12 h in a dark bottle at room temperature. A working solution consisting of 0.5 mL Avertin stock in 39.5 mL 0.9% saline is mixed and filter sterilized, for a final working concentration of 20 mg/mL. It can then be stored at 4°C and used for up to 1 wk [167].

Intravenous access was provided by removal of fur from the neck area, followed by preparation with iodine. A small incision was made in the skin to provide access to the internal jugular vein, and rhGAA was injected directly into the venous bloodstream. The

incision was closed and analgesics were delivered subcutaneously. The dosing schedule was timed to match the half-life of rhGAA — mice were dosed once per wk.

Assessment of Skeletal Muscle Function

After reaching a surgical plane of anesthesia, soleus muscles were surgically excised and placed in a cooled dissecting chamber containing Krebs-Henseleit solution, equilibrated with a 95%O₂/ 5%CO₂ gas mixture. The intact muscles were then vertically suspended between two lightweight Plexiglas clamps connected to force transducers (Model FT03, Grass Instruments, West Warwick, RI) in a water-jacketed tissue bath containing Krebs-Henseleit solution equilibrated with a 95%O₂/ 5%CO₂ gas (bath ~37 ± 0.5°C, pH ~ 7.4 ± 0.05, osmolality ~ 290 mOsm). Transducer outputs were amplified and differentiated by operational amplifiers and underwent A/D conversion for analysis using a computer based data acquisition system (Polyview, Grass Instruments).

In vitro contractile measurements began with empirical determination of the muscle's optimal length (L₀) for isometric tetanic tension development. The muscle was field-stimulated using a stimulator (Model S48, Grass Instruments) along its entire length with platinum electrodes. Muscle length was progressively increased until maximal isometric twitch tension was obtained. Once the highest twitch force was achieved, all contractile properties were measured isometrically at L₀. The force-frequency relationship was examined using previously described methods [168].

Results

Expression and Enzymatic Activity in *Gaa*^{-/-} Mice After Intravenous Delivery of rhGAA

We first examined the enzymatic activity in muscles from rhGAA-treated *Gaa*^{-/-} mice. Uptake of active rhGAA was observed in the hearts, livers, and skeletal muscles of

treated mice, and in all cases uptake was more significant with delivery of the BI preparation than with the HP and GZ preparations, as shown in Figure 3-1.

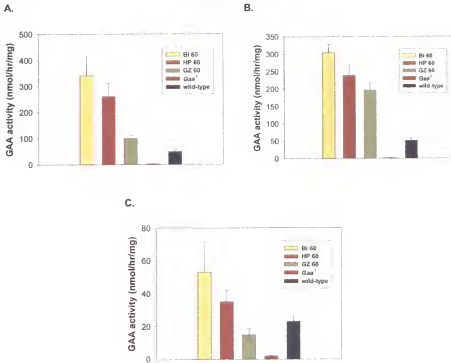


Figure 3-1. Enzymatic activities after intravenous delivery of rhGAA. Purified rhGAA (60mg/kg) was delivered intravenously once per week for 2 wk. Three different preparations were administered: BI, HP, and GZ. All of the preparations resulted in supra-normal levels of activity in the (A) heart, (B) liver, and (C) skeletal muscle.

Restoration of Skeletal Muscle Contractile Force in *Gaa*^{-/-} Mice After Intravenous Delivery of rhGAA

We tested the contractile properties of soleus muscles of treated *Gaa*^{-/-} mice using isometric force-frequency relationships as in Chapter 2. *Gaa*^{-/-} mice exhibit an age-dependent impairment of skeletal muscle function. To test the effect of restoration of GAA activity on contractile dysfunction in *Gaa*^{-/-} mice, isometric force generation was tested at the end of 2 wk of treatment (Figure 3-2). Despite restoration of high levels of enzymatic activity, we did not observe a full restoration of contractile function.

Surprisingly, there was also no measurable difference in soleus FFR among mice from

the three different treatment groups; we expected that the BI preparation would lead to improvements in function compared to the HP and (in particular) the GZ preparation. However, all of the treated mice did perform better than the untreated $Gaa^{-/-}$, indicating this dose may have some limited therapeutic benefit.

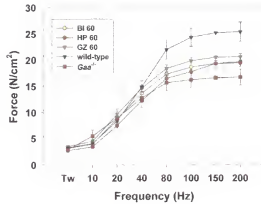


Figure 3-2. Isometric force-frequency relationships in soleus muscles of $Gaa^{-/-}$ mice after intravenous delivery of rhGAA. Note that despite high levels of enzyme activity, full restoration of contractile function remained elusive at this dose.

Discussion

Pompe disease is caused by a deficiency of GAA in all tissues, but is manifested primarily as cardiac and skeletal muscle weakness. We have long believed that restoration of enzymatic activity held the potential to reverse disease progression and lead to functional recovery. However, in treated $Gaa^{-/-}$ mice, we did not observe a return to fully normal function, suggesting that damage to the muscle (as part of the pathogenesis of GSDII) may be irreversible.

The results from our ERT study were equivocal in some sense because of the unanticipated result that the highest levels of phosphorylation and *in vitro* M6P receptor binding (HP) did not lead to the most significant transfer of activity to various tissues. Similarly, we did not expect to see such similar functional characteristics given the

seemingly broad range of activities in the heart, skeletal muscle, and liver. The causes of these results warrant further investigation, but several possibilities exist.

Highly phosphorylated rhGAA may have been preferentially bound and processed by various tissues, and as a result may have been turned over faster than the other two preparations. Since the final sacrifice and tissue processing occurred 1 wk after the last dosing, it is possible that higher levels of uptake and transfer of activity may have occurred but were not present at the sacrifice date. More careful study and exposition of the pharmacodynamics of the various rhGAA preparations would indicate whether this does actually occur. This result would also explain the confounding result that vastly different levels of enzymatic activity led to very similar restoration of muscle function. If the pharmacologic effect of early uptake of rhGAA led to significant clearance of glycogen, early turnover of the protein may still be accompanied by improvements in function — assuming that re-accumulation of glycogen and resumption of pathogenesis was slower than the beneficial effects of glycogen clearance. Future studies will investigate these possibilities more carefully.

CHAPTER 4

SKELETAL MUSCLE-DIRECTED RECOMBINANT ADENO-ASSOCIATED VIRUS MEDIATED GENE THERAPY FOR GSDII

Because of the transient expression of vector-delivered transgenes *in vivo* after recombinant adenoviral and non-viral vector delivery, we have constructed recombinant adeno-associated viral (rAAV) vectors that express human and mouse GAA (rAAV-*hGAA* and rAAV-*mGaa*, respectively). Adeno-associated virus (AAV) has gained widespread attention in recent years as a potential vector for recombinant gene transfer in humans [169]. AAV is a nonpathogenic, single-stranded DNA-containing human parvovirus that requires helper viruses, such as adenovirus or herpesvirus, or other factors in order to replicate. Recombinant AAV vectors contain none of the wild-type viral genes and retain only the characteristic inverted terminal repeats (ITRs), the only *cis*-acting sequences required for recombinant viral replication. Early studies in our laboratory and others [65,66,104,105] demonstrated that intramuscularly delivered rAAV2 is able to direct sustained expression of reporter and therapeutic genes.

We report here the successful use of rAAV2 vectors to direct the synthesis of both human and murine GAA *in vitro* and *in vivo*, resulting in restoration of enzymatic activity and skeletal muscle contractility. We also extend our studies to include rAAV1 and demonstrate broad and substantial skeletal muscle tropism for this serotype compared to rAAV2, as demonstrated by nearly one log greater expression in treated skeletal muscles of various fiber types.

Methods and Materials

Molecular Cloning of rAAV Vectors Carrying the Human and Murine GAA Genes

The human and murine GAA cDNAs (*hGAA* and *mGaa*), respectively, were constructed as described previously [55]. The full-length cDNAs were placed under the transcriptional control of the cytomegalovirus (CMV) immediate early promoter in the mammalian expression plasmid pCI (Clontech, Palo Alto, CA), yielding pCI-*hGAA* and pCI-*mGaa*. The expression cassettes were then cloned into p43.2, a plasmid containing both of the AAV inverted terminal repeats (ITRs). The human plasmid, p43.2-*hGAA*, was generated via *EcoRI*–*XbaI*, and p43.2-*mGaa* was similarly cloned via *SpeI*–*MunI*. A control recombinant AAV vector plasmid (pAAV- β gal) carrying the *Escherichia coli* β -galactosidase gene under the transcriptional control of the CMV promoter has been described previously [64].

To confirm the enzymatic activity of recombinant GAA produced from p43.2-*hGAA* and p43.2-*mGaa*, rAAV vector plasmids were transfected into COS-1 cells, and GAA activity was measured 72 h after transfection, as described below. An 8- to 10-fold increase in activity was observed after transfection with p43.2-*hGAA* or p43.2-*mGaa*, compared to untransfected cells or cells transfected with pAAV- β gal (data not shown). DNA sequences for the two rAAV-GAA plasmids were confirmed by the Johns Hopkins University DNA Analysis Facility using an automated sequencing protocol. Infectious rAAV-*hGAA*, rAAV-*mGaa*, and rAAV- β gal vectors were packaged and titered as described previously [74,87]. The current packaging protocol yields AAV particles that have a ratio of DNA-containing to infectious particle ratio of < 100. High-titer stocks (up to 10^{11} infectious units (iu)/mL) were fully characterized by SDS/PAGE and silver stain,

infectious center assay, particle count, and electron microscopy. rAAV1-*mGaa* vectors were produced and isolated using similar techniques.

Cell Lines and *In Vitro* and *In Vivo* Viral Transduction

Cultured cells were maintained in 5% CO₂ at 37°C. GAA-deficient fibroblasts isolated from an infant with GSDII (GM04912) were obtained from the NIGMS Mutant Cell Repository (Camden, NJ). Normal human skeletal muscle cells were obtained from Clonetics Corporation (Walkersville, MD).

GM04912 cells were cultured in 24-well plates at a density of 10⁵ in growth medium (GM; 20% [vol/vol] fetal calf serum (FCS) in DMEM). *In vitro* transduction with rAAV2 was performed in Opti-MEM, and after viral adsorption, cells were cultured in 2% FCS in DMEM. Normal and deficient human myoblasts were seeded in 24-well plates at a density of 2 x 10⁴ cells/cm² and cultured to confluence in GM. Once the cells reached confluence, differentiation medium (DM; 2% [vol/vol] horse serum in DMEM) was substituted to induce myoblast fusion and myotube formation. After 14 d of incubation in DM, myotubes were transduced with purified rAAV2 vectors in Opti-MEM. DM was reintroduced after viral adsorption. All media and sera were purchased from Life Technologies (Gaithersburg, MD).

All animal procedures were performed in accordance with the guidelines of the University of Florida Institutional Animal Care and Use Committee. Delivery of recombinant viral vectors to mouse skeletal muscle has been previously described. Balb/c mice were anesthetized with inhaled methoxyflurane, and 10⁹ iu of rAAV2-*hGAA* or rAAV2-*βgal* were injected into the tibialis anterior muscle after minimal exposure of the muscle *via* a single incision. For intramuscular rAAV2-*mGaa* experiments, rAAV2-

mGaa (10^9 iu) was injected into the quadriceps muscle of *Gaa*^{-/-} mice using minimal exposure; mice were then sutured as described before. Control mice of the same genetic background (129X1 x C57BL/6) were injected with identical volumes of sterile saline.

Assays of GAA Activity and Glycogen Content

Enzymatic activity assays for GAA were performed as described previously: Transduced tissue culture cells were harvested and lysed in a commercial lysis buffer (Analytic Luminescence Lab). Alternatively, harvested muscle tissues were homogenized in sterile water, then subjected to 3 freeze-thaw cycles. Lysates were centrifuged, and clarified supernatants were assayed for GAA activity by measuring the cleavage of the synthetic substrate 4-methylumbelliferyl- α -D-glucoside (Sigma M9766, Sigma-Aldrich, St. Louis, MO) after incubation for 1 h at 37°C. Successful cleavage yielded a product that emits at 448 nm when excited at 360 nm, as measured with an FLx800 microplate fluorescence reader (Bio-Tek Instruments, Winooski, VT) at 460 nm. Protein concentration was measured using the Bio-Rad DC Protein Assay Kit (Bio-Rad, Hercules, CA), with bovine serum albumin as a standard. Data are represented as nanomoles of substrate cleaved in one hour per milligram of total protein in the lysate (nmol/h/mg). Glycogen concentration was assessed by measuring the amount of glucose released from tissue homogenates after treatment with amyloglucosidase as described previously [57].

Immunocytochemistry

For immunofluorescence microscopy, cells on coverslips were fixed with 50% methanol/50% acetone (vol/vol) at -20°C for 15 min. Samples were blocked with 50% FBS / 50% PBS (vol/vol) for 1 h at room temperature, then incubated for 1 h at 25°C

with a previously described rabbit-derived anti-hGAA antiserum, diluted 1:1000 in phosphate-buffered saline (PBS) with 50% FCS and 0.01% NaN_3 . Cells were washed in PBS 3 times and incubated for 1 h at 25°C with fluorescein isothiocyanate-conjugated goat anti-rabbit antibody. The slips were again washed 3 times, mounted with an aqueous/dry-mounting medium (Biomedex, Foster City, CA) and examined with fluorescence microscopy. For localization of human GAA in the lysosomal compartment, transduced cells were fixed and probed simultaneously with a mouse monoclonal antibody recognizing human lysosome-associated membrane protein 1 (LAMP-1) and rabbit anti-human acid α -glucosidase antiserum. Cells were incubated with tetramethyl rhodamine-conjugated goat anti-mouse IgG and fluorescein-conjugated goat anti-rabbit IgG.

Perchloric Acid Extraction and ^1H -NMR Spectroscopy

Mice were fasted overnight to lower background glycogen to minimal levels. Upon sacrifice, samples were prepared by rapid freezing in liquid nitrogen and pulverization into a fine powder. Liquid nitrogen was evaporated and the powder was transferred to a 15 mL polypropylene tube containing 3 mL 7% (vol/vol) perchloric acid in 50 mM NaH_2PO_4 . The sample was vortexed repeatedly and centrifuged at 4°C and 4,000 rpm for 15 min. The supernatant was transferred to a new tube and neutralized to pH 7.0 with 5 M potassium hydroxide, leading to precipitate formation. The precipitate was removed by centrifugation; the supernatant was transferred to a new tube, and paramagnetic metals and excess salts were removed by incubation with pre-washed Chelex beads at a 1:8 ratio for 20 min at 4°C. The mixture was filtered through a 0.22 μm filter and lyophilized overnight. Samples were resuspended in D_2O for spectroscopy.

Proton nuclear magnetic resonance ($^1\text{H-NMR}$) measurements were performed using a Bruker Avance 500 spectrometer with an 11.75 T Magnex. Spectra were collected under unsaturated conditions at 25°C and pH 7.0 (TR = 5 s, sweep width = 6.666 kHz, pulse width = 5.5 μsec , number of averages = 256, number of points = 40,000). Integrated areas and chemical shifts were referenced to the total creatine peak (3.0 ppm) for each sample.

Assessment of Skeletal Muscle Function

Direct intramuscular injections of rAAV2-*mGaa* (2×10^9 iu) or lactated Ringer's were performed in the soleus muscle of *Gaa*^{-/-} mice. After 6 wk, the mechanical function of the muscles was assessed. *Gaa*^{-/-} and 129X1 x C57BL/6 controls were anesthetized via intraperitoneal (IP) injection of sodium pentobarbital. After reaching a surgical plane of anesthesia, the soleus muscles are surgically excised and placed in a cooled dissecting chamber containing Krebs-Henseleit solution, equilibrated with a 95% O₂ / 5% CO₂ gas mixture. The intact muscles are then vertically suspended between 2 lightweight Plexiglas clamps connected to force transducers (Model FT03, Grass Instruments, West Warwick, RI) in a water-jacketed tissue bath containing Krebs-Henseleit solution equilibrated with a 95% O₂ / 5% CO₂ gas (bath $\sim 37 \pm 0.5^\circ\text{C}$, pH $\sim 7.4 \pm 0.05$, osmolality ~ 290 mOsm). Transducer outputs are amplified and differentiated by operational amplifiers and undergo A/D conversion for analysis using a computer-based data acquisition system (Polyview, Grass Instruments).

In vitro contractile measurements begin with empirical determination of the muscle's optimal length (L_0) for isometric tetanic tension development. The muscle is field-stimulated using a stimulator (Model S48, Grass Instruments) along its entire length with platinum electrodes. Muscle length is progressively increased until maximal

isometric twitch tension is obtained. Once the highest twitch force is achieved, all contractile properties are measured isometrically at L_0 . The force-frequency relationship is examined using previously described methods [168].

Results

Expression and Enzymatic Activity in GSDII cells After *In Vitro* Transduction With rAAV2-*hGAA*

We first examined the expression of recombinant human GAA in deficient fibroblasts and myotubes from patients with GSDII. Deficient fibroblasts have no GAA activity, whereas deficient myotubes retain 50-80% of the GAA activity of normal human myotubes. Fourteen days after rAAV2-*hGAA* transduction, GAA activity in deficient fibroblasts reached 30% of normal with a multiplicity of infection (moi) of 10, whereas GAA activities of 150% normal were observed at an moi of 100 (Figure 4-1A). In deficient myotubes transduced with rAAV2-*hGAA* at an moi of 10, a 10-fold increase (360.0 ± 122.9 v. 32.0 ± 5.3 nmol/h/mg) in enzymatic activity was observed 2 wk after transduction (Figure 4-1B). These data indicate that rAAV2-*hGAA* is capable of restoring GAA activity in deficient cells *in vitro* in a dose-dependent manner.

To confirm that recombinant human GAA was being properly expressed and localized intracellularly, we probed for vector-derived human GAA protein in transduced, deficient cells. Immunofluorescent staining of human deficient fibroblasts transduced with rAAV2-*hGAA* (Figure 4-1C) showed that the protein is correctly targeted to the cytoplasm with a lysosomal distribution pattern. We confirmed lysosomal targeting of GAA by testing for co-localization of GAA and LAMP-1, a specific marker for mature lysosomes. As shown in Figure 4-1C, positive staining for human GAA (green; left panel) was coincident with the LAMP-1 staining (red; middle panel), indicating that

GAA protein expressed from rAAV2-*hGAA* is indeed transported to lysosomes; a digitally merged representation demonstrates co-localization in yellow (Figure 4-1C, right panel).

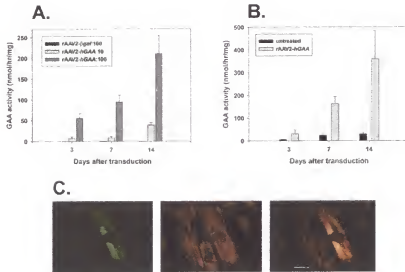


Figure 4-1. *In vitro* expression and lysosomal targeting of GAA in cells from GSDII patients. (A) Fibroblasts of GSDII patients were transduced with rAAV2-*hGAA* or rAAV2- β gal and harvested after 3, 7, or 14 d. Bar graph = mean \pm SEM of GAA activities from triplicate cultures. (B) GSDII myoblasts were harvested after 3, 7, or 14 d after infection with rAAV2-*hGAA*. Bar graph = mean \pm SEM of GAA activities from triplicate cultures. (C) Fibroblasts from a GSDII patient incubated with an anti-hGAA antibody and a FITC-conjugated secondary antibody 8 d after infection with rAAV2-*hGAA* (green). The same cells were also incubated with an anti-LAMP-1 antibody and a rhodamine-conjugated secondary antibody (red). Digitally merged FITC/rhodamine image shows co-localization in yellow (confirming sorting of human GAA to the lysosomal compartment). Bar = 25 μ m.

Stable, Long-Term Expression of Human or Mouse GAA in Mouse Muscle After *In Vivo* Delivery of rAAV2 Vectors

To examine the efficiency and stability of rAAV2-mediated expression of GAA, we tested the vectors *in vivo* by injecting 10^9 iu of rAAV2-*hGAA* into the tibialis anterior (TA) muscles of Balb/c mice. GAA expression was then assessed at 1 wk, 4 wk, 10 wk, and 6 mo after treatment (Figure 4-2). We found that GAA enzymatic activity was

increased over 150% in the TA muscles at 1 wk (168.1 ± 16.0 nmol/h/mg treated v. 62.0 ± 3.1 control), and this level of activity was maintained or increased over 6 mo, with the highest activities observed at the latest timepoint (397.9 ± 113.3 nmol/h/mg). The control group, which was injected with rAAV2- β gal, showed no change in GAA enzymatic activity over the same period. These data demonstrate that the rAAV2 is capable of expressing GAA efficiently, and that the expression is stable for up to 6 mo after a single intramuscular injection.

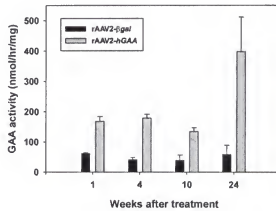


Figure 4-2. Expression of recombinant human GAA in Balb/c mice after transduction with rAAV2-hGAA. Adult mice were treated with 10^9 iu of rAAV2-hGAA in the tibialis anterior muscle, muscle tissues were isolated at the time points indicated, and assayed for GAA activity. Bar graph represents mean \pm SEM GAA activity in 5 animals (wk 1 and 4) or 4 animals (wk 10 and 24).

To provide further assurance that the observed enzymatic activities were not caused by increased basal production in the Balb/c strain, we treated knockout mice (*Gaa*^{-/-}) with rAAV2-mGaa. These mice have little or no residual GAA activity and have been shown to recapitulate many of the pathologic manifestations observed in human GSDII patients. Twelve weeks after intramuscular delivery of 10^9 iu of rAAV2-mGaa, we observed

normal levels of GAA enzyme activity in the knockout mice (32.6 ± 14.7 nmol/h/mg), as compared to 129X1 x C57BL/6 control mice (39.7 ± 1.0 nmol/h/mg) (Figure 4-3).

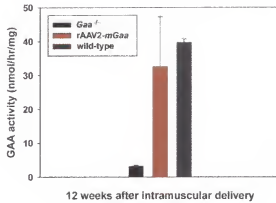


Figure 4-3. rAAV2-*mGaa*-mediated transduction of skeletal muscle in *Gaa*^{-/-} mice. Adult *Gaa*^{-/-} mice were treated with 10^9 iu of rAAV2-*mGaa* in the quadriceps femoris muscle. 129X1 x C57BL/6 controls and untreated *Gaa*^{-/-} mice were sham-injected with sterile saline. Muscle tissues were isolated at 12 wk after treatment and assayed for GAA activity. Bar graph represents mean \pm SEM GAA activity for 5 mice in each group.

Preservation of Skeletal Muscle Contractile Force in Knockout Mice After Direct Intramuscular Delivery of rAAV2-*mGaa*

We tested the contractile properties of soleus muscles of knockout and wild-type hybrid mice, using isometric force-frequency relationships as an index of contractile function. *Gaa*^{-/-} mice exhibit an age-dependent impairment of skeletal muscle function (Figure 4-4, open squares), as evidenced by their decreased maximal tetanic force (16.71 ± 1.52 N/cm²) at higher stimulation frequencies compared to the matched control strain (20.86 ± 1.88 N/cm²; filled circles). This impairment is observed as early as 3 mo of age (Fig. 4) and progressively worsens over the lifespan of the animal.

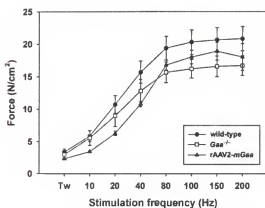


Figure 4-4. Force-frequency relationships of intact soleus muscles after direct intramuscular delivery of rAAV2-*mGaa*. 2×10^9 iu of rAAV2-*mGaa* were directly delivered to the soleus muscles of 2-mo-old *Gaa*^{-/-} mice ($n = 3$). Muscles were isolated 6 wk after treatment, tested for isometric force generation, and compared to untreated 129X1 x C57BL/6 (wild-type) ($n = 6$) and *Gaa*^{-/-} mice ($n = 5$), respectively.

To test the effect of restoration of GAA activity on contractile dysfunction in *Gaa*^{-/-} mice, we injected 2×10^9 iu of rAAV2-*mGaa* directly into the soleus muscles of 6-wk-olds. Isometric force generation was tested 6 wk later, at 3 mo of age (Figure 4-4, filled triangles). At the maximal stimulation frequency (200 Hz), treated *Gaa*^{-/-} mice had intermediate contractile force (18.03 ± 2.05 N/cm²) relative to untreated *Gaa*^{-/-} and wild-type controls. Similar relationships in isometric tension were observed between wild-type, treated, and untreated *Gaa*^{-/-} mice from 80 to 150 Hz, indicating some amelioration of the muscle function deficit over a range of physiologically relevant forces.

Treatment of *Gaa*^{-/-} Mice With rAAV1-*mGaa* Leading to Rapid Overexpression of GAA and Glycogen Clearance

Since rAAV2-mediated gene replacement led to wild-type levels of GAA enzymatic activity, we tested the ability AAV serotype 1 vectors to restore GAA activity as well. We injected 4×10^{10} total particles (as assessed by dot-blot analysis) of rAAV1-*mGaa* directly into the tibialis anterior (TA) muscles of 2-mo-old *Gaa*^{-/-} mice ($n = 4$), and

the mice were sacrificed 2 wk later. TA muscles were harvested, pooled, and homogenized. GAA activities (Figure 4-5, left panel) in treated *Gaa*^{-/-} tissues (461.5 nmol/h/mg) were nearly eight times wild-type (65 nmol/h/mg). Glycogen contents of TA muscles from untreated and treated GAA mice were 1.756 and 0.0219 μ mol glucose/mg protein, respectively, compared to 0.128 μ mol glucose/mg protein for wild-type mice. Proton nuclear magnetic resonance (¹H-NMR) spectra of perchloric acid extracts from the same treated and untreated tissues showed a pronounced glycogen peak for *Gaa*^{-/-} mice and complete amelioration of glycogen accumulation in rAAV1-*mGaa* treated mice. Taken together, these findings indicate a dramatic reversal of glycogen accumulation after transduction with rAAV1-*mGaa*.

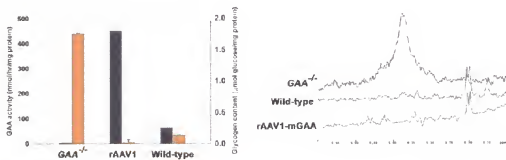


Figure 4-5. rAAV1-*mGaa*-mediated transduction of tibialis anterior in *Gaa*^{-/-} mice. (A) 4×10^{10} particles of rAAV1-*mGaa* were directly delivered to the tibialis anterior muscles of 2-mo-old *Gaa*^{-/-} mice ($n = 4$). Muscles were harvested, pooled, and homogenized 2 wk after treatment and compared to untreated 129X1 x C57BL/6 (wild-type) and *Gaa*^{-/-} mice, respectively. (B) *In vitro* glycogen content determination for the same muscle homogenates. (C) Stacked ¹H-NMR spectra from the same homogenates after perchloric acid extraction. Glycogen peaks are observed at 5.4 ppm.

Treatment of Various Skeletal Muscles with rAAV1-*mGaa* Leads to Overexpression of GAA in *Gaa*^{-/-} Mice

We decided to test rAAV1 vectors carrying the *mGaa* cDNA in *Gaa*^{-/-} to determine whether rAAV1 vectors have a preference for certain skeletal muscle groups. Figure 4-6

illustrates the lack of a clear preference among the three tested tissues. As in Figure 4-5, transduction with rAAV1 vectors led mGaa expression that was several-fold greater than wild-type in the soleus, tibialis anterior, and quadriceps muscles. In the cases of the soleus and quadriceps, we were able to test 2 different doses, and a dose-dependent relationship was clearly observed.

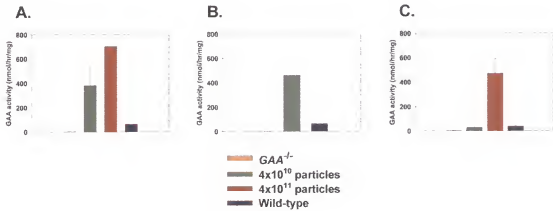


Figure 4-6. rAAV1-*mGaa*-mediated transduction of various skeletal muscles in *Gaa*^{-/-} mice. Muscles were directly injected with 4×10^{10} or 4×10^{11} particles of rAAV1-*mGaa*. Muscles were harvested and homogenized 2-4 wk after treatment and compared to untreated 129X1 x C57BL/6 (wild-type) and *Gaa*^{-/-} mice, respectively. (A) Soleus. (B) Tibialis anterior. (C) Quadriceps femoris.

We noted that detection of GAA activity appears to be in some ways related to the size of the muscle tested. Because our assays are performed on total muscle homogenates, it is possible that positive transduction may be diluted in larger tissues (such as the quadriceps femoris) due to a smaller number of transduced fibers relative to the total volume of the bulk tissue. In other words, since the dose in these cases has been delivered on a particle-to-particle basis rather than a particle-to-tissue mass basis, the potency of viral transduction may not be fully appreciated in larger tissues since the number of transducing units delivered to those tissues was smaller on a per gram (g^{-1})

basis. Nevertheless, these results confirm the potency of rAAV1 vectors in muscle tissues that either predominantly slow- or fast-twitch.

Discussion

Pompe disease is caused by a deficiency of GAA in all tissues, but is manifested primarily as cardiac and skeletal muscle weakness. Recently, several murine knockout models of GSDII have been developed [29], all of which mimic, according to one index or another, the myopathic phenotype associated with GSDII. The *Gaa*^{-/-} mouse used in these studies accumulates lysosomal glycogen and suffers from generalized skeletal myopathy, manifested in part in decreased locomotor activity. Our objective was to achieve sustained restoration of GAA activity from direct intramuscular delivery to cardiac or skeletal muscle. Additionally, we sought to test the ability of vector-derived GAA to restore contractile function in deficient muscle tissue.

We constructed recombinant adeno-associated viruses that encode the full-length human and mouse GAA cDNAs and tested their ability to restore GAA activity *in vitro* in GAA-deficient fibroblasts and myotubes. Previous work in our laboratory and others had demonstrated the efficient transduction of these tissues with adenoviral vectors and indicated the utility of these cells as an *in vitro* system to evaluate potential therapies [55-57]. In this report, high-level expression of recombinant human GAA was achieved in both GAA-deficient fibroblasts and myotubes transduced *in vitro* with rAAV2-*hGAA*, demonstrating that the human GAA cDNA is capable of directing synthesis of functional GAA protein in the context of rAAV2.

In vivo experiments confirmed that rAAV2-*hGAA* and rAAV2-*mGaa* were able to direct long-term enzymatic activity in treated mice. Stable expression of recombinant human GAA was observed for up to 6 mo after a single intramuscular injection of

rAAV2-*hGAA*. In treated *Gaa*^{-/-} animals, near-normal levels of mouse GAA activity were observed in skeletal muscle 12 wk after administration of 10⁹ iu (~10¹³ genomes/kg); concomitant improvement of muscle contractile function was observed in the higher frequency (i.e., clinically relevant) stimulation range. These results are consistent with previous observations of efficient skeletal muscle transduction with rAAV2 vectors, as demonstrated with reporter and therapeutic genes [105,107-109], as well as with genes for muscle contractile apparatus proteins [118], and another lysosomal storage disease, mucopolysaccharidosis VII.

The clinical heterogeneity of GSDII suggests that potential therapies must address the primary enzymatic deficiency in both skeletal and cardiac muscle. Numerous reports have indicated that circulating recombinant GAA, either purified protein or viral vector-derived, might serve as an effective method of delivery of GAA to muscle tissue. Several groups, including our own, have sought to take advantage of cell surface mannose 6-phosphate receptors to mediate the transport of circulating enzyme to the lysosomal compartments of individual cells. Studies with intravenous delivery of recombinant human GAA protein have indicated that this strategy may be beneficial in *Gaa*^{-/-} mice and human subjects [48,50]. Ongoing investigation will determine whether clinically relevant circulating enzyme concentrations can be sustained, particularly given the potential for neutralizing antibody responses to intravenously administered recombinant enzyme replacement therapy.

Recent data, from *Gaa*^{-/-} transgenic mice that express human GAA in a conditional, muscle-specific manner, indicate that several-fold overexpression of human GAA was required in order to achieve systemic restoration of GAA activity in non-muscle tissues.

Given these data, the near-normal enzymatic activity observed after intramuscular delivery of rAAV2-*mGaa* (Figure 4-3A) is not likely to provide sufficient circulating concentrations of GAA for systemic correction; in fact, no change in enzymatic activity was observed in the liver, heart, or uninjected (distal) skeletal muscles with the enzymatic activities reported here (data not shown). By contrast, GAA activities after intramuscular delivery of rAAV1-*mGaa* resulted in nearly eight times wild-type enzyme activity levels (Figure 4-5), with concomitant clearance of glycogen from the injected tissue. Because of the relative size of the tibialis anterior muscle, we did not seek, in this study, to substantially increase circulating concentrations of recombinant GAA secreted from muscle. However, these data suggest that a larger, well-perfused muscle may be capable of serving as a production site for systemic therapy for GSDII. Further studies are underway to address this question.

We should note that the metrics used to analyze phenotypic correction of GSDII in both mice and humans are an area of active development in our laboratory and others. One potentially clinically important outcome is the co-localization of both active GAA enzyme and the clearance of lysosomal glycogen. To date, clinical trials with both intravenously delivered CHO- and transgenic rabbit milk-derived human GAA have led to variable increases GAA enzymatic activity in skeletal and cardiac muscle, with achieved developmental milestones and reductions in cardiac mass. However, despite these promising observations, reductions in total tissue glycogen content have been reported in only one patient among the seven patients studied in 2 separate trials. As shown in Figure 4-5, we have recently begun to employ magnetic resonance imaging and spectroscopy techniques in an effort to better understand the dynamics of glycogen

clearance in vector-treated *Gaa*^{-/-} mice. The initial observations suggest that this technique will be very useful in longitudinal studies of treated mice. In addition to glycogen content, important morphological characteristics of skeletal muscle will also be evaluated in future studies.

The use of rAAV1 serotype vectors will only expand in the coming months and years as their efficacy is evaluated in a host of tissue targets. Pruchnic *et al.* [109] believed that rAAV2 serotype vectors (while effective in many muscle tissues) had a preference for slow-twitch skeletal muscle compared to fast-twitch. We have not directly evaluated this possibility for rAAV1 vectors, but indirectly provide evidence that fiber-type tropism may not be a factor in rAAV1 transduction. We are certain that future studies will further investigate this question. When they are discovered, the identification of skeletal muscle receptors for rAAV1 may greatly assist in determining the muscle-type tropisms of rAAV1 (if any exist).

We have described the use of recombinant adeno-associated virus vectors to correct the primary enzymatic defect in GSDII. These data suggest that adeno-associated virus-mediated gene transfer represents a feasible and potentially powerful strategy for the delivery of gene products to specific myopathic tissue. Given the short half-life of GAA *in vivo* (~ 7 d), gene therapy vectors with capabilities for both high-level and long-term, persistent transgene expression will be required.

We anticipate that direct delivery of rAAV vectors will have broad applicability for the delivery of a variety of recombinant gene products to myopathic tissue and for the treatment of many inherited forms of skeletal and cardiac myopathy. Our results indicate that a variety of transduction of efficiencies may exist among rAAV serotypes when

delivered to skeletal muscle tissues. We believe that these differences may be exploited in the future to provide appropriate levels of transduction for specific applications. Using specific serotypes; in specific skeletal muscles; and tailored injection volumes and carrier vehicles, it may be possible to rationally design gene therapy delivery and dosing regimens based on the target organs and the desired level of gene expression.

CHAPTER 5

CROSS-CORRECTION AFTER RECOMBINANT ADENO-ASSOCIATED VIRUS DELIVERY TO SKELETAL MUSCLE

The promising results acquired with rAAV1-*mGaa* delivery to skeletal muscles prompted us to attempt to use skeletal muscle as a platform for systemic cross-correction. As mentioned in Chapter 1, we are attempting to transduce a defined muscle bed with rAAV1 vectors with the expectation that the injected tissue will overexpress active GAA; and we further anticipate that this overexpression will lead to secretion of GAA, providing a circulating pool of enzyme that can bind to cell-surface mannose 6-phosphate receptors (M6PRs) of other tissues and be trafficked to the lysosomal compartment.

To this end, we treated *Gaa*^{-/-} mice with two doses of rAAV1 carrying genes encoding GAA. In the first pilot experiment, mice were treated with 4×10^{10} and 4×10^{11} particles of rAAV1-*mGaa* to establish the potential for cross-correction. Following this study, we initiated a second study in which mice were treated with 7.5×10^{11} particles of rAAV1-*hGAA*, carrying the human *GAA* gene. The rationale for the second study was two-fold: to use a higher dose in an attempt to make an incremental improvement compared to the first study; and to test the human transgene in an animal model in anticipation of initiation of a preclinical protocol. Additionally, a subset of animals was neonatally tolerized *via* subcutaneous injection of recombinant human GAA (rhGAA) in an effort to blunt or prevent an immune response to the human *GAA* gene product.

Methods and Materials

Molecular Cloning of rAAV Vectors Carrying the Human and Murine GAA Genes

The human and murine GAA cDNAs (*hGAA* and *mGaa*), respectively, were constructed as described previously with a modification of the human GAA cDNA described by Schleissing [170]. In that case, the 5' untranslated region (5' UTR) was removed from the *hGAA* gene, yielding a 2.8 kb cassette renamed *hGAA2.8*. Dr. Schleissing characterized the enzymatic activities of these truncations *in vitro* and *in vivo* and validated their identity and potency. Viral vectors based on these transgenes were produced as described in the preceding chapter.

In Vivo Viral Transduction

All animal procedures were performed in accordance with the guidelines of the University of Florida Institutional Animal Care and Use Committee. Delivery of recombinant viral vectors to mouse skeletal muscle has been previously described. *Gaa*^{-/-} mice were anesthetized with inhaled methoxyflurane, and 4×10^{10} or 4×10^{11} particles rAAV1-*mGaa* (Study 1) or 7.5×10^{11} particles rAAV1-*hGAA2.8* (Study 2) were directly injected into the quadriceps femoris muscles — injected doses were divided equally between both quadriceps in order to accommodate the injectate volume. Animals were bled weekly to facilitate enzyme-linked immunosorbent assay (ELISA) for development of serum antibodies against human GAA.

Assays of GAA Activity

Enzymatic activity assays for GAA were performed as described previously: Harvested muscle tissues were homogenized in sterile water using Lysing Matrix D (Qbiogene, Carlsbad, CA) in a FastPrep FP120 (Qbiogene), centrifuged, and clarified supernatants were assayed for GAA activity by measuring the cleavage of the synthetic

substrate 4-methylumbelliferyl- α -D-glucoside (Sigma M9766, Sigma-Aldrich, St. Louis, MO; 75 mM in DMSO) after incubation for 1 h at 37°C, as described in the previous chapter. Fluorescence was measured using a FLx800 microplate fluorescence reader (Bio-Tek Instruments, Winooski, VT), and protein concentration was determined using the Bio-Rad DC Protein Assay Kit (Bio-Rad, Hercules, CA), with bovine serum albumin as a standard. Data are again represented as nanomoles of substrate cleaved in one hour per milligram of total protein in the lysate (nmol/h/mg).

Assessment of Skeletal Muscle Function

Ten weeks after delivery of rAAV1-*hGAA*2.8, the isometric force-frequency relationships of the soleus muscles were assessed. Six-month-old *Gaa*^{-/-} and age-matched 129X1 x C57BL/6 controls were tested as described in previous chapters.

Assessment of Immune Response to hGAA

Serum samples were obtained weekly *via* tail vein bleeds of anesthetized animals. Whole blood was collected in Microtainer tubes (Becton Dickinson, Franklin Lakes, NJ), spun at 5500 rpm for 10 min, and serum was removed and stored at -20°C. Microtiter plates were coated overnight at 4°C with 200 μ L of 0.5 mg/mL human GAA in 0.1 M NaHCO₃ (pH 8.2). Wells were washed 3 times with 300 μ L of PBS/Tween 20; blocked with blocking reagent (300 μ L of 10% fetal bovine serum (FBS)) for 2 h at room temperature; then washed once more prior to adding samples and standards. Serum samples were diluted 1:80 in blocking reagent and added to the wells in a total volume of 100 μ L. Serial dilutions of rabbit-anti-human GAA antibody (from 1:500 to 1:5 x 10⁶) were used to generate a standard curve. Samples and standards were incubated for 1 h at room temperature. Washing was repeated and 100 μ L of sheep anti-mouse IgG-HRP-

linked antibody (Amersham Pharmacia Biotech, Piscataway, NJ; diluted 1:10,000) was added to sample wells and 100 μ L of donkey anti-rabbit-IgG-HRP-linked antibody (also diluted 1:10,000) was added to standard wells for 30 min at room temperature. After incubation, wells were washed again and 100 μ L of tetramethyl benzidine (Sigma-Aldrich, St Louis, MO) was added to wells for 1-3 min. The reaction was stopped with 100 μ L of 1 N H_2SO_4 and absorbance was measured at 450 nm. A standard curve was generated using absorbance units and dilution of the rabbit anti-human GAA antibody. Absorbance values of samples were converted to 1/dilution to obtain a positive correlation between the reported units and absorbance readings.

Histological Assessment of Glycogen Clearance

Segments of treated and untreated diaphragm were also fixed overnight in 2% glutaraldehyde in PBS, embedded in epon, sectioned, and stained with periodic acid-Schiff (PAS) by standard methods.

Results

Study 1: Evidence of Cross-Correction of Distal Tissues with rAAV1-*mGaa* Delivery to Quadriceps Femoris in *Gaa*^{-/-} Mice

Mice treated with 4×10^{10} or 4×10^{11} particles of rAAV1-*mGaa* were sacrificed and tested for enzymatic activities in injected and distal tissues. The results are shown in Table 5-1, and are expressed in terms of percent of wild-type activity. The activities in injected tissues (quadriceps femoris) are shown in Figure 4-6C, and correspond to approximately 1X and 10X wild-type activity, respectively. As stated in Chapter 4, these activities are higher than measured with any attempted dose of rAAV2.

Table 5-1. Percent of wild-type acid α -glucosidase activities in various *Gaa*^{-/-} tissues after quadriceps femoris delivery of rAAV1-*mGaa*.

	4 x 10 ¹⁰ particles	4 x 10 ¹¹ particles
Heart	2.54 ± 0.19%	10.58 ± 4.71%
Liver	1.60 ± 0.21%	2.47 ± 0.21%
Soleus	1.93 ± 1.33%	6.03 ± 6.81%
Diaphragm	1.70 ± 0.21%	2.72 ± 0.53%
Tibialis anterior	1.78 ± 0.59%	13.51 ± 0.75%
Gastrocnemius	2.49 ± 0.46%	70.91 ± 31.89%

These data indicate some transfer of GAA activity from transduced tissues to distal tissues and are the first demonstration of potential cross-correction after intramuscular delivery of rAAV carrying a gene encoding for acid α -glucosidase. However, positive results were not observed at the lower dose and were not uniformly observed at the higher dose.

Varied Enzymatic Activities in Injected and Distal Muscles after High-Dose Delivery of rAAV1-hGAA to Quadriceps Femoris

We decided to further investigate the potential for muscle-directed cross-correction using a higher dose of rAAV1. We also decided to use vectors carrying the human *GAA* cDNA in the hopes that the data would confirm our initial result and provide important data for the initiation of a preclinical safety and efficacy study. Finally, we used a model of neonatal tolerance developed in our laboratory by Kerry Cresawn to try to ameliorate potential immune responses to human GAA. We tolerized 9 neonatal (1-d-old) *Gaa*^{-/-} mice with single subcutaneous bolus injections of purified recombinant human GAA (rhGAA). Ten additional, naïve *Gaa*^{-/-} mice were included in the study and were not tolerized. Mice in both groups were treated with 7.5 x 10¹¹ particles of rAAV1-*hGAA*2.8 between 75 and 90 d of age; doses were administered intramuscularly into the quadriceps femoris.

The biochemical results of this study are summarized in Tables 5-2 and 5-3, and indicate a variegated response to both gene delivery and neonatal tolerization. In summary, none of the treated *Gaa*^{-/-} mice responded with unequivocal cross-correction. In particular animals with high levels of GAA activity in some tissues were not recapitulated in other tissues, and the results did not align along any particular pattern — anatomic, metabolic, or otherwise. Likewise, subjects with the highest levels of GAA activity in the injected tissue (quadriceps femoris) did not uniformly have higher levels of enzymatic activity in distal muscle tissues.

Table 5-2. Acid α -glucosidase activities in *Gaa*^{-/-} hindlimb tissues after quadriceps femoris delivery of rAAV1-*hGAA*.

	SOL	GAST	TA	EDL	QUAD
Wild-type	5.23 \pm 0.45	5.91 \pm 0.73	12.21 \pm 0.72	31.06 \pm 3.66	5.53 \pm 0.21
	4.69 – 6.47	5.16 – 7.58	10.5 – 14.01	22.6 – 37.35	5.04 – 6.05
<i>Gaa</i> ^{-/-}	0.39 \pm 0.07	0.43 \pm 0.19	0.26 \pm 0.06	0.64 \pm 0.11	0.06 \pm 0.03
	0.16 – 0.62	0.08 – 1.17	0.24 – 0.42	0.42 – 0.94	0.03 – 0.08
Naïve	0.41 \pm 0.04	0.57 \pm 0.18	0.37 \pm 0.07	2.40 \pm 0.91	3.83 \pm 2.31
	0.34 – 0.52	0.15 – 1.34	0.22 – 0.63	0.79 – 6.17	0.02 – 14.92
Tolerized	0.47 \pm 0.07	0.53 \pm 0.19	1.96 \pm 1.31	3.26 \pm 0.61	24.94 \pm 12.9
	0.32 – 0.87	0.16 – 1.27	0.31 – 8.47	1.64 – 5.36	0.18 – 99.84

Table 5-3. Acid α -glucosidase activities in *Gaa*^{-/-} various cardiac, smooth, and skeletal muscle tissues after quadriceps femoris delivery of rAAV1-*hGAA*.

	HRT	DIA	TRI	TNG	BLD
Wild-type	9.30 \pm 1.20	4.95 \pm 0.56	6.59 \pm 0.30	8.47 \pm 0.70	20.46 \pm 3.15
	7.51 – 12.83	3.29 – 5.83	5.89 – 7.24	7.01 – 10.37	12.2 – 26.57
<i>Gaa</i> ^{-/-}	0.42 \pm 0.24	0.17 \pm 0.02	0.18 \pm 0.02	0.37 \pm 0.05	0.64 \pm 0.06
	0.03 – 1.10	0.11 – 0.23	0.11 – 0.22	0.20 – 0.49	0.48 – 0.86
Naïve	0.13 \pm 0.03	0.16 \pm 0.03	0.22 \pm 0.03	0.28 \pm 0.02	0.54 \pm 0.07
	0.06 – 0.20	0.06 – 0.27	0.11 – 0.35	0.18 – 0.33	0.41 – 0.84
Tolerized	0.27 \pm 0.09	0.14 \pm 0.03	0.22 \pm 0.03	0.30 \pm 0.03	0.99 \pm 0.52
	0.03 – 0.58	0.09 – 0.27	0.15 – 0.33	0.22 – 0.42	0.33 – 4.13

Partial Preservation of Soleus Contractile Force in *Gaa*^{-/-} Mice after High-Dose Delivery of rAAV1-hGAA to Quadriceps Femoris

We tested the effect of rAAV1-*hGAA* delivery to the quadriceps on contractile dysfunction in *Gaa*^{-/-} mouse soleus muscles. Isometric force-frequency relationships (FFR) were tested at the 10-wk timepoint. At stimulation frequencies from 80 to 200 Hz, both groups of treated *Gaa*^{-/-} mice displayed intermediate contractile forces relative to age-matched, untreated *Gaa*^{-/-} and wild-type controls. No differences were observed between naïve and tolerized, rAAV1-treated mice. Differences between tolerized mice and *Gaa*^{-/-} were significant at 150 and 200 Hz stimulation frequencies, and significant differences were recorded between naïve and *Gaa*^{-/-} mice between 80 and 200 Hz ($p < 0.05$ in all cases).

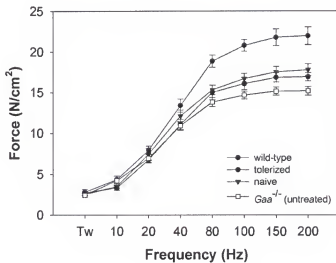


Figure 5-1. Force-frequency relationships of intact soleus muscles after intramuscular delivery of rAAV1-*hGAA* to the quadriceps femoris. 7.5×10^{11} particles of rAAV1-*hGAA*2.8 were injected in the quadriceps femoris muscles of naïve and tolerized *Gaa*^{-/-} mice. Muscles were isolated 10 wk after treatment, tested for isometric force generation, and compared to age-matched, wild-type (129X1 x C57BL/6) and *Gaa*^{-/-} mice, respectively.

High-Dose rAAV1-*hGAA* Treatment Leads to a Rapid Immune Response to the *GAA* Transgene

Because the *Gaa*^{-/-} mice used in these studies do not synthesize either mouse *Gaa* or human *GAA* protein, we tested whether or not rAAV1-*hGAA* treated mice would mount an immune response to human *GAA*. We tested two groups of animals: naïve *Gaa*^{-/-} mice and neonatally tolerized *Gaa*^{-/-} mice. Serial serum samples were collected weekly beginning the week of vector delivery, and enzyme-linked immunosorbent assays (ELISAs) were performed to measure the amount of anti-h*GAA* antibody present in treated mouse serum. Figure 5-2 shows anti-h*GAA* antibody titers from naïve mice; Figure 5-3 represents antibody levels in neonatally tolerized mice; and Figure 5-4 shows (for comparison) the average anti-h*GAA* antibody titers for the two groups.

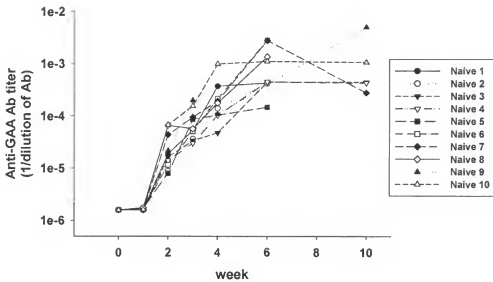


Figure 5-2. Naïve anti-h*GAA* antibody titers. Serial bleedings were performed weekly, and antibody titers were measured at the end of the study.

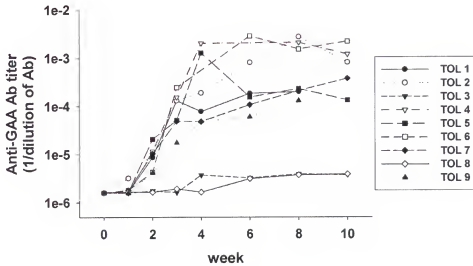


Figure 5-3. Tolerized anti-hGAA antibody titers. Neonatal *Gaa*^{-/-} mice were tolerized using rhGAA prior to rAAV1-*hGAA* delivery. Serial bleedings were performed weekly, and antibody titers were measured at the end of the study.

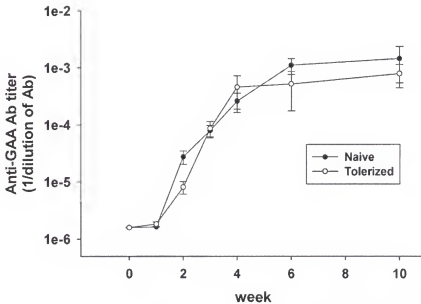


Figure 5-4. Average anti-hGAA antibody titers for naïve and tolerized groups. Data represent means \pm SEM for each timepoint.

As expected, anti-hGAA antibody titers from naïve mice (Figure 5-2) were detected very early after rAAV1 delivery; rose rapidly in the first 2-4 wk after transduction; and remained extremely high throughout the course of the study. Unfortunately, similar results were observed in neonatally tolerized mice (Figure 5-3). Based on prior experience from our laboratory (K.Cresawn, data not shown), we expected neonatal tolerance to protect treated animals from mounting an immune response to the human transgene. In 2 out of 9 animals we did observe a depressed antibody response as we had hoped (TOL 3 and TOL 8). However, these lower titers did not correspond to higher levels of cross-correction or activity in treated quadriceps muscles. As seen in Figure 5-4, the average anti-hGAA antibody titers for the two groups were remarkably similar and followed the same general timecourse.

Discussion

The two studies described in this chapter were designed to test the ability of vector-mediated overexpression of hGAA in null-animal skeletal muscles to systemically correct the enzymatic deficiency and related pathogenesis. The first study was intended to establish a reference point for cross-correction with rAAV1 vectors. The second study sought to build upon the experience from the first and to establish the efficacy of rAAV1 carrying the human *GAA* cDNA. Raben *et al.* [32] reported that several-fold overexpression of human *GAA* was required in order to achieve systemic restoration of *GAA* activity in non-muscle tissues. We believed that rAAV1-mediated overexpression might be able to provide enough circulating material to lead to uptake of hGAA in distal tissues.

Mice treated with 4×10^{10} or 4×10^{11} particles of rAAV1-*mGaa* had restored enzymatic activity and some evidence of cross-correction. The data in this case were

highly variable and in some cases merely suggestive. However, there were enough instances of potential correction to justify further investigation. As we noted in the previous chapter, the levels of expression were lower than in the tibialis anterior. We attributed this to the mass effect of quadriceps muscle compared to tibialis; we believed that a higher dose of vector in the quadriceps (with perhaps more spread) might lead to similar specific activities. On a per gram basis, transduction of the quadriceps might be similar to tibialis.

The second study did not provide consistent data to support or discount this hypothesis. Unfortunately, the experimental design may have also confounded our efforts. We changed not only the dose of vector but also the transgene. We have no evidence to suggest that mouse Gaa protein is less immunogenic than human GAA in null mice, but our results could have been affected by the difference in gene product or the immune response to it. Furthermore, we have no data (and none exists in the literature at this point) to indicate whether or not rAAV1 vectors have increased tropism for dendritic cells (compared to rAAV2 vectors). It is possible that a limiting dose of rAAV1 exists for murine skeletal muscle, above which transduction of dendritic and other immunomodulatory cells becomes a factor in long-term expression.

The early, robust, and persistent immune response to rAAV1-derived hGAA was not wholly unanticipated, but did lead to new questions regarding the stability of transduction. Using a tolerized mouse model, we sought to account for this possibility. Unfortunately, the levels of expression after rAAV1 delivery were high enough to break the immune tolerance; alternatively, the animals may not have been effectively tolerized in the first place. This is not to say that the tolerization dose of immunogen was

inappropriate, either temporally or in concentration, but vector delivery component of the study occurred well after the tolerization event. This circumstance arose because of delays in production of purified rAAV1-*hGAA* and may be an important variable to consider in the design of future studies using neonatal tolerization.

Variable enzymatic activities were observed in the injected tissues, despite substantial immune responses in all treated animals. This result suggests that a variety of individual responses occurred among individual subjects. In some cases, early, robust expression may have been accompanied by equally robust immune responses.

We have employed the use of knockout mice in attempt to achieve homogeneous responses to gene transfer interventions. However, our mice (as well as humans and other species) have a heterogeneous (in this case hybrid) genetic background. Polymorphisms and differential expression of any number of modifier genes between 129X1 and C57BL/6 mice could account for some of the observed variability. Since individual mice could have varying contributions from these two strains, we cannot rule out genetic contributions to differences in immune response or transgene stability.

Despite variable enzymatic activities in injected tissues and distal tissues; robust immune responses in naïve and tolerized mice; and no evidence of substantial, long-term correction in the soleus, we measured a significant difference in isometric force-frequency relationships, particularly with regards to maximal force generation. These results were surprising (given the preponderance of other data) for two reasons: the forces measured in treated mice contradict the enzymatic activity data, and the data are remarkably similar for naïve and tolerized mice. Taken in concert with the enzymatic activity and immune response data, the functional data suggest that low levels of cross-

correction may have been achieved. This correction may have occurred because of a transient transfer of active enzyme that was subsequently cleared; a continuous uptake of enzymatic activity that is below the levels of detection; or some other modulatory effect that is systemic in nature but not detectable at the myocyte level. This may include effects on circulating cell types and inhibition or stimulation of signaling pathways within myocytes or in other cell types. We speculate that pathophysiology in GSDII myocytes is related to not only glycogen content and storage but also substantial regulation of cell signaling. It may be the case that amelioration of signaling defects will impart functional correction without substantial glycogen clearance. This may also explain the variegation of phenotypes observed in human GSDII subjects with similar or identical genetic defects and/or enzymatic activities.

We have described the use of recombinant adeno-associated virus serotype 1 (rAAV1) vectors to correct the primary enzymatic defect in GSDII. Our data confirm the skeletal muscle tropism for rAAV1 and indicate that (in some cases) transfer of material from transduced tissue to distal, affected tissues may be possible. We also report, for the first time, a substantial immune response to rAAV1 transgenes, and show that this response may be fairly robust, despite efforts to tolerize mice prior to gene delivery.

CHAPTER 6

RECOMBINANT ADENO-ASSOCIATED VIRUS-MEDIATED GENE THERAPY FOR MYOCARDIAL DISEASE IN GSDII

Genetic interventions for myocardial disorders could reverse or prevent a host of conditions that are currently serious public health and health care delivery challenges. While gene therapeutics have been under development for nearly a decade, few have resulted in expression levels or persistence that can be qualified as successful or therapeutic. Nevertheless, recombinant adeno-associated virus vectors have been demonstrated to transduce cardiac tissue and persist within the myocardium, and we describe their application to GSDII.

Experimental Design and Rationale

The studies outlined in this chapter encompass a number of different strategies to address gene delivery and restoration of myocardial GAA enzymatic activity. As noted in Chapter 1, these strategies can include delivery of a correct copy of the *GAA* gene *in cis* or delivery of active GAA enzyme *in trans*. We have employed rAAV vectors to attempt both strategies. We have delivered rAAV vectors directly to the myocardium of *Gaa*^{-/-} mice *via* direct injection into the ventricular wall in order to directly transduce the heart. In parallel and in contrast, we have also delivered rAAV vectors intramuscularly to the quadriceps femoris, as described in the previous chapter, in the hopes that overexpression in the quadriceps will provide secreted, circulating GAA; this circulating pool can then be endocytosed by cardiac and other tissues.

Methods and Materials

All animal procedures were performed in accordance with the guidelines of the University of Florida Institutional Animal Care and Use Committee (IACUC).

Intramyocardial Injections

To facilitate direct injection into cardiac muscle, adult *Gaa*^{-/-} and control mice were anesthetized with an intraperitoneal (IP) injection of a ketamine/xylazine (100mg/kg ketamine; 15mg/kg xylazine) cocktail. Animals were placed in a supine position in a sterile surgical field. The trachea was exposed and a 22G catheter was introduced to facilitate ventilation using an SAR-830AP rodent ventilator (CWE, Ardmore, PA). The animal was ventilated at 110 breaths/min with a tidal volume of 0.2 cc/min. A left thoracotomy was performed, and the ribs were retracted to give full visualization of the left ventricle. Injections of 10 to 50 μ L were carried out with a 29-gauge insulin syringe. The ribs and skin were closed, and the animal was weaned from the ventilator. All animals were monitored overnight for pain or distress and for 1 wk or longer for infection or other complications.

In Vitro Cardiomyocyte Transduction with rAAV1

The preparation of neonatal cardiomyocytes takes two days. The first day is divided into two main activities: 1) media and plate preparation; and 2) dissection, cell isolation, and plating. The second day consists of fibroblast growth arrest and senescent cell culture. All procedures are performed in a sterile tissue culture hood using sterile technique.

Media and plate preparation

First, collagenase (0.1% w/v) is dissolved in 10X trypsin (100 mg/100 mL) in a 37°C water bath, and passed through a filter flask. Plating media consisting of 10% fetal

bovine serum (FBS) and 5% horse serum (HS) is prepared in base media with penicillin-streptomycin supplement, and then filtered into 500 mL or 1 L flask. The base medium consists of Dulbecco's modified Eagle's medium (DMEM) and medium M199 in a 4:1 ratio. Culture media is prepared with 5% HS in base media with penicillin-streptomycin supplement, and then filtered into 500 mL flask.

Collagen-coated plates are prepared by covering plates (or wells) with collagen, allowing them to rest for 5-10 min, and then aspirating the collagen. Plates are then air-dried for 1 h, followed by rinsing with sterile PBS and aspirating.

Dissection, cell isolation, and plating

Neonatal rats (no more than 1 d old) are anesthetized with 20 μ L Nembutol (sodium pentobarbital) per rat and rinsed with 80-90% ethanol. Rats are decapitated with sterile scissors and a midline incision is made from the top of the sternum to the abdomen. Pressure is applied to the sides of the chest cavity, causing the heart to protrude from the thoracic space. The heart is removed with sterile forceps and rinsed in cold PBS in a 50 mL conical tube.

After collecting 5-7 hearts, the PBS is aspirated and the hearts are poured into the lid of a 10 cm dish. The hearts are blotted to remove excess PBS and transferred to the 10 cm dish. Using two sterile scalpels, the hearts are minced in the dish while being kept somewhat moist with small amounts of PBS. The minced hearts are transferred to a 50 mL conical tube on ice and covered with a small amount of cold PBS until another batch of 5-7 hearts can be similarly processed.

Once all of the hearts have been collected they are transferred to a new 50 mL conical tube with 10 mL of warmed trypsin/collagenase. The tube is vortexed and shaken vigorously and placed in a 37°C water bath. The tube is vortexed and shaken every 10

min for 30 min. The contents are permitted to settle and the supernatant is gently aspirated and collected in a new 50 mL conical tube, leaving the pellet. The pellet is processed with another 10 mL warmed trypsin/collagenase and incubated, vortexed, and shaken (as before) for another 30 min. These steps are repeated until no pellet remains. One mL of FBS is added to the supernatant; the contents are pipetted up and down and then spun at 1250 rpm for 5 min. The supernatant is gently aspirated and discarded, leaving both “fluffy” and “dark” layers of pelleted material. This processed pellet is resuspended in 1-2 mL of FBS and kept in the water bath until all of the pellets from the trypsin/collagenase step have been processed.

Resuspended pellets are pooled in 30 mL of plating media (consisting of 10% FBS and 5% HS) and plated in T225 flask. The flask is incubated in a 37°C tissue culture incubator for 50 min. The flask is rocked back and forth lightly and then stood on end. Media are collected and placed into a new 50 mL conical tube. The flask is rinsed lightly with 10 mL fresh plating media and collected again. Collected media are filtered through a cell filter into new 50 mL conical tube and spun at 1250 rpm for 5 min. The resulting pellet is resuspended into an appropriate volume of plating media, pipetted up and down, and then aliquoted into the PBS-rinsed, collagen-coated plates, wells, or slides.

Fibroblast growth arrest

Plating media (10% FBS and 5% HS) and PBS are warmed in a 37°C water bath. Media are aspirated from the plated cells and then the cells are washed vigorously 3 times with PBS. Mitomycin C (50 uL) is added to 5 mL plating media and added to the cells for 3-3.5 h (while incubated in tissue culture incubator). After incubation, the cells are washed 3-4 times with PBS

Senescent cell culture

Culture media (5% HS) is added to the cells and they are returned to the tissue culture incubator. The cells ordinarily start to contract after 2-3 d and should remain viable for 2-3 wk.

Results

Intramyocardial Delivery of rAAV

After intramyocardial injections (10^9 iu rAAV-*mGaa*) in *Gaa*^{-/-} mice we observed similar levels of expression as in skeletal muscle (Figure 6-1, left panel), demonstrating that recombinant murine GAA expression can be directed by rAAV-*mGaa* in both skeletal and cardiac muscle in *Gaa*^{-/-} mice.

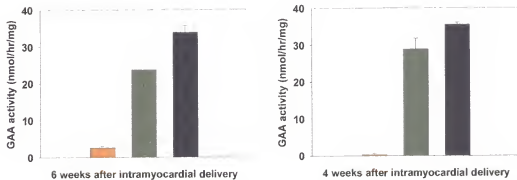


Figure 6-1. Restoration of GAA activity after intramyocardial injection of rAAV2 and rAAV1. (A) 10^9 infectious units of rAAV2-*mGaa* were directly injected into the left-ventricular free wall of *Gaa*^{-/-} mice. (B) 10^{10} particles rAAV1-*hGAA* were delivered. Animals were sacrificed either 4 or 6 wk after injection. Data are plotted as means and standard error. Yellow = *Gaa*^{-/-}, green = treated animals, blue = wild-type.

In a small cohort, we also tested the ability of rAAV1-*hGAA* to direct myocardial synthesis of GAA. Surprisingly, we saw very a little difference between rAAV1-mediated and rAAV2-mediated expression, in contrast to our previous findings in skeletal muscle.

In Vitro Transduction of Rat Cardiomyocytes with rAAV1, 2, and 5

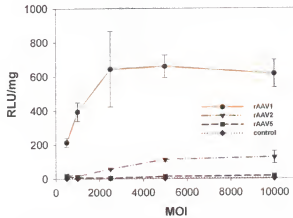


Figure 6-2. *In vitro* transduction of neonatal rat cardiomyocytes with three serotypes of rAAV- β gal. Neonatal rat cardiomyocytes were infected with increasing MOIs of rAAV1, 2, and 5, respectively, and incubated for 4 wk.

Intramuscular Delivery of rAAV1-*hGAA* and Cross-Correction of the Myocardium

We injected the *quadriceps femoris* muscles of *Gaa*^{-/-} mice in an attempt to generate a pool of circulating rhGAA. In a pilot study, we injected 4×10^{11} particles of rAAV1-*hGAA* directly into the quadriceps. Six weeks after intramuscular injection, we measured the enzymatic activity not only in the quadriceps but also several other tissues, including the heart. Enzymatic activities in the heart reached 10% of normal, indicating some transfer of material from the quadriceps to the myocardium (Table 5-1).

Discussion

Our data indicate that rAAV2-*mGaa* delivery to the myocardium of *Gaa*^{-/-} mice effectively restores GAA enzymatic activity, and is among the first examples of rAAV-mediated delivery of a therapeutic gene to the myocardium. Svensson *et al.* described both direct intramyocardial delivery and intracoronary perfusion as potential methods for efficient rAAV delivery to the myocardium using β -galactosidase as a reporter [131]. Recently, direct delivery of rAAV encoding recombinant vascular endothelial growth

factor (rVEGF) has been used to induce neovascularization in an ischemic mouse model. Likewise, Kawada *et al.* have demonstrated restoration of cardiac function in dystrophic mice after direct intramural delivery of rAAV expressing δ -sarcoglycan [120,121]. The present work represents the first attempt to use adeno-associated virus vectors to address a metabolic cardiomyopathy.

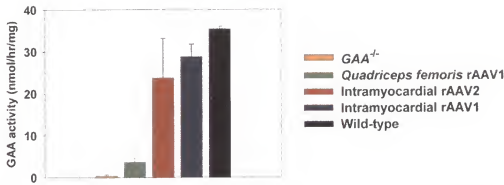


Figure 6-3. Current status of rAAV-mediated gene therapy for myocardial disease in GSDII. Data are reported from treated $Gaa^{-/-}$ mice and wild-type controls, and indicate GAA enzymatic activity after cross-correction (quadriceps femoris delivery) and direct rAAV2 and rAAV1 delivery to the myocardium, respectively.

We have also demonstrated that rAAV1-*hGAA* delivery to the myocardium can effectively restore GAA enzymatic activity. We note that our results were not of the same scale as in skeletal muscle vis à vis rAAV2. We also note that the delivered transgene in this case was also different, and may account for the difference in expression. Future work, employing more effective delivery methods, will provide a better understanding of the potential for rAAV1-mediated transduction of the heart.

Finally, cross-correction of the heart after delivery to other organs remains a real and achievable goal. Our preliminary work in skeletal muscle shows some potential. Other work in our laboratory may lead to more effective transduction of the liver — with even higher levels of enzymatic transfer.

CHAPTER 7

RECOMBINANT ADENO-ASSOCIATED VIRUS DELIVERY TO THE MURINE DIAPHRAGM

Mouse models of human disease provide invaluable opportunities to evaluate the potential efficacy of candidate therapies. Gene therapy strategies in particular have benefited enormously from the profusion of knockout and transgenic mice that recapitulate the genetic and pathophysiologic features of human diseases. Congenital myopathies, including the muscular dystrophies, have been widely investigated as targets for gene therapy interventions, and the diaphragm is often cited as one of the important target organs for functional correction [171].

The mouse diaphragm presents unique challenges in terms of delivery of therapeutic agents due to its small size and thickness, which preclude direct injection into the muscle. Intravenous or intra-arterial delivery of vectors may be effective alternatives and are currently under investigation [172,173]; however, isolation of blood vessels that specifically perfuse the diaphragm is also difficult in the mouse. Systemic delivery of vectors may eventually require the application of capsid-based targeting methods that have recently been reported [174-180].

As stated in Chapter 1, recombinant adeno-associated virus is a single-stranded DNA-containing, non-pathogenic human parvovirus that is being widely investigated as a therapeutic vector for a host of muscle disorders [64,66,70,104]. Six serotypes of the virus (AAV1-6) were originally described, and two more have recently been identified in rhesus macaques [95]. Using helper plasmids expressing various combinations of the

AAV2 *rep* and AAV1, 2, and 5 *cap* genes, respectively, our group and others have demonstrated efficient cross-packaging of AAV2 genomes into particles containing the AAV1, 2, or 5 capsid proteins [100,101,103,181]. The various serotype vectors have demonstrated distinct tropisms for different tissue types *in vivo*, due in part to their putative cell surface receptors. Although several reports have indicated that rAAV1 vectors efficiently transduce skeletal muscle in general [97,98,111,113], no study to date has reported which of the serotypes, if any, might transduce the diaphragm in particular.

The aim of this study is to provide a safe, effective, and uniform method for delivery of recombinant adeno-associated virus vectors to the mouse diaphragm in order to evaluate their potential as therapeutic agents. We evaluate the ability of rAAV serotypes 1, 2, and 5 to transduce the mouse diaphragm. We further describe the application of a gel-based delivery method and demonstrate its utility for delivery of rAAV1, 2, and 5 to the mouse diaphragm. Our results are the first to demonstrate efficient, uniform expression of a transgene in the murine diaphragm using rAAV vectors. Finally, we assess the utility of this method using a mouse model (*Gaa*^{-/-}) of glycogen storage disease type II (GSDII) [28], an autosomal recessive disorder that is characterized by respiratory insufficiency secondary to diaphragmatic weakness in affected juveniles [10]. We believe the method we describe may have broad applicability for delivery of gene therapy vectors not only to the diaphragm but perhaps to other tissues as well.

Methods and Materials

Packaging and Purification of Recombinant AAV1, 2, and 5 vectors

The recombinant AAV2 plasmids pAAV-*βgal* [64] and p43.2-*GAA* [98] have been described previously. Recombinant AAV vectors were generated, purified, and titered at

the University of Florida Powell Gene Therapy Center Vector Core Lab as previously described [101]. Recombinant AAV particles based on serotypes 1, 2, and 5 were produced using pAAV-*βgal*, whereas only rAAV1 particles (rAAV1-*GAA*) were packaged with p43.2-*GAA*.

Vector-Vehicle Preparation

A sterile, bacteriostatic, water-soluble, glycerin-based gel was used as a vehicle for vector application to the diaphragm (K-Y® Sterile, Johnson & Johnson Medical, Arlington, TX). Individual doses of virus were diluted in sterile phosphate buffered saline (PBS) for a total volume of 10 μL and then added to 150 μL of gel in a 2 mL microcentrifuge tube. The virus-vehicle suspension was vortexed for 1 min and then centrifuged for 1 min at maximum speed. Free virus was diluted in sterile PBS for a total volume of 50 μL.

***In Vivo* Delivery**

All animal studies were performed in accordance with the guidelines of the University of Florida Institutional Animal Care and Use Committee. Adult 129X1 x C57BL/6 (wild-type) or *Gaa*^{-/-} mice [28] were anesthetized using 2% isoflurane and restrained supine on a warmed operating surface. In a sterile field, after reaching a surgical plane of anesthesia, a midline incision was made through the skin extending from the xyphoid process to the suprapubic region. An incision was made through the abdominal wall following the *linea alba*. The abdominal walls were retracted laterally and the intestines were displaced to the left side of the animal and covered with sterile gauze soaked in warm saline. The gall bladder was carefully separated from the rib cage, and the liver was carefully retracted from the diaphragm using sterile cotton swabs.

While lifting the xyphoid, free virus or virus mixed with vehicle were applied directly to the abdominal surface of the diaphragm. Free virus was applied using a pipet. To facilitate application of the gel to the diaphragm, a 22 G needle was used to puncture the bottom of the microcentrifuge tube and a plunger from a 3 cc syringe was used to force the gel through the hole and onto the diaphragm surface (Figure 7-1). In some cases, a cotton-tipped applicator was used to ensure even spread over the entire diaphragm. After 5 min the intestines were returned to their original position, the abdominal muscles were sutured, and the skin was finally closed. Subcutaneous ampicillin (20-100 mg/kg) and buprenorphine (0.1 mg/kg) were administered prior to removing the animal from anesthesia.

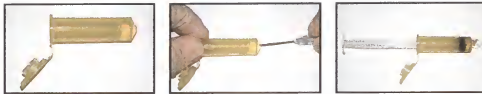


Figure 7-1. Gel-based delivery preparation. (A) rAAV vectors are mixed in a 2 mL microcentrifuge tube and then centrifuged briefly. (B) The tube is punctured using a 22G needle, creating an aperture through which the virus-gel suspension can be propelled. (C) A plunger from a standard 3cc syringe is used to push the vector from the tube, enabling its application to the diaphragmatic surface. The oblique, bottom surface of the microcentrifuge tube is used to distribute the vector-gel suspension evenly on the surface.

Assays of β -galactosidase and GAA Enzymatic Activity

Six weeks after the surgical procedure and gene delivery, tissue lysates were assayed for enzyme activity using the Galacto-Star chemiluminescent reporter gene assay system (Tropix Inc., Bedford, MA). Protein concentrations for tissue lysates were determined using the Bio-Rad *DC* Protein Assay Kit (Bio-Rad, Hercules, CA). For rAAV1-*GAA* treated animals, enzymatic activity assays for GAA were performed 6 wk

after vector delivery as described previously [98]. Tissue homogenates were assayed for GAA activity by measuring the cleavage of the synthetic substrate 4-methylumbelliferyl- α -D-glucoside (Sigma M9766, Sigma-Aldrich, St. Louis, MO) after incubation for 1 h at 37°C. Successful cleavage yielded a fluorescent product that emits at 448 nm, as measured with an FLx800 microplate fluorescence reader (Bio-Tek Instruments, Winooski, VT). Protein concentration was measured as described above. Data are represented as nanomoles of substrate cleaved in one hour per milligram of total protein in the lysate (nmol/h/mg).

Histological Assessment of Glycogen Clearance

Segments of treated and untreated diaphragm were also fixed overnight in 2% glutaraldehyde in PBS, embedded in epon, sectioned, and stained with periodic acid-Schiff (PAS) by standard methods.

Biodistribution of Vector Genomes

Tissues were removed using sterile instruments and snap-frozen in liquid nitrogen. Total cellular DNA was extracted from tissue homogenates using a QIAGEN DNeasy kit per the manufacturer's instructions (QIAGEN, Valencia, CA). Nested PCR reactions were performed as follows: 1.5 μ g total DNA was used as a template for the initial PCR amplification using the sense primer 5'-AGCTGGCGTAATAGCGAAGA-3' and reverse primer 5'-CGCGTCTCTCCAGGTAGCGAA-3', yielding a 1486-bp product. The PCR product was purified using the QIAGEN MinElute PCR purification kit per the manufacturer's instructions, followed by PCR amplification using the sense primer 5'-CGGTGATGGTCTGCGTTGGAG-3' and reverse primer 5'-TCGACGTTTCAGACGTAGTGT-3', resulting in a final product of 333 bp. All reactions

were performed under the following conditions: hot start denaturation at 94°C for 5 min, followed by 30 cycles of denaturation at 94°C for 1 min, annealing at 62°C for 1 min, and extension at 72°C for 2 min. Products were electrophoresed analyzed using a 2% agarose gel.

Results

Efficiency of Transduction Using Gel-Based Delivery of rAAV *In Vivo*

We investigated the efficiency of rAAV delivery using the gel-based method compared to free virus delivery using β -galactosidase as a reporter gene (Figure 7-2A). Direct particle-to-particle comparisons of histochemistry from free virus-treated animals (left column) versus gel-based delivery (right column) indicate an increased efficiency of transduction for all serotypes using the latter method. Quantitative analysis of tissue lysates from these animals using the Galacto-Star enzymatic assay for β -galactosidase confirms these results (Figure 7-2B). Activities for subjects treated with gel-vector suspensions had higher activities for all 3 serotypes.

Varying Tropisms of rAAV Serotypes 1, 2, and 5 for Diaphragm *In Vivo*

The results from Figures 7-2A and 7-2B also indicate a distinct gradient of tropism for mouse diaphragm among the 3 tested serotypes. Qualitatively, rAAV1 vectors led to the most intense staining in both the free virus and gel-based conditions. Differences between rAAV2 and rAAV5 were hard to distinguish in the free virus case due to the low levels of transduction for both vectors, but the gel-mediated subjects demonstrated a clear preference for rAAV2 compared to rAAV5. These results are further verified in Figure 7-2B, which indicates higher levels of enzyme activity for rAAV2-gel suspensions compared to rAAV5. Taken together, the results of histochemical staining and enzymatic activity indicate 1) a substantial increase in viral transduction using a physical delivery

system and 2) a clearly enhanced mouse diaphragm tropism for rAAV1, and a potentially important difference between rAAV2 and rAAV5.

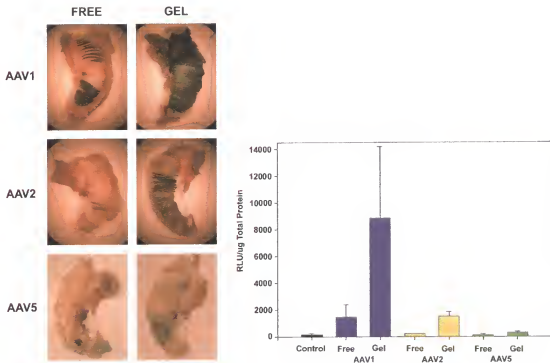


Figure 7-2. Free virus and gel-based delivery of rAAV- β gal vectors based on AAV serotypes 1, 2, and 5. Adult wild-type mice (129X1xC57BL/6) were treated with 10^{11} particles of rAAV- β gal, with virus either directly applied to the diaphragm or applied using the gel-based method. (A) Histochemical (X-gal) stained diaphragm segments from treated animals. Each row corresponds to the respective serotype (AAV1, 2, and 5, respectively) and columns represent application of free virus (left) or virus-gel suspension (right) respectively. (B) Quantitative assay of β -galactosidase activity from the same animals. The bar graph represents mean \pm SEM β -galactosidase activity for 3 mice in each group.

Biochemical Correction of Diaphragms of *Gaa*^{-/-} Mice with Gel-Based Delivery of rAAV1-GAA

Having demonstrated increased transduction of the mouse diaphragm using the gel-based method, we assessed the ability of this method to restore enzymatic activity in a mouse model of glycogen storage disease type II (GSDII; MIM 232300), a lysosomal glycogen storage disease caused by a lack or deficiency of the lysosomal enzyme, acid a-

glucosidase (GAA; EC 3.2.1.20). The mouse model of this disease stores glycogen in all tissues, with significant pathologies in the heart and skeletal muscle [6]. We have previously characterized the use of rAAV vectors to restore enzymatic and functional activity in skeletal and cardiac muscle in these mice [98]. Coupled with our new findings using a gel-based delivery method, we hypothesized that gel-based delivery of rAAV1-*GAA* would be able to restore GAA activity in *Gaa*^{-/-} diaphragms and, in turn, reverse lysosomal glycogen accumulation.

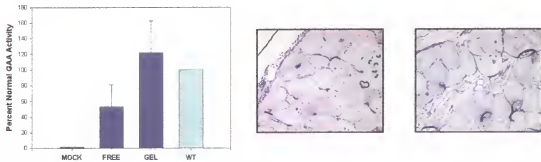


Figure 7-3. rAAV1-*hGAA*-mediated transduction of diaphragms *Gaa*^{-/-} mice. (A) Adult *Gaa*^{-/-} mice were treated with 10^{11} particles of rAAV1-*hGAA* in the quadriceps muscle. Wild-type (wt) and untreated *Gaa*^{-/-} (mock) mice were used as controls. Muscle tissues were isolated at 6 wk after treatment and assayed for GAA activity. The bar graph represents mean \pm SEM GAA activity for 3 mice in each group. (B) Representative sections of sections from free vector (left) and gel-based vector treated (right) *Gaa*^{-/-} mouse diaphragms, stained for glycogen using periodic acid-Schiff's reagent. Glycogen containing vacuoles and regions acquire a pink stain using this technique.

Using rAAV1-*GAA* vectors, we found increases in diaphragmatic transduction in *Gaa*^{-/-} mice similar to those seen in control mice with β -galactosidase vector. GAA enzymatic activities were restored to 50% of wild-type with free vector, and were further increased to 120% of normal levels using a vector-gel suspension (Figure 7-3A). These activities had a profound effect in glycogen storage, as assessed by periodic acid-Schiff's reagent (PAS) staining (Figure 7-3B). Dark pink vacuoles are observed in free vector

treated diaphragms from *Gaa*^{-/-} mice compared to a near-complete reversal of glycogen accumulation from diaphragms of gel-treated mice.

Biodistribution of rAAV Genomes After Gel-Based Delivery

Since a secondary advantage of physical delivery systems may be the ability to restrict viral spread, we also sought to determine which tissues endocytosed our viral vectors after gel-based delivery. We collected and homogenized various tissues from rAAV1-*βgal*-gel treated mice and extracted total cellular DNA. Using a nested PCR technique, we amplified a portion of the *β*-galactosidase gene from vector genomes (Figure 7-4). As expected, vector genomes could be detected in treated diaphragms. We could not detect vector genomes in any other tissue examined, including sections of the peritoneal wall and liver adjacent to the diaphragm.

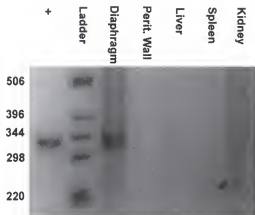


Figure 7-4. Biodistribution of rAAV1 vector genomes after gel-based delivery. Nested PCR was used to amplify AAV genomes carrying the *β*-galactosidase gene after isolating tissues from gel-based rAAV1-*βgal* treated mice. Total cellular DNA was extracted and AAV genomes were amplified using primers specific for the *βgal* transgene. The expected product is 333 bp, and the positive control is the vector plasmid that was used to package the rAAV particles.

Discussion

Transduction events for recombinant adeno-associated viruses can be separated into five general stages: 1) binding and entry (endocytosis), 2) endosomal processing and escape, 3) transcytosis, 4) nuclear import and uncoating, and 5) genome conversion, including second-strand synthesis (or alternatively self-complementation) followed by genome concatemerization and/or integration into the host chromosome. We have sought in this report to enhance the first step of this process using a physical method to prolong viral dwell time -- we expect to increase the efficiency of transduction by providing longer viral particle exposure times to receptors on target tissues.

Carrier molecules and delivery agents have been used extensively for gene therapy applications, particularly for non-viral gene delivery. With regards to viral vectors, recombinant adenoviruses have been used in concert with a variety of agents in order to increase or prolong bioavailability, thereby enhancing the efficiency of delivery. March and colleagues [182] reported the use of poloxamer 407, a hydrogel which exhibits potentially useful, thermo-reversible gelation, enabling formulation at low temperature with subsequent hardening to a robust gel at room and physiologic temperatures. They demonstrated increased transduction of vascular smooth muscle cells *in vitro*, with similar findings reported *in vivo* by Van Belle *et al.* [183]. Unfortunately, poloxamers have recently been shown to have adverse effects on adeno-associated virus stability [184]. Likewise, thixotropic solutions have also shown promise for enhancing adenovirus-mediated transduction of airway epithelia [185]. Several other promising agents have also been effectively used with adenovirus vectors, including beta-cyclodextrins, surfactants, and collagen or gelatin-based matrices.

While extensive testing of potential adenovirus formulations has been reported, few similar studies are extant for adeno-associated viruses. Most of the available literature describes formulations that increase stability for storage or purification, but few reports address the need for augmented physical delivery of viral particles *in vivo*. We have previously described the use of microsphere-conjugated rAAV for systemic delivery of viral vectors [186]. In that study, we were able to achieve high-efficiency transduction of cells in targeted tissue beds by increasing vector dwell time. Similarly, a number of groups are currently developing capsid-modified rAAV vectors to target specific vascular beds upon systemic delivery. To date, however, we are unaware of other examples of physical delivery agents or methods to improve rAAV delivery to tissue surfaces, such as skin, blood vessel adventitia, or diaphragm. The method that we describe has been specifically applied to the diaphragm, but we anticipate that this formulation or similar ones will have broad utility for a variety of tissues, both for preclinical proof-of-principle studies and perhaps for eventual clinical applications.

Previous studies of gene transfer to the diaphragm in rodents have been attempted *via* delivery of non-viral or adenoviral gene transfer vectors. Liu *et al.* recently described a method for systemic delivery of plasmid DNA carrying the full-length dystrophin gene with subsequent targeting to the diaphragm in *mdx* mice [173], a mouse strain with X-linked muscular dystrophy that mimics the diaphragmatic degeneration observed in Duchenne muscular dystrophy [187]. In that study, which used no carrier molecules, plasmid DNA was delivered intravenously *via* tail vein followed by transient (8-second) occlusion of the vena cava at the level of the diaphragm. High levels of gene expression were measured in diaphragm homogenates the next day and for 180 d [173], implicating

dwelling time as potentially the most significant determinant of successful gene transfer to the diaphragm with naked DNA. Two reports [188,189], by Petrof, Yang, and colleagues, also indicated successful direct injection of recombinant adenoviruses carrying a mini-dystrophin gene to the diaphragms of *mdx* mice. Both studies demonstrated high levels of expression focally, presumably due to the delivery method. Transient gene expression, caused by vector-related, dose-dependent inflammation, made assessment of the uniformity of gene expression difficult, but even with focal expression the authors observed measurable improvements in contractile function. More recently, Sakamoto *et al.* have developed an *mdx* strain that is transgenic for a micro-dystrophin construct [116], which is within the packaging capacity of rAAV. We are hopeful that the combination of the micro-dystrophin transgene and gel-based delivery of rAAV will soon lead to uniform phenotypic correction in diaphragms of *mdx* mice.

Comparisons of rAAV serotype tropisms for skeletal muscle have already been reported [97,98,111,113]. Several recombinant AAV vectors based on alternative serotypes have demonstrated greater transduction efficiencies in skeletal muscle than serotype 2. In particular, several reports have shown nearly one log greater expression of a variety of transgenes when packaged in rAAV1 capsids compared to rAAV2. Similar findings have been reported with rAAV6, although this serotype has not been as widely used. We note that the eight-fold over-expression of GAA in Gaa-deficient diaphragms after delivery of free rAAV1-GAA compared to serotype 2 (Figure 7-2B, AAV1-Free v. AAV2-Free) is nearly identical to our prior observations after direct intramuscular administration of the same 2 vectors in tibialis anterior muscles of *Gaa*^{-/-} mice [98], indicating a conserved rAAV1 tropism for skeletal muscle.

CHAPTER 8

CONCLUSIONS AND FUTURE DIRECTIONS

The application of biotherapeutics to clinical problems is the logical extension of the last 40 years of biomedical research. From the development of recombinant DNA to the large-scale manufacture of biological agents, new strategies to address disease are under continuous development and improvement.

Lysosomal storage disorders present unique challenges for new classes of biotherapeutics. A dedicated cell-surface and intracellular receptor; unique organelle biogenesis and maturation; and a diverse cargo of cellular debris and byproducts, all in an acidic environment give rise to a biological milieu that is distinct from any other compartment, yet exists in the context of a complete organism. Coupled with the variegated tissues and organs of pathogenesis, these disorders will present uniform opportunities as a group and unique challenges as individual syndromes.

Glycogen storage disease type II is a classic lysosomal storage disorder and is an excellent target for a host of potential therapies. Recombinant protein therapeutics are in clinical trials and show some promise although the results of the trials are not yet available. However, despite their similarity in glycosylation and site of action, these agents have not had the same potency as some of their counterparts for other lysosomal diseases. Issues related to immune response, dosing regimens and routes, differential uptake in various tissues, and manufacturing capacity continue to present concerns, though current efforts are attempting to address each of these challenges.

Gene therapies, and recombinant adeno-associated viral gene therapy in particular, continue to provide hope for a correct alternative. The data from this study indicates that rAAV1 vectors have broad tropism for skeletal muscle; that these vectors can restore enzymatic activity to affected tissues and clear glycogen; and that this restoration may lead to functional preservation and/or recovery in muscle tissues. We have demonstrated, in several studies, the skeletal muscle tropism of rAAV1 vectors and have shown the ability of physical delivery methods to augment the already substantial transduction efficiency of rAAV1 in the diaphragm.

Preclinical, rAAV gene therapy studies for GSDII will need to address some of the new questions posed by our work. These questions are several-fold:

- Is overexpression of GAA cytotoxic, as suggested by Raben and potentially observed in our high-dose rAAV1 study?
- Is the age of treatment critical, as proposed by Reuser in the first enzyme replacement trials? Is muscle damage in GSDII reversible, and/or should therapy include stimulation of muscle regeneration (either pharmacologically or otherwise)?
- Do rAAV1 vectors infect dendritic cells or modulate immune responses differently than rAAV2 or other serotype vectors? Does the route of administration (intramuscular v. other modalities) substantially alter the immune response to rAAV-mediated transgenes?
- Are there combinations or modifications of current technologies that can enhance rAAV-mediated therapy for GSDII including tissue-specific or regulatable promoters; epitope-targeted or primate-derived rAAV vectors; or combinations of pharmacologic agents and gene therapy vectors?

Our laboratory and others are currently addressing these questions and others. The work of Kerry Cresawn in our laboratory will be critical to understanding the immune response in rAAV-mediated therapies and strategies for blunting that response. Her work will also provide a second platform for cross-correction with new vectors to transduce the

liver. Despite these remaining questions, gene therapy for GSDII is poised (for the first time) to enter preclinical toxicity testing. We are hopeful that the results of those trials will provide a justification for human trials and a viable therapeutic modality for GSDII patients.

REFERENCES

1. Hoyert DL, Arias E, Smith BL, Murphy SL, Kochanek KD. Deaths: final data for 1999. *Natl Vital Stat Rep.* 2001;49:1-113.
2. State of Florida Department of Health. Florida vital statistics annual report 2000. http://www9.myflorida.com/Planning_eval/vital_statistics/00vitals/00VSCOMP.pdf. Accessed 10-29-2001. Electronic Citation.
3. Nabel EG. Gene therapy for cardiovascular disease. *Circulation.* 1995;91:541-548.
4. Hajjar RJ, del Monte F, Matsui T, Rosenzweig A. Prospects for gene therapy for heart failure. *Circ Res.* 2000;86:616-621.
5. Hers HG. Alpha-glucosidase deficiency in generalized glycogen storage disease (Pompe's disease). *Biochem J.* 1963;86:11.
6. Hirschhorn R, Reuser AJJ. Glycogen storage disease II: acid-alpha glucosidase (acid maltase) deficiency. In: Scriver CR, Beaudet AL, Sly WS, Valle D, editors. *Metabolic Basis of Inherited Disease.* New York: McGraw Hill, 2000: 3389-3420.
7. Reuser AJ, Kroos MA, Hermans MM, Bijvoet AG, Verbeet MP, Van Diggelen OP, Kleijer WJ, Van der Ploeg AT. Glycogenosis type II (acid maltase deficiency). *Muscle Nerve.* 1995;3:S61-S69.
8. van den Hout HM, Hop W, Van Diggelen OP, Smeitink JA, Smit GP, Poll-The BT, Bakker HD, Loonen MC, de Klerk JB, Reuser AJ, Van der Ploeg AT. The natural course of infantile Pompe's disease: 20 original cases compared with 133 cases from the literature. *Pediatrics.* 2003;112:332-340.
9. Engel AG, Gomez MR, Seybold ME, Lambert EH. The spectrum and diagnosis of acid maltase deficiency. *Neurology.* 1973;23:95-106.
10. Moufarrej NA, Bertorini TE. Respiratory insufficiency in adult-type acid maltase deficiency. *South Med J.* 1993;86:560-567.
11. Papapetropoulos T, Paschalis C, Manda P. Myopathy due to juvenile acid maltase deficiency affecting exclusively the type I fibres. *J Neurol Neurosurg Psychiatry.* 1984;47:213-215.

12. Ausems MG, Lochman P, Van Diggelen OP, Ploos van Amstel HK, Reuser AJ, Wokke JH. A diagnostic protocol for adult-onset glycogen storage disease type II. *Neurology*. 1999;52:851-853.
13. Bodamer OA, Leonard JV, Halliday D. Dietary treatment in late-onset acid maltase deficiency. *Eur J Pediatr*. 1997;156 Suppl 1:S39-S42.
14. Radojevic V, Humm AM, Rosler KM, Lauterburg T, Burgunder JM. Abnormal trafficking of sarcolemmal proteins in alpha-glucosidase deficiency. *Acta Neuropathol (Berl)*. 2003;105:373-380.
15. Slonim AE, Coleman RA, McElligot MA, Najjar J, Hirschhorn K, LaBadie GU, Mrak R, Evans OB, Shipp E, Presson R. Improvement of muscle function in acid maltase deficiency by high-protein therapy. *Neurology*. 1983;33:34-38.
16. Watson JG, Gardner-Medwin D, Goldfinch ME, Pearson AD. Bone marrow transplantation for glycogen storage disease type II (Pompe's disease). *N Engl J Med*. 1986;314:385.
17. Bodamer OA, Halliday D, Leonard JV. The effects of l-alanine supplementation in late-onset glycogen storage disease type II. *Neurology*. 2000;55:710-712.
18. Bodamer OA, Haas D, Hermans MM, Reuser AJ, Hoffmann GF. L-alanine supplementation in late infantile glycogen storage disease type II. *Pediatr Neurol*. 2002;27:145-146.
19. Mayes PA. Metabolism of Glycogen. In: Murray RK, Granner DK, Mayes PA, Rodwell VW, editors. *Harper's Biochemistry*. Stamford, CT: Appleton & Lange, 2000: 199-207.
20. Raben N, Plotz P, Byrne BJ. Acid alpha-glucosidase deficiency (glycogenosis type II, Pompe disease). *Curr Mol Med*. 2002;2:145-166.
21. Kornfeld S. Lysosomal enzyme targeting. *Biochem Soc Trans*. 1990;18:367-374.
22. Hasilik A, Neufeld EF. Biosynthesis of lysosomal enzymes in fibroblasts. Synthesis as precursors of higher molecular weight. *J Biol Chem*. 1980;255:4937-4945.
23. Hoefsloot LH, Willemsen R, Kroos MA, Hoogeveen-Westerveld M, Hermans MM, Van der Ploeg AT, Oostra BA, Reuser AJ. Expression and routing of human lysosomal alpha-glucosidase in transiently transfected mammalian cells. *Biochem J*. 1990;272:485-492.
24. Fuller M, Van der Ploeg A, Reuser AJ, Anson DS, Hopwood JJ. Isolation and characterisation of a recombinant, precursor form of lysosomal acid alpha-glucosidase. *Eur J Biochem*. 1995;234:903-909.

25. Wisselaar HA, Kroos MA, Hermans MM, van Beeumen J, Reuser AJ. Structural and functional changes of lysosomal acid alpha-glucosidase during intracellular transport and maturation. *J Biol Chem*. 1993;268:2223-2231.
26. Neufeld EF. Lysosomal storage diseases. [Review]. *Annu Rev Biochem*. 1991;60:257-80:257-280.
27. Van der Ploeg AT, Loonen MC, Bolhuis PA, Busch HM, Reuser AJ, Galjaard H. Receptor-mediated uptake of acid alpha-glucosidase corrects lysosomal glycogen storage in cultured skeletal muscle. *Pediatr Res*. 1988;24:90-94.
28. Raben N, Nagaraju K, Lee E, Kessler P, Byrne B, Lee L, LaMarca M, King C, Ward J, Sauer B, Plotz P. Targeted disruption of the acid alpha-glucosidase gene in mice causes an illness with critical features of both infantile and adult human glycogen storage disease type II. *J Biol Chem*. 1998;273:19086-19092.
29. Bijvoet AG, van de Kamp EH, Kroos MA, Ding JH, Yang BZ, Visser P, Bakker CE, Verbeet MP, Oostra BA, Reuser AJ, Van der Ploeg AT. Generalized glycogen storage and cardiomegaly in a knockout mouse model of Pompe disease. *Hum Mol Genet*. 1998;7:53-62.
30. Raben N, Nagaraju K, Lee E, Plotz P. Modulation of disease severity in mice with targeted disruption of the acid alpha-glucosidase gene. *Neuromuscul Disord*. 2000;10:283-291.
31. Kamphoven JH, Stubenitsky R, Reuser AJ, Van der Ploeg AT, Verdouw PD, Duncker DJ. Cardiac remodeling and contractile function in acid alpha-glucosidase knockout mice. *Physiol Genomics*. 2001;5:171-179.
32. Raben N, Lu N, Nagaraju K, Rivera Y, Lee A, Yan B, Byrne B, Meikle PJ, Umaphysivam K, Hopwood JJ, Plotz PH. Conditional tissue-specific expression of the acid alpha-glucosidase (GAA) gene in the GAA knockout mice: implications for therapy. *Hum Mol Genet*. 2001;10:2039-2047.
33. Gossen M, Bujard H. Tight control of gene expression in mammalian cells by tetracycline-responsive promoters. *Proc Natl Acad Sci U S A*. 1992;89:5547-5551.
34. Grabowski GA. Perspectives on gene therapy for lysosomal storage diseases that affect hematopoiesis. *Curr Hematol Rep*. 2003;2:356-362.
35. de Barse T, Jacquemin P, Van Hoof F, Hers HG. Enzyme replacement in Pompe disease: an attempt with purified human acid alpha-glucosidase. *Birth Defects Orig Artic Ser*. 1973;9:184-190.
36. Reuser AJ, Kroos MA, Ponne NJ, Wolterman RA, Loonen MC, Busch HF, Visser WJ, Bolhuis PA. Uptake and stability of human and bovine acid alpha-glucosidase in cultured fibroblasts and skeletal muscle cells from glycogenosis type II patients. *Exp Cell Res*. 1984;155:178-189.

37. Van der Ploeg AT, Kroos M, van Dongen JM, Visser WJ, Bolhuis PA, Loonen MC, Reuser AJ. Breakdown of lysosomal glycogen in cultured fibroblasts from glycogenosis type II patients after uptake of acid alpha- glucosidase. *J Neurol Sci.* 1987;79:327-336.
38. Hermans MM, Wisselaar HA, Kroos MA, Oostra BA, Reuser AJ. Human lysosomal alpha-glucosidase: functional characterization of the glycosylation sites. *Biochem J.* 1993;289 (Pt 3):681-686.
39. Martiniuk F, Mehler M, Pellicer A, Tzall S, La Badie G, Hobart C, Ellenbogen A, Hirschhorn R. Isolation of a cDNA for human acid alpha-glucosidase and detection of genetic heterogeneity for mRNA in three alpha-glucosidase-deficient patients. *Proc Natl Acad Sci U S A.* 1986;83:9641-9644.
40. Hoefsloot LH, Hoogeveen-Westerveld M, Kroos MA, van Beeumen J, Reuser AJ, Oostra BA. Primary structure and processing of lysosomal alpha-glucosidase; homology with the intestinal sucrase-isomaltase complex. *EMBO J.* 1988;7:1697-1704.
41. Van Hove JL, Yang HW, Wu JY, Brady RO, Chen YT. High-level production of recombinant human lysosomal acid alpha-glucosidase in Chinese hamster ovary cells which targets to heart muscle and corrects glycogen accumulation in fibroblasts from patients with Pompe disease. *Proc Natl Acad Sci U S A.* 1996;93:65-70.
42. Kikuchi T, Yang HW, Pennybacker M, Ichihara N, Mizutani M, Van Hove JL, Chen YT. Clinical and metabolic correction of pompe disease by enzyme therapy in acid maltase-deficient quail. *J Clin Invest.* 1998;101:827-833.
43. Bijvoet AG, Kroos MA, Pieper FR, De Boer HA, Reuser AJ, Van der Ploeg AT, Verbeet MP. Expression of cDNA-encoded human acid alpha-glucosidase in milk of transgenic mice. *Biochim Biophys Acta.* 1996;1308:93-96.
44. Bijvoet AG, Van Hirtum H, Kroos MA, van de Kamp EH, Schoneveld O, Visser P, Brakenhoff JP, Weggeman M, van Corven EJ, Van der Ploeg AT, Reuser AJ. Human acid alpha-glucosidase from rabbit milk has therapeutic effect in mice with glycogen storage disease type II. *Hum Mol Genet.* 1999;8:2145-2153.
45. Bijvoet AG, Kroos MA, Pieper FR, Van d, V, De Boer HA, Van der Ploeg AT, Verbeet MP, Reuser AJ. Recombinant human acid alpha-glucosidase: high level production in mouse milk, biochemical characteristics, correction of enzyme deficiency in GSDII KO mice. *Hum Mol Genet.* 1998;7:1815-1824.
46. Reuser AJ, Van Den HH, Bijvoet AG, Kroos MA, Verbeet MP, Van der Ploeg AT. Enzyme therapy for Pompe disease: from science to industrial enterprise. *Eur J Pediatr.* 2002;161 Suppl 1:S106-S111.

47. Van den Hout H, Reuser AJ, Vulto AG, Loonen MC, Cromme-Dijkhuis A, Van der Ploeg AT. Recombinant human alpha-glucosidase from rabbit milk in Pompe patients. *Lancet*. 2000;356:397-398.
48. Van den Hout JM, Reuser AJ, de Klerk JB, Arts WF, Smeitink JA, Van der Ploeg AT. Enzyme therapy for pompe disease with recombinant human alpha-glucosidase from rabbit milk. *J Inherit Metab Dis*. 2001;24:266-274.
49. Winkel LP, Kamphoven JH, Van Den Hout HJ, Severijnen LA, Van Doorn PA, Reuser AJ, Van der Ploeg AT. Morphological changes in muscle tissue of patients with infantile Pompe's disease receiving enzyme replacement therapy. *Muscle Nerve*. 2003;27:743-751.
50. Amalfitano A, Bengur AR, Morse RP, Majure JM, Case LE, Veerling DL, Mackey J, Kishnani P, Smith W, McVie-Wylie A, Sullivan JA, Hoganson GE, Phillips JA, III, Schaefer GB, Charrow J, Ware RE, Bossen EH, Chen YT. Recombinant human acid alpha-glucosidase enzyme therapy for infantile glycogen storage disease type II: results of a phase I/II clinical trial. *Genet Med*. 2001;3:132-138.
51. National Institutes of Health. ClinicalTrials.gov, a service of the National Institutes of Health. <http://www.clinicaltrials.gov/ct/search>. Accessed 10-1-2003. Electronic Citation.
52. Raben N, Danon M, Gilbert AL, Dwivedi S, Collins B, Thurberg BL, Mattaliano RJ, Nagaraju K, Plotz PH. Enzyme replacement therapy in the mouse model of Pompe disease. *Mol Genet Metab*. 2003;80:159-169.
53. Hoefsloot LH, Hoogeveen-Westerveld M, Reuser AJ, Oostra BA. Characterization of the human lysosomal alpha-glucosidase gene. *Biochem J*. 1990;272:493-497.
54. Zaretsky JZ, Candotti F, Boerkoel C, Adams EM, Yewdell JW, Blaese RM, Plotz PH. Retroviral transfer of acid alpha-glucosidase cDNA to enzyme-deficient myoblasts results in phenotypic spread of the genotypic correction by both secretion and fusion. *Hum Gene Ther*. 1997;8:1555-1563.
55. Pauly DF, Johns DC, Matelis LA, Lawrence JH, Byrne BJ, Kessler PD. Complete correction of acid alpha-glucosidase deficiency in Pompe disease fibroblasts in vitro, and lysosomally targeted expression in neonatal rat cardiac and skeletal muscle. *Gene Ther*. 1998;5:473-480.
56. Nicolino MP, Puech JP, Kremer EJ, Reuser AJ, Mbebi C, Verdiere-Sahuque M, Kahn A, Poenaru L. Adenovirus-mediated transfer of the acid alpha-glucosidase gene into fibroblasts, myoblasts and myotubes from patients with glycogen storage disease type II leads to high level expression of enzyme and corrects glycogen accumulation. *Hum Mol Genet*. 1998;7:1695-1702.

57. Amalfitano A, McVie-Wylie AJ, Hu H, Dawson TL, Raben N, Plotz P, Chen YT. Systemic correction of the muscle disorder glycogen storage disease type II after hepatic targeting of a modified adenovirus vector encoding human acid-alpha-glucosidase. *Proc Natl Acad Sci U S A*. 1999;96:8861-8866.
58. Pauly DF, Fraites TJ, Toma C, Bayes HS, Huie ML, Hirschhorn R, Plotz PH, Raben N, Kessler PD, Byrne BJ. Intercellular transfer of the virally derived precursor form of acid alpha-glucosidase corrects the enzyme deficiency in inherited cardioskeletal myopathy Pompe disease. *Hum Gene Ther*. 2001;12:527-538.
59. Flotte TR, Ferkol TW. Genetic therapy. Past, present, and future. *Pediatr Clin North Am*. 1997;44:153-178.
60. Martiniuk F, Chen A, Mack A, Donnabella V, Slonim A, Bulone L, Arvanitopoulos E, Raben N, Plotz P, Rom WN. Helios gene gun particle delivery for therapy of acid maltase deficiency. *DNA Cell Biol*. 2002;21:717-725.
61. Flotte TR, Carter BJ. Adeno-associated virus vectors for gene therapy. *Gene Ther*. 1995;2:357-362.
62. Berns KI, Giraud C. Biology of adeno-associated virus. *Curr Top Microbiol Immunol*. 1996;218:1-23.
63. Podsakoff G, Wong KK, Jr., Chatterjee S. Efficient gene transfer into nondividing cells by adeno-associated virus-based vectors. *J Virol*. 1994;68:5656-5666.
64. Kessler PD, Podsakoff GM, Chen X, McQuiston SA, Colosi PC, Matelis LA, Kurtzman GJ, Byrne BJ. Gene delivery to skeletal muscle results in sustained expression and systemic delivery of a therapeutic protein. *Proc Natl Acad Sci U S A*. 1996;93:14082-14087.
65. Xiao X, Li J, Samulski RJ. Efficient long-term gene transfer into muscle tissue of immunocompetent mice by adeno-associated virus vector. *J Virol*. 1996;70:8098-8108.
66. Clark KR, Sferra TJ, Johnson PR. Recombinant adeno-associated viral vectors mediate long-term transgene expression in muscle. *Hum Gene Ther*. 1997;8:659-669.
67. Berns KI, Linden RM. The cryptic life style of adeno-associated virus. *Bioessays*. 1995;17:237-245.
68. Samulski RJ. Adeno-associated virus: integration at a specific chromosomal locus. *Curr Opin Genet Dev*. 1993;3:74-80.

69. Walsh CE, Liu JM, Xiao X, Young NS, Nienhuis AW, Samulski RJ. Regulated high level expression of a human gamma-globin gene introduced into erythroid cells by an adeno-associated virus vector. *Proc Natl Acad Sci U S A*. 1992;89:7257-7261.
70. Muzyczka N. Use of adeno-associated virus as a general transduction vector for mammalian cells. *Curr Top Microbiol Immunol*. 1992;158:97-129.
71. Kotin RM, Siniscalco M, Samulski RJ, Zhu XD, Hunter L, Laughlin CA, McLaughlin S, Muzyczka N, Rocchi M, Berns KI. Site-specific integration by adeno-associated virus. *Proc Natl Acad Sci U S A*. 1990;87:2211-2215.
72. Summerford C, Samulski RJ. Membrane-associated heparan sulfate proteoglycan is a receptor for adeno-associated virus type 2 virions. *J Virol*. 1998;72:1438-1445.
73. Qing K, Mah C, Hansen J, Zhou S, Dwarki V, Srivastava A. Human fibroblast growth factor receptor 1 is a co-receptor for infection by adeno-associated virus 2 [see comments]. *Nat Med*. 1999;5:71-77.
74. Xiao X, Li J, Samulski RJ. Production of high-titer recombinant adeno-associated virus vectors in the absence of helper adenovirus. *J Virol*. 1998;72:2224-2232.
75. Kaplitt MG, Leone P, Samulski RJ, Xiao X, Pfaff DW, O'Malley KL, During MJ. Long-term gene expression and phenotypic correction using adeno-associated virus vectors in the mammalian brain. *Nat Genet*. 1994;8:148-154.
76. Peel AL, Zolotukhin S, Schrimsher GW, Muzyczka N, Reier PJ. Efficient transduction of green fluorescent protein in spinal cord neurons using adeno-associated virus vectors containing cell type-specific promoters. *Gene Ther*. 1997;4:16-24.
77. Klein RL, Meyer EM, Peel AL, Zolotukhin S, Meyers C, Muzyczka N, King MA. Neuron-specific transduction in the rat septohippocampal or nigrostriatal pathway by recombinant adeno-associated virus vectors. *Exp Neurol*. 1998;150:183-194.
78. Flotte TR, Solow R, Owens RA, Afione S, Zeitlin PL, Carter BJ. Gene expression from adeno-associated virus vectors in airway epithelial cells. *Am J Respir Cell Mol Biol*. 1992;7:349-356.
79. Beck SE, Laube BL, Barberena CI, Fischer AC, Adams RJ, Chesnut K, Flotte TR, Guggino WB. Deposition and expression of aerosolized rAAV vectors in the lungs of Rhesus macaques. *Mol Ther*. 2002;6:546-554.
80. Flotte TR, Zeitlin PL, Reynolds TC, Heald AE, Pedersen P, Beck S, Conrad CK, Brass-Ernst L, Humphries M, Sullivan K, Wetzel R, Taylor G, Carter BJ, Guggino WB. Phase I trial of intranasal and endobronchial administration of a recombinant adeno-associated virus serotype 2 (rAAV2)-CFTR vector in adult cystic fibrosis patients: a two-part clinical study. *Hum Gene Ther*. 2003;14:1079-1088.

81. Lipkowitz MS, Hanss B, Tulchin N, Wilson PD, Langer JC, Ross MD, Kurtzman GJ, Klotman PE, Klotman ME. Transduction of renal cells in vitro and in vivo by adeno-associated virus gene therapy vectors. *J Am Soc Nephrol.* 1999;10:1908-1915.
82. Chen S, Agarwal A, Glushakova OY, Jorgensen MS, Salgar SK, Poirier A, Flotte TR, Croker BP, Madsen KM, Atkinson MA, Hauswirth WW, Berns KI, Tisher CC. Gene delivery in renal tubular epithelial cells using recombinant adeno-associated viral vectors. *J Am Soc Nephrol.* 2003;14:947-958.
83. Ponnazhagan S, Mukherjee P, Yoder MC, Wang XS, Zhou SZ, Kaplan J, Wadsworth S, Srivastava A. Adeno-associated virus 2-mediated gene transfer in vivo: organ-tropism and expression of transduced sequences in mice. *Gene.* 1997;190:203-210.
84. Snyder RO, Miao CH, Patijn GA, Spratt SK, Danos O, Nagy D, Gown AM, Winther B, Meuse L, Cohen LK, Thompson AR, Kay MA. Persistent and therapeutic concentrations of human factor IX in mice after hepatic gene transfer of recombinant AAV vectors. *Nat Genet.* 1997;16:270-276.
85. Mount JD, Herzog RW, Tillson DM, Goodman SA, Robinson N, McClelland ML, Bellinger D, Nichols TC, Arruda VR, Lothrop CD, Jr., High KA. Sustained phenotypic correction of hemophilia B dogs with a factor IX null mutation by liver-directed gene therapy. *Blood.* 2002;99:2670-2676.
86. During MJ, Xu R, Young D, Kaplitt MG, Sherwin RS, Leone P. Peroral gene therapy of lactose intolerance using an adeno-associated virus vector. *Nat Med.* 1998;4:1131-1135.
87. Zolotukhin S, Byrne BJ, Mason E, Zolotukhin I, Potter M, Chesnut K, Summerford C, Samulski RJ, Muzyczka N. Recombinant adeno-associated virus purification using novel methods improves infectious titer and yield. *Gene Ther.* 1999;6:973-985.
88. Conway JE, ap Rhys CMJ, Zolotukhin I, Zolotukhin S, Muzyczka N, Hayward GS, Byrne BJ. High-titer recombinant adeno-associated virus production utilizing a recombinant herpes simplex virus type I vector expressing AAV-2 Rep and Cap. *Gene Ther.* 1999;6:973-985.
89. Conway JE, Chesnut K, Zolotukhin I et al. Production and purification systems for recombinant Adeno-associated virus type 2 vectors. In: Cid-Arregui A, Garcia-Carranca A, editors. *Viral Vectors: Basic Science and Gene Therapy.* Natick, MA: Eaton Publishing, 2000.
90. Casto BC, Atchison RW, Hammon WM. Studies on the relationship between adeno-associated virus type I (AAV- I) and adenoviruses. I. Replication of AAV-I in certain cell cultures and its effect on helper adenovirus. *Virology.* 1967;32:52-59.

91. Bantel-Schaal U, zur HH. Characterization of the DNA of a defective human parvovirus isolated from a genital site. *Virology*. 1984;134:52-63.
92. Parks WP, Green M, Pina M, Melnick JL. Physicochemical characterization of adeno-associated satellite virus type 4 and its nucleic acid. *J Virol*. 1967;1:980-987.
93. Rutledge EA, Halbert CL, Russell DW. Infectious clones and vectors derived from adeno-associated virus (AAV) serotypes other than AAV type 2. *J Virol*. 1998;72:309-319.
94. Chiorini JA, Kim F, Yang L, Kotin RM. Cloning and characterization of adeno-associated virus type 5. *J Virol*. 1999;73:1309-1319.
95. Gao GP, Alvira MR, Wang L, Calcedo R, Johnston J, Wilson JM. Novel adeno-associated viruses from rhesus monkeys as vectors for human gene therapy. *Proc Natl Acad Sci U S A*. 2002;99:11854-11859.
96. Gao G, Alvira MR, Somanathan S, Lu Y, Vandenberghe LH, Rux JJ, Calcedo R, Sanmiguel J, Abbas Z, Wilson JM. Adeno-associated viruses undergo substantial evolution in primates during natural infections. *Proc Natl Acad Sci U S A*. 2003;100:6081-6086.
97. Chao H, Monahan PE, Liu Y, Samulski RJ, Walsh CE. Sustained and complete phenotype correction of hemophilia b mice following intramuscular injection of aav1 serotype vectors. *Mol Ther*. 2001;4:217-222.
98. Fraites TJ, Jr., Schleissing MR, Shanely RA, Walter GA, Cloutier DA, Zolotukhin I, Pauly DF, Raben N, Plotz PH, Powers SK, Kessler PD, Byrne BJ. Correction of the enzymatic and functional deficits in a model of Pompe disease using adeno-associated virus vectors. *Mol Ther*. 2002;5:571-578.
99. Duan D, Sharma P, Yang J, Yue Y, Dudas L, Zhang Y, Fisher KJ, Engelhardt JF. Circular intermediates of recombinant adeno-associated virus have defined structural characteristics responsible for long-term episomal persistence in muscle tissue [In Process Citation]. *J Virol*. 1998;72:8568-8577.
100. Rabinowitz JE, Rolling F, Li C, Conrath H, Xiao W, Xiao X, Samulski RJ. Cross-packaging of a single adeno-associated virus (AAV) type 2 vector genome into multiple AAV serotypes enables transduction with broad specificity. *J Virol*. 2002;76:791-801.
101. Zolotukhin S, Potter M, Zolotukhin I, Sakai Y, Loiler S, Fraites TJ, Jr., Chiodo VA, Phillipsberg T, Muzyczka N, Hauswirth WW, Flotte TR, Byrne BJ, Snyder RO. Production and purification of serotype 1, 2, and 5 recombinant adeno-associated viral vectors. *Methods*. 2002;28:158-167.

102. Kaludov N, Handelman B, Chiorini JA. Scalable purification of adeno-associated virus type 2, 4, or 5 using ion-exchange chromatography. *Hum Gene Ther.* 2002;13:1235-1243.
103. Grimm D, Kay MA, Kleinschmidt JA. Helper virus-free, optically controllable, and two-plasmid-based production of adeno-associated virus vectors of serotypes 1 to 6. *Mol Ther.* 2003;7:839-850.
104. Fisher KJ, Jooss K, Alston J, Yang Y, Haecker SE, High K, Pathak R, Raper SE, Wilson JM. Recombinant adeno-associated virus for muscle directed gene therapy. *Nat Med.* 1997;3:306-312.
105. Snyder RO, Spratt SK, Lagarde C, Bohl D, Kaspar B, Sloan B, Cohen LK, Danos O. Efficient and stable adeno-associated virus-mediated transduction in the skeletal muscle of adult immunocompetent mice. *Hum Gene Ther.* 1997;8:1891-1900.
106. Su H, Lu R, Kan YW. Adeno-associated viral vector-mediated vascular endothelial growth factor gene transfer induces neovascular formation in ischemic heart. *Proc Natl Acad Sci U S A.* 2000;97:13801-13806.
107. Herzog RW, Hagstrom JN, Kung SH, Tai SJ, Wilson JM, Fisher KJ, High KA. Stable gene transfer and expression of human blood coagulation factor IX after intramuscular injection of recombinant adeno-associated virus. *Proc Natl Acad Sci U S A.* 1997;94:5804-5809.
108. Song S, Morgan M, Ellis T, Poirier A, Chesnut K, Wang J, Brantly M, Muzyczka N, Byrne BJ, Atkinson M, Flotte TR. Sustained secretion of human alpha-1-antitrypsin from murine muscle transduced with adeno-associated virus vectors. *Proc Natl Acad Sci U S A.* 1998;95:14384-14388.
109. Pruchnic R, Cao B, Peterson ZQ, Xiao X, Li J, Samulski RJ, Epperly M, Huard J. The use of adeno-associated virus to circumvent the maturation-dependent viral transduction of muscle fibers. *Hum Gene Ther.* 2000;11:521-536.
110. Summerford C, Bartlett JS, Samulski RJ. AlphaVbeta5 integrin: a co-receptor for adeno-associated virus type 2 infection [see comments]. *Nat Med.* 1999;5:78-82.
111. Chao H, Liu Y, Rabinowitz J, Li C, Samulski RJ, Walsh CE. Several log increase in therapeutic transgene delivery by distinct adeno-associated viral serotype vectors. *Mol Ther.* 2000;2:619-623.
112. Hildinger M, Auricchio A, Gao G, Wang L, Chirmule N, Wilson JM. Hybrid vectors based on adeno-associated virus serotypes 2 and 5 for muscle-directed gene transfer. *J Virol.* 2001;75:6199-6203.
113. Hauck B, Xiao W. Characterization of tissue tropism determinants of adeno-associated virus type 1. *J Virol.* 2003;77:2768-2774.

114. Fabb SA, Wells DJ, Serpente P, Dickson G. Adeno-associated virus vector gene transfer and sarcolemmal expression of a 144 kDa micro-dystrophin effectively restores the dystrophin-associated protein complex and inhibits myofibre degeneration in nude/mdx mice. *Hum Mol Genet.* 2002;11:733-741.
115. Harper SQ, Hauser MA, DelloRusso C, Duan D, Crawford RW, Phelps SF, Harper HA, Robinson AS, Engelhardt JF, Brooks SV, Chamberlain JS. Modular flexibility of dystrophin: implications for gene therapy of Duchenne muscular dystrophy. *Nat Med.* 2002;8:253-261.
116. Sakamoto M, Yuasa K, Yoshimura M, Yokota T, Ikemoto T, Suzuki M, Dickson G, Miyagoe-Suzuki Y, Takeda S. Micro-dystrophin cDNA ameliorates dystrophic phenotypes when introduced into mdx mice as a transgene. *Biochem Biophys Res Commun.* 2002;293:1265-1272.
117. Yuasa K, Sakamoto M, Miyagoe-Suzuki Y, Tanouchi A, Yamamoto H, Li J, Chamberlain JS, Xiao X, Takeda S. Adeno-associated virus vector-mediated gene transfer into dystrophin-deficient skeletal muscles evokes enhanced immune response against the transgene product. *Gene Ther.* 2002;9:1576-1588.
118. Li J, Dressman D, Tsao YP, Sakamoto A, Hoffman EP, Xiao X. rAAV vector-mediated sarcoglycan gene transfer in a hamster model for limb girdle muscular dystrophy. *Gene Ther.* 1999;6:74-82.
119. Xiao X, Li J, Tsao YP, Dressman D, Hoffman EP, Watchko JF. Full functional rescue of a complete muscle (TA) in dystrophic hamsters by adeno-associated virus vector-directed gene therapy. *J Virol.* 2000;74:1436-1442.
120. Kawada T, Sakamoto A, Nakazawa M, Urabe M, Masuda F, Hemmi C, Wang Y, Shin WS, Nakatsuru Y, Sato H, Ozawa K, Toyo-oka T. Morphological and physiological restorations of hereditary form of dilated cardiomyopathy by somatic gene therapy. *Biochem Biophys Res Commun.* 2001;284:431-435.
121. Kawada T, Nakazawa M, Nakauchi S, Yamazaki K, Shimamoto R, Urabe M, Nakata J, Hemmi C, Masui F, Nakajima T, Suzuki J, Monahan J, Sato H, Masaki T, Ozawa K, Toyo-oka T. Rescue of hereditary form of dilated cardiomyopathy by rAAV-mediated somatic gene therapy: amelioration of morphological findings, sarcolemmal permeability, cardiac performances, and the prognosis of TO-2 hamsters. *Proc Natl Acad Sci U S A.* 2002;99:901-906.
122. Greelish JP, Su LT, Lankford EB, Burkman JM, Chen H, Konig SK, Mercier IM, Desjardins PR, Mitchell MA, Zheng XG, Leferovich J, Gao GP, Balice-Gordon RJ, Wilson JM, Stedman HH. Stable restoration of the sarcoglycan complex in dystrophic muscle perfused with histamine and a recombinant adeno-associated viral vector. *Nat Med.* 1999;5:439-443.

123. Cordier L, Hack AA, Scott MO, Barton-Davis ER, Gao G, Wilson JM, McNally EM, Sweeney HL. Rescue of skeletal muscles of gamma-sarcoglycan-deficient mice with adeno-associated virus-mediated gene transfer. *Mol Ther.* 2000;1:119-129.
124. Dressman D, Araishi K, Imamura M, Sasaoka T, Liu LA, Engvall E, Hoffman EP. Delivery of alpha- and beta-sarcoglycan by recombinant adeno-associated virus: efficient rescue of muscle, but differential toxicity. *Hum Gene Ther.* 2002;13:1631-1646.
125. Kearns WG, Afione SA, Fulmer SB, Pang MC, Erikson D, Egan M, Landrum MJ, Flotte TR, Cutting GR. Recombinant adeno-associated virus (AAV-CFTR) vectors do not integrate in a site-specific fashion in an immortalized epithelial cell line. *Gene Ther.* 1996;3:748-755.
126. Ponnazhagan S, Erikson D, Kearns WG, Zhou SZ, Nahreini P, Wang XS, Srivastava A. Lack of site-specific integration of the recombinant adeno-associated virus 2 genomes in human cells. *Hum Gene Ther.* 1997;8:275-284.
127. Song S, Laipis PJ, Berns KI, Flotte TR. Effect of DNA-dependent protein kinase on the molecular fate of the rAAV2 genome in skeletal muscle. *Proc Natl Acad Sci U S A.* 2001;98:4084-4088.
128. Kaplitt MG, Xiao X, Samulski RJ, Li J, Ojamaa K, Klein IL, Makimura H, Kaplitt MJ, Strumpf RK, Diethrich EB. Long-term gene transfer in porcine myocardium after coronary infusion of an adeno-associated virus vector. *Ann Thorac Surg.* 1996;62:1669-1676.
129. Maeda Y, Ikeda U, Shimpō M, Ueno S, Ogasawara Y, Urabe M, Kume A, Takizawa T, Saito T, Colosi P, Kurtzman G, Shimada K, Ozawa K. Efficient gene transfer into cardiac myocytes using adeno-associated virus (AAV) vectors. *J Mol Cell Cardiol.* 1998;30:1341-1348.
130. Maeda Y, Ikeda U, Shimpō M, Shibuya M, Monahan J, Urabe M, Ozawa K, Shimada K. Adeno-associated virus-mediated vascular endothelial growth factor gene transfer into cardiac myocytes. *J Cardiovasc Pharmacol.* 2000;36:438-443.
131. Svensson EC, Marshall DJ, Woodard K, Lin H, Jiang F, Chu L, Leiden JM. Efficient and stable transduction of cardiomyocytes after intramyocardial injection or intracoronary perfusion with recombinant adeno-associated virus vectors. *Circulation.* 1999;99:201-205.
132. Logeart D, Hatem SN, Heimburger M, Le Roux A, Michel JB, Mercadier JJ. How to optimize in vivo gene transfer to cardiac myocytes: mechanical or pharmacological procedures? *Hum Gene Ther.* 2001;12:1601-1610.

133. Champion HC, Georgakopoulos D, Haldar S, Wang L, Wang Y, Kass DA. Robust Adenoviral and Adeno-Associated Viral Gene Transfer to the In Vivo Murine Heart. Application to Study of Phospholamban Physiology. *Circulation*. 2003.
134. Chu D, Sullivan CC, Weitzman MD, Du L, Wolf PL, Jamieson SW, Thistlethwaite PA. Direct comparison of efficiency and stability of gene transfer into the mammalian heart using adeno-associated virus versus adenovirus vectors. *J Thorac Cardiovasc Surg*. 2003;126:671-679.
135. Hoshijima M, Ikeda Y, Iwanaga Y, Minamisawa S, Date MO, Gu Y, Iwatate M, Li M, Wang L, Wilson JM, Wang Y, Ross J, Jr., Chien KR. Chronic suppression of heart-failure progression by a pseudophosphorylated mutant of phospholamban via in vivo cardiac rAAV gene delivery. *Nat Med*. 2002;8:864-871.
136. Iwatate M, Gu Y, Dieterle T, Iwanaga Y, Peterson KL, Hoshijima M, Chien KR, Ross J. In vivo high-efficiency transcortical gene delivery and Cre-LoxP gene switching in the adult mouse heart. *Gene Ther*. 2003;10:1814-1820.
137. Post H, Kajstura J, Lei B, Sessa WC, Byrne B, Anversa P, Hintze TH, Recchia FA. Adeno-associated virus mediated gene delivery into coronary microvessels of chronically instrumented dogs. *J Appl Physiol*. 2003;95:1688-1694.
138. Yasukawa H, Yajima T, Duplain H, Iwatate M, Kido M, Hoshijima M, Weitzman MD, Nakamura T, Woodard S, Xiong D, Yoshimura A, Chien KR, Knowlton KU. The suppressor of cytokine signaling-1 (SOCS1) is a novel therapeutic target for enterovirus-induced cardiac injury. *J Clin Invest*. 2003;111:469-478.
139. Yue Y, Li Z, Harper SQ, Davisson RL, Chamberlain JS, Duan D. Microdystrophin gene therapy of cardiomyopathy restores dystrophin-glycoprotein complex and improves sarcolemma integrity in the mdx mouse heart. *Circulation*. 2003;108:1626-1632.
140. Bosch A, Perret E, Desmaris N, Heard JM. Long-term and significant correction of brain lesions in adult mucopolysaccharidosis type VII mice using recombinant AAV vectors. *Mol Ther*. 2000;1:63-70.
141. Daly TM, Ohlemiller KK, Roberts MS, Vogler CA, Sands MS. Prevention of systemic clinical disease in MPS VII mice following AAV-mediated neonatal gene transfer. *Gene Ther*. 2001;8:1291-1298.
142. Elliger SS, Elliger CA, Aguilar CP, Raju NR, Watson GL. Elimination of lysosomal storage in brains of MPS VII mice treated by intrathecal administration of an adeno-associated virus vector. *Gene Ther*. 1999;6:1175-1178.
143. Hartung SD, Reddy RG, Whitley CB, McIvor RS. Enzymatic correction and cross-correction of mucopolysaccharidosis type I fibroblasts by adeno-associated virus-mediated transduction of the alpha-L-iduronidase gene. *Hum Gene Ther*. 1999;10:2163-2172.

144. Jung SC, Han IP, Limaye A, Xu R, Gelderman MP, Zerfas P, Tirumalai K, Murray GJ, During MJ, Brady RO, Qasba P. Adeno-associated viral vector-mediated gene transfer results in long-term enzymatic and functional correction in multiple organs of Fabry mice. *Proc Natl Acad Sci U S A*. 2001;98:2676-2681.
145. Park J, Murray GJ, Limaye A, Quirk JM, Gelderman MP, Brady RO, Qasba P. Long-term correction of globotriaosylceramide storage in Fabry mice by recombinant adeno-associated virus-mediated gene transfer. *Proc Natl Acad Sci U S A*. 2003;100:3450-3454.
146. Takahashi H, Hirai Y, Migita M, Seino Y, Fukuda Y, Sakuraba H, Kase R, Kobayashi T, Hashimoto Y, Shimada T. Long-term systemic therapy of Fabry disease in a knockout mouse by adeno-associated virus-mediated muscle-directed gene transfer. *Proc Natl Acad Sci U S A*. 2002;99:13777-13782.
147. Criswell DS, Powers SK, Herb RA, Dodd SL. Mechanism of specific force deficit in the senescent rat diaphragm. *Respir Physiol*. 1997;107:149-155.
148. Herb RA, Powers SK, Criswell DS, Caiozzo VJ, Vrabas IS, Dodd SL. Alterations in phenotypic and contractile properties of the rat diaphragm: influence of hypothyroidism. *J Appl Physiol*. 1996;80:2163-2170.
149. Schiaffino S, Gorza L, Sartore S, Saggin L, Ausoni S, Vianello M, Gundersen K, Lomo T. Three myosin heavy chain isoforms in type 2 skeletal muscle fibres. *J Muscle Res Cell Motil*. 1989;10:197-205.
150. Wehrens XH, Kirchhoff S, Doevendans PA. Mouse electrocardiography: an interval of thirty years. *Cardiovasc Res*. 2000;45:231-237.
151. Georgakopoulos D, Mitzner WA, Chen CH, Byrne BJ, Millar HD, Hare JM, Kass DA. In vivo murine left ventricular pressure-volume relations by miniaturized conductance micromanometry. *Am J Physiol*. 1998;274:H1416-H1422.
152. Chaves AA, Dech SJ, Nakayama T, Hamlin RL, Bauer JA, Carnes CA. Age and anesthetic effects on murine electrocardiography. *Life Sci*. 2003;72:2401-2412.
153. Chu V, Otero JM, Lopez O, Morgan JP, Amende I, Hampton TG. Method for non-invasively recording electrocardiograms in conscious mice. *BMC Physiol*. 2001;1:6.
154. Maguire CT, Bevilacqua LM, Wakimoto H, Gehrmann J, Berul CI. Maturational atrioventricular nodal physiology in the mouse. *J Cardiovasc Electrophysiol*. 2000;11:557-564.
155. Saba S, Vanderbrink BA, Luciano B, Aronovitz MJ, Berul CI, Reddy S, Housman D, Mendelsohn ME, Estes NA, III, Wang PJ. Localization of the sites of conduction abnormalities in a mouse model of myotonic dystrophy. *J Cardiovasc Electrophysiol*. 1999;10:1214-1220.

156. Gardin JM, Siri FM, Kitsis RN, Edwards JG, Leinwand LA. Echocardiographic assessment of left ventricular mass and systolic function in mice. *Circ Res.* 1995;76:907-914.
157. Suga H. Paul Dudley White International Lecture: cardiac performance as viewed through the pressure-volume window. *Jpn Heart J.* 1994;35:263-280.
158. Sagawa K, Maughan WL, Suga H et al. Cardiac contraction and the pressure-volume relationship. 1988.
159. Feldman MD, Erikson JM, Mao Y, Korcarz CE, Lang RM, Freeman GL. Validation of a mouse conductance system to determine LV volume: comparison to echocardiography and crystals. *Am J Physiol Heart Circ Physiol.* 2000;279:H1698-H1707.
160. Feldman MD, Mao Y, Valvano JW, Pearce JA, Freeman GL. Development of a multifrequency conductance catheter-based system to determine LV function in mice. *Am J Physiol Heart Circ Physiol.* 2000;279:H1411-H1420.
161. Georgakopoulos D, Kass DA. Estimation of parallel conductance by dual-frequency conductance catheter in mice. *Am J Physiol Heart Circ Physiol.* 2000;279:H443-H450.
162. Bruneau BG, Bao ZZ, Fatkin D, Xavier-Neto J, Georgakopoulos D, Maguire CT, Berul CI, Kass DA, Kuroski-de Bold ML, de Bold AJ, Conner DA, Rosenthal N, Cepko CL, Seidman CE, Seidman JG. Cardiomyopathy in *Irx4*-deficient mice is preceded by abnormal ventricular gene expression. *Mol Cell Biol.* 2001;21:1730-1736.
163. McConnell BK, Jones KA, Fatkin D, Arroyo LH, Lee RT, Aristizabal O, Turnbull DH, Georgakopoulos D, Kass D, Bond M, Niimura H, Schoen FJ, Conner D, Fischman DA, Seidman CE, Seidman JG, Fischman DH. Dilated cardiomyopathy in homozygous myosin-binding protein-C mutant mice. *J Clin Invest.* 1999;104:1235-1244.
164. McConnell BK, Fatkin D, Semsarian C, Jones KA, Georgakopoulos D, Maguire CT, Healey MJ, Mudd JO, Moskowitz IP, Conner DA, Giewat M, Wakimoto H, Berul CI, Schoen FJ, Kass DA, Seidman CE, Seidman JG. Comparison of two murine models of familial hypertrophic cardiomyopathy. *Circ Res.* 2001;88:383-389.
165. Georgakopoulos D, Christe ME, Giewat M, Seidman CM, Seidman JG, Kass DA. The pathogenesis of familial hypertrophic cardiomyopathy: early and evolving effects from an alpha-cardiac myosin heavy chain missense mutation. *Nat Med.* 1999;5:327-330.

166. Dodd SL, Powers SK, Vrabas IS, Criswell D, Stetson S, Hussain R. Effects of clenbuterol on contractile and biochemical properties of skeletal muscle. *Med Sci Sports Exerc.* 1996;28:669-676.
167. Papaioannou VE, Fox JG. Efficacy of tribromoethanol anesthesia in mice. *Lab Anim Sci.* 1993;43:189-192.
168. Brooks SV, Faulkner JA. Contractile properties of skeletal muscles from young, adult and aged mice. *J Physiol.* 1988;404:71-82.
169. Monahan PE, Samulski RJ. AAV vectors: is clinical success on the horizon? *Gene Ther.* 2000;7:24-30.
170. Schleissing, M. R. Biochemical and functional analysis after in utero delivery of recombinant adeno-associated virus to a mouse model of glycogen storage disease type II. 11-25-2003. Electronic Citation.
171. Petrof BJ. Respiratory muscles as a target for adenovirus-mediated gene therapy. *Eur Respir J.* 1998;11:492-497.
172. Baranov A, Glazkov P, Kiselev A, Ostapenko O, Mikhailov V, Ivaschenko T, Sabetsky V, Baranov V. Local and distant transfection of mdx muscle fibers with dystrophin and LacZ genes delivered in vivo by synthetic microspheres. *Gene Ther.* 1999;6:1406-1414.
173. Liu F, Nishikawa M, Clemens PR, Huang L. Transfer of full-length Dmd to the diaphragm muscle of Dmd(mdx/mdx) mice through systemic administration of plasmid DNA. *Mol Ther.* 2001;4:45-51.
174. Buning H, Ried MU, Perabo L, Gerner FM, Huttner NA, Enssle J, Hallek M. Receptor targeting of adeno-associated virus vectors. *Gene Ther.* 2003;10:1142-1151.
175. Muller OJ, Kaul F, Weitzman MD, Pasqualini R, Arap W, Kleinschmidt JA, Trepel M. Random peptide libraries displayed on adeno-associated virus to select for targeted gene therapy vectors. *Nat Biotechnol.* 2003.
176. Perabo L, Buning H, Kofler DM, Ried MU, Girod A, Wendtner CM, Enssle J, Hallek M. In vitro selection of viral vectors with modified tropism: the adeno-associated virus display. *Mol Ther.* 2003;8:151-157.
177. Ponnazhagan S, Mahendra G, Kumar S, Thompson JA, Castillas M, Jr. Conjugate-based targeting of recombinant adeno-associated virus type 2 vectors by using avidin-linked ligands. *J Virol.* 2002;76:12900-12907.
178. Shi W, Arnold GS, Bartlett JS. Insertional mutagenesis of the adeno-associated virus type 2 (AAV2) capsid gene and generation of AAV2 vectors targeted to alternative cell-surface receptors. *Hum Gene Ther.* 2001;12:1697-1711.

179. Shi W, Bartlett JS. RGD inclusion in VP3 provides adeno-associated virus type 2 (AAV2)-based vectors with a heparan sulfate-independent cell entry mechanism. *Mol Ther.* 2003;7:515-525.
180. Wu P, Xiao W, Conlon T, Hughes J, Agbandje-McKenna M, Ferkol T, Flotte T, Muzyczka N. Mutational analysis of the adeno-associated virus type 2 (AAV2) capsid gene and construction of AAV2 vectors with altered tropism [In Process Citation]. *J Virol.* 2000;74:8635-8647.
181. Xiao W, Chirmule N, Berta SC, McCullough B, Gao G, Wilson JM. Gene therapy vectors based on adeno-associated virus type 1. *J Virol.* 1999;73:3994-4003.
182. March KL, Madison JE, Trapnell BC. Pharmacokinetics of adenoviral vector-mediated gene delivery to vascular smooth muscle cells: modulation by poloxamer 407 and implications for cardiovascular gene therapy. *Hum Gene Ther.* 1995;6:41-53.
183. Van Belle E, Maillard L, Rivard A, Fabre JE, Couffinhal T, Kearney M, Branellec D, Feldman LJ, Walsh K, Isner JM. Effects of poloxamer 407 on transfection time and percutaneous adenovirus-mediated gene transfer in native and stented vessels. *Hum Gene Ther.* 1998;9:1013-1024.
184. Croyle MA, Cheng X, Wilson JM. Development of formulations that enhance physical stability of viral vectors for gene therapy. *Gene Ther.* 2001;8:1281-1290.
185. Seiler MP, Luner P, Moninger TO, Karp PH, Keshavjee S, Zabner J. Thixotropic solutions enhance viral-mediated gene transfer to airway epithelia. *Am J Respir Cell Mol Biol.* 2002;27:133-140.
186. Mah C, Fraites TJ, Jr., Zolotukhin I, Song S, Flotte TR, Dobson J, Batich C, Byrne BJ. Improved method of recombinant AAV2 delivery for systemic targeted gene therapy. *Mol Ther.* 2002;6:106-112.
187. Stedman HH, Sweeney HL, Shrager JB, Maguire HC, Panettieri RA, Petrof B, Narusawa M, Leferovich JM, Sladky JT, Kelly AM. The mdx mouse diaphragm reproduces the degenerative changes of Duchenne muscular dystrophy. *Nature.* 1991;352:536-539.
188. Petrof BJ, Acsadi G, Jani A, Massie B, Bourdon J, Matusiewicz N, Yang L, Lochmuller H, Karpati G. Efficiency and functional consequences of adenovirus-mediated in vivo gene transfer to normal and dystrophic (mdx) mouse diaphragm. *Am J Respir Cell Mol Biol.* 1995;13:508-517.
189. Yang HW, Kikuchi T, Hagiwara Y, Mizutani M, Chen YT, Van Hove JL. Recombinant human acid alpha-glucosidase corrects acid alpha-glucosidase-deficient human fibroblasts, quail fibroblasts, and quail myoblasts. *Pediatr Res.* 1998;43:374-380.

BIOGRAPHICAL SKETCH

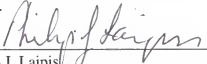
Thomas J. Fraites, Jr. was born in Flushing, NY, in 1974. He graduated from Niceville Senior High School (Niceville, FL) in 1992 and attended the Johns Hopkins University in Baltimore, MD. In 1997, Tom received his B.S. in biomedical engineering, with a concentration in materials science and a minor in philosophy. While at Johns Hopkins, he studied *in situ* cardiac mechanics with David Kass, M.D., and cardiovascular cellular response to mechanical stimuli with Barry J. Byrne, M.D., Ph.D.

In December 2000, Tom completed the joint MS/MBA program at the University of Florida, in the Department of Molecular Genetics and Microbiology and the Warrington College of Business. He is a recipient of the Outstanding Research Award and Travel Grant from the American Society of Gene Therapy (ASGT) and is a Predoctoral Fellow of the American Heart Association. Tom enrolled as a doctoral student in the Interdisciplinary Graduate Program (IDP) at the University of Florida College of Medicine in August 2000. He intends to pursue a career in product development for cardiovascular applications, and looks forward to the clinical application of gene therapeutics for GSDII.


I certify that I have read this study and that in my opinion it conforms to acceptable standards of scholarly presentation and is fully adequate, in scope and quality, as a dissertation for the degree of Doctor of Philosophy.


Barry J. Byrne, Chair
Professor of Molecular Genetics and
Microbiology

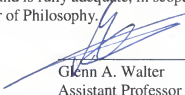
I certify that I have read this study and that in my opinion it conforms to acceptable standards of scholarly presentation and is fully adequate, in scope and quality, as a dissertation for the degree of Doctor of Philosophy.


Philip J. Laipis
Professor of Biochemistry and Molecular
Biology

I certify that I have read this study and that in my opinion it conforms to acceptable standards of scholarly presentation and is fully adequate, in scope and quality, as a dissertation for the degree of Doctor of Philosophy.


Jörg Bungert
Assistant Professor of Biochemistry and
Molecular Biology


I certify that I have read this study and that in my opinion it conforms to acceptable standards of scholarly presentation and is fully adequate, in scope and quality, as a dissertation for the degree of Doctor of Philosophy.


Glenn A. Walter
Assistant Professor of Physiology and
Functional Genomics

This dissertation was submitted to the Graduate Faculty of the College of Medicine and to the Graduate School and was accepted as partial fulfillment of the requirements for the degree of Doctor of Philosophy.

December 2003


Wayne J. McCormack
Dean, College of Medicine


Shafiq M. Abbas
Dean, Graduate School